

Universitätsklinik für Herz- und Thoraxchirurgie der Medizinischen Fakultät der
Otto-von-Guericke-Universität Magdeburg



**Blood Monocyte Phenotypes and Effect of Selenium on
Mononuclear Cells in Coronary Artery Disease: A Special
Focus on Monocyte Migration Markers and STAT-3/IL-6 Axis**

DISSERTATION

zur Erlangung des Doktorgrades

Dr. med.

(doctor medicinae)

an der Medizinischen Fakultät

der Otto-von-Guericke-Universität Magdeburg

vorgelegt von:

Anna Ball

geb. am:

03.09.1991 in Potsdam

Magdeburg 2024

Bibliographic Information:

Ball, Anna:

Blood Monocyte Phenotypes and Effect of Selenium on Mononuclear Cells in Coronary Artery Disease: A Special Focus on Monocyte Migration Markers and STAT-3/IL-6 Axis.
- 2024. - 69 pages, 27 illustrations, 15 tables

Abstract

Chronic inflammation is a key factor in the development of atherosclerosis, the underlying pathological mechanism of coronary artery disease (CAD), where circulating blood monocytes play a crucial role. These monocytes are classified into three subtypes: classical, intermediate and non-classical. Further, pro-inflammatory cytokines secreted by the mononuclear cells are pivotal in sustaining the state of inflammation in CAD. Hence, the main aim of the study was (i) to investigate the existing state of inflammation among CAD patients in terms of (a) monocytes subtypes and (b) pro-inflammatory cytokines and (ii) to intervene the inflamed state with a therapeutic concentration of selenium, *in-vitro*. The study found that CAD patients exhibited ongoing inflammation, characterized by (i) alterations in monocyte subtypes, including a decrease in classical monocytes and an increase in non-classical monocytes, (ii) heightened CCR1 expression in classical monocytes, suggesting potential differentiation towards inflamed monocytes or macrophages, and (iii) elevated IL-6 cytokine levels. Selenium *in-vitro* treatment diminished the conversion of classical monocytes into the intermediate and non-classical subsets. Moreover, selenium *in-vitro* intervention was found to minimize inflammation by hampering the STAT-3 activity and thereby lowering the production of pro-inflammatory cytokines, including IL-6 and TNF- α , by CAD mononuclear cells. In conclusion, the study highlights the potential of selenium to modulate the inflammatory processes and might hold promising potential as a therapeutic approach for CAD patients.

Keywords:

Coronary Artery Disease, Monocytes, Monocyte Migration Markers, IL-6 and TNF- α cytokines, STAT-3

Contents

List Of Abbreviations	v
1. Introduction	1
1.1. Coronary Artery Disease (CAD)	1
1.1.A. Terms and Definitions associated with CAD	1
1.1.B. Epidemiological Reports of CAD	4
1.1.C. Risk Factors of CAD	5
1.1.D. Pathogenesis of CAD	6
1.2. Immunological Aspects	8
1.2.A. Blood Monocytes and Monocyte Subpopulations	8
1.2.B. Monocyte Migration Markers	12
1.2.C. Selenium	15
1.2.D. IL-6-STAT-3-Pathway	17
1.3. Chronic Inflammation and the Combined Impact of Monocytes and IL-6- STAT-3-Pathway in CAD	18
1.4. Aims and Objectives	20
2. Materials	21
2.1. Biological Materials and Ethical Approval	21
2.2. Materials Corresponding to the Methods	21
2.2.A. FACS	21
2.2.B. ELISA	23
2.2.C. RT-PCR	24
2.2.D. Cell Culture and Selenium Treatment	25
2.2.E. WB	25
2.3. General Lab Materials	29
2.3.A. General Chemicals, Media, Buffers and Solutions	29
2.3.B. Consumables	30
2.3.C. Laboratory Materials	31
2.3.D. Laboratory Devices and Software	31

3. Methods	33
3.1. Collection of Subjects: CAD Patients and Normal Controls	33
3.2. Sample Preparation: Isolation of PBMC	33
3.3. Phenotyping of Monocyte Subsets and Migration Markers by FACS	34
3.4. Plasma Quantification of Pro-inflammatory Cytokines in CAD and Normal Control	39
3.5. Therapeutic Intervention with Selenium on CAD Mononuclear Cells	40
3.5.A. Pharmacokinetic Selenium Dose Evaluation by RT-PCR	40
3.5.B. Cell Culture and Selenium Treatment	43
3.5.C. Selenium Intervention on the Frequencies of Monocytes Subsets and Expression of Monocyte Migration Markers in CAD Mononuclear Cells	44
3.5.D. Selenium Intervention on Phosphorylation of STAT-3 Transcription Factor in CAD Mononuclear Cells	44
3.5.E. Selenium Intervention on Pro-inflammatory Cytokines in CAD Mononuclear Cells	51
3.6. Statistical Analysis	51
4. Results	52
4.1. Phenotyping of Monocyte Subsets and Migration Markers in CAD Patients and Normal Controls	52
4.2. Plasma Quantification of Pro-inflammatory Cytokines in CAD Patients and Normal Controls	54
4.3. Therapeutic Intervention with Selenium on CAD Mononuclear Cells	55
4.3.A. Pharmacokinetic Selenium Dose Evaluation Study by Real-Time PCR.	55
4.3.B. Selenium Intervention on the Frequencies of Monocyte Subsets and Expression of Monocyte Migration Markers in CAD Mononuclear Cells	56
4.3.C. Selenium Intervention on Phosphorylation Status of STAT3 Tran- scription Factor in CAD Mononuclear Cells	58
4.3.D. Selenium Intervention on the Cell Supernatant Levels of Pro-inflammatory Cytokines from CAD Mononuclear Cells	59

5. Discussion	60
5.1. Phenotyping of Monocyte Subsets and Migration Markers in CAD Patients and Normal Control	60
5.2. Plasma Quantification of Pro-inflammatory Cytokines in CAD Patients and Normal Control	63
5.3. Therapeutic Intervention with Selenium	64
5.4. Conclusion and Outlook	67
6. Summary	69
Bibliography	VIII
Acknowledgment	XX
Curriculum Vitae	XXII

List Of Abbreviations

ACS	Acute Coronary Syndrome	ELISA	Enzyme-linked Immunosorbent Assay
AMI	Acute Myocardial Infarction	ESC	European Society of Cardiology
APC	Allophycocyanin	FACS	Fluorescence-Activated Cell Sorting
BV	Brilliant Violet	fcX	Fc Receptor Blocking Solution
CABG	Coronary Bypass Grafting	FITC	Fluoresceinisothiocyanat
CAD	Coronary Artery Disease	GPX	Glutathione Peroxidases
CCL2	Chemokine Ligand Type 2	ICAM-1	Intercellular Adhesion Molecule-1
CCL3	Chemokine Ligand Type 3	IHD	Ischemic Heart Disease
CCL5	Chemokine Ligand Type 5	IL-1β	Interleukin-1 Beta
CCR1	C-C Chemokine Receptor Type 1	IL-6	Interleukin-6
CCR2	C-C Chemokine Receptor Type 2	JAK	Janus Kinase
CCR5	C-C Chemokine Receptor Type 5	L/D	Life Dead
CCS	Chronic Coronary Syndrome	LDL	Low Density Lipoprotein
CD	Cluster of Differentiation	LPS	Lipopolysaccharides
CVD	Cardiovascular Disease	M1	Classical Monocytes
CX₃CL₁	Chemokine C-X3-C motif ligand 1	M2	Intermediate Monocytes
CX₃CR₁	Chemokine C-X3-C motif receptor 1	M3	Non-Classical Monocytes
DVD	Double-Vessel Disease	MCP-1	Monocytes Chemoattractant Protein-1
e.g.	exempli gratia, for example		

MFI	Median Fluorescent Intensity	RT-PCR	Real-time Polymerase Chain Reaction
Mil	Million	sec	Seconds
min	Minutes	Se	Selenium
MPS	Mononuclear Phagocyte System	STAT-3	Signal Transducer and Activator of Transcription Type 3
NF-κB	Nuclear Factor Kappa B	STAT	Signal Transducer and Activator of Transcription
NSTEMI	Non ST-Elevation Myocardial Infarction	STEMI	ST-elevation Myocardial Infarction
PBMC	Peripheral Blood Mononuclear Cells	SVD	Single-Vessel Disease
PCI	Percutaneous Coronary Intervention	Temp.	Temperature
PCR	Polymerase Chain Reaction	TLR4	Toll-like Receptor 4
Pe-Cy7	PE-Cyanine 7	TNF-α	Tumor Necrosis Factor Alpha
Pe	Phycoerythrin	TVD	Triple-Vessel Disease
pSTAT-3	Phosphorylated Signal Transducer and Activator of Transcription type 3	VCAM-1	Vascular Cell Adhesion Molecule-1
ROS	Reactive Oxygen Species	WB	Western Blot
rpm	Revolutions per Minute	WHO	World Health Organization

1. Introduction

Chronic inflammation is the main pathological driver for the development and of atherosclerosis, which is regarded to be the underlying pathophysiological mechanism for coronary artery disease (CAD). The progression of chronic inflammation is mediated by infiltrating inflammatory cells that are being recruited to the coronary arteries leading to occlusion of lumen and subsequent ischaemia, where circulating blood monocytes are considered to be one of the pivotal inflammatory cells. The main content of this doctoral thesis is focused on investigating the circulating blood monocytes, their subsets and functional migration markers, as well as plasma levels of pro-inflammatory cytokines in context to define the state of inflammation in CAD compared to normal control. A unique emphasis is placed on investigating intervention with selenium to mitigate this ongoing inflammation. This trace element is explored for its capacity to modulate the inflammatory landscape. Of particular interest are changes in the frequencies of monocyte subsets and the expression of migration markers, levels of pro-inflammatory cytokines, namely tumor necrosis factor alpha (TNF- α) and interleukin-6 (IL-6), and the signal transducer and activator of transcription type 3 (STAT-3)/IL-6 signaling pathway within blood mononuclear cells. Through this complex examination, the thesis seeks to illuminate key factors contributing to CAD-related inflammation and to shed light on novel avenues for intervention.

1.1. Coronary Artery Disease (CAD)

1.1.A. Terms and Definitions associated with CAD

Atherosclerosis is the main underlying principal mechanism of all cardiovascular diseases (CVDs) including CAD, acute myocardial infarction (AMI), stroke, carotid artery occlusion, ischaemic cerebrovascular disease and peripheral vascular disease. CAD is a condition that results in reduced blood supply to the heart muscle and subsequently to ischemic heart disease (IHD). There are two main manifestations of IHD: chronic and acute.

- **Chronic ischaemic heart disease** refers to a long-standing, ongoing condition in which the blood flow to the heart muscle is consistently reduced or compromised due to narrowed coronary arteries. In alignment with the term acute coronary syndrome (ACS), the European Society of Cardiology (ESC) has currently designated chronic

ischaemic heart disease or stable ischaemic heart disease (SIHD) as chronic coronary syndrome (CCS) [1]. This narrowing is often caused by the build-up of fatty deposits and plaque on the inner walls of the arteries, a condition known as CAD due to atherosclerosis. As the narrowing progresses, it can lead to ischaemia of the heart muscle, an imbalance between oxygen supply and demand. This can result in the primary symptom of IHD, which is angina pectoris (chest pain or discomfort), and sometimes shortness of breath during physical exercise. Chronic ischaemic heart disease can also lead to more serious complications like heart failure over time if not managed properly.

- **Acute ischaemic heart disease**, commonly denoted as acute coronary syndrome (ACS), on the other hand, refers to sudden and severe episodes of reduced blood supply to the heart muscle. The foremost recognized manifestation of acute ischaemic heart disease is acute myocardial infarction (AMI), popularly termed as heart attack. ACS encompasses ST-elevation myocardial infarction (STEMI), non-ST elevation myocardial infarction (NSTEMI), and unstable angina. Again, the leading symptom is angina pectoris.
 - ST-elevation myocardial infarction (STEMI): A severe form of heart attack, where there is a complete obstruction of a coronary artery, typically caused by a thrombus forming on a ruptured plaque within the artery, leading to significant damage to the heart muscle. In contrast to the other manifestations of ACS, the extent of myocardial damage in STEMI affects all layers of the heart wall from the endocardium to the epicardium (transmural infarction). It is characterized by kinetics of cardiac biomarkers, namely troponin, and elevated ST-segments on an electrocardiogram (ECG).
 - Non ST-elevation myocardial infarction (NSTEMI): A type of heart attack where there is a partial blockage of a coronary artery, resulting in damage to the heart muscle. It is characterized by kinetics of troponin but without significant ST-segment elevation on an ECG.
 - Unstable angina: A condition where there is a temporary and partial blockage of a coronary artery due to a ruptured atherosclerotic plaque, causing angina pectoris due to inadequate blood supply to the heart muscle. It is characterized by neither kinetics of troponin nor significant ST-segment elevation on an ECG.

The ischaemia of the heart muscle, caused by the lack of blood flow, can cause rapid damage to the heart muscle (necrosis), leading to chest pain, shortness of breath, nausea, and potentially life-threatening complications. Quick medical intervention is crucial

in treating acute ischaemic heart disease to minimize heart muscle damage and improve survival rates. Significant CAD is a condition where there is at least a 50 % luminal narrowing in one of the epicardial coronary arteries. CAD is classified based on the vascular territory affected: triple-vessel disease (TVD) is a severe type of significant CAD where there is significant stenosis in any three of the major epicardial coronary arteries, namely LAD (Left Anterior Descending), LCX (Left Circumflex), and RCA (Right Coronary Artery). TVD is related with higher incidences of major adverse cardiac events and mortality compared to double-vessel disease (DVD) and single-vessel disease (SVD), with significant stenosis in any two or one of the major epicardial coronary arteries, respectively [2]. According to the 2021 ACC/AHA/SCAI Guideline for Coronary Artery Revascularization, angiographic features contributing to the increasing complexity of CAD include: multivessel disease; left main or proximal left anterior descending artery lesion; chronic total occlusion and lesion length greater than 20 mm, next to others [3]. One of the treatment options for significant CAD are either percutaneous coronary intervention (PCI) or coronary bypass grafting (CABG), as both methods ensure the reperfusion, subsequent reoxygenation of the ischaemic area, next to pharmacological treatment. The procedure of revascularization shows a survival benefit over medical therapy alone: Both CABG and PCI procedures can improve the prognosis, provided that the indication is appropriate [4]. Especially patients with left main CAD, TVD and ischemic cardiomyopathy have shown a survival benefit with CABG over medical therapy [3]. PCI is a minimal-invasive procedure to re-open the blocked artery, introducing a drug-eluting stent through the radial or femoral arteries. In contrast, CABG is a surgical procedure commonly performed to treat severe CAD, creating new pathways to facilitate uninterrupted blood flow to the heart and to avoid ischaemia by bypassing blocked or narrowed coronary arteries. In CABG autologous vessels, either left internal mammary arteries (LIMA), radial arteries or saphenous veins are used to bypass one or more affected coronary vessels [3]. Moreover, CABG is traditionally performed using a cardiopulmonary bypass machine (on pump), while the newer procedures facilitate surgery without using cardiopulmonary bypass machine (off-pump). Both techniques remain controversial, especially in terms of post-surgical inflammation and mortality [5, 6]. Criteria to choose a revascularization procedure [3] include (a) consideration of disease complexity and comorbidities, (b) technical feasibility for treatment, and (c) an intense discussion of the local heart team (cardiologists and cardiac surgeons). Usually, for patients with complex CAD and a significant left main stenosis, CABG is recommended improving the survival rate [3]. Furthermore, patients with diabetes who have TVD should undergo surgical revascularization [3]. Moreover, when making treatment decisions for patients undergoing surgical revascularization for

CAD, it is important to factor in the assessment of a patient’s surgical risk [3]. This can be accomplished, for instance, by using tools such as the Euroscore or Society of Thoracic Surgeons Score.

1.1.B. Epidemiological Reports of CAD

CAD is one among the CVDs and is categorized into non-communicable diseases. According to the World Health Organization (WHO), CAD is a rising burden, as death due to non-communicable diseases are substantially increasing, while deaths related to infectious diseases, nutritional deficiencies, and maternal with perinatal conditions are slowly declining [8]. Actually, as per the WHO, CVDs are

ICD-10	Cause of death	Deceased ¹	% ²
I25	Chronic ischemic heart disease	74 485	21.9
I21	Acute myocardial infarction	45 181	13.3
I50	Heart failure	35 131	10.3
I11	Hypertensive heart disease	23 363	6.9
I48	Atrial fibrillation and atrial flutter	21 719	6.4
I63	Cerebral infarction	15 177	4.5
I69	Sequelae of cerebrovascular disease	12 584	3.7
I64	Stroke. not specified as haemorrhage or infarction	10 629	3.1
I35	Aortic valve stenosis	10 616	3.1
I10	Essential (primary) hypertension	10 432	3.1
1: Without stillbirths and without declarations of presumed death			
2: From all cardiovascular diseases			

Figure 1.1. Total mortality from CVD in 2021, German Federal Statistical Office [7]

projected to be the first leading cause of death globally associated with 17.8 million deaths annually in 2019 and CAD is projected to be the third leading cause of death worldwide [9, 10]. Noteworthy, as per the data provided by the German Federal Statistical Office (Statistisches Bundesamt), as shown in Figure 1.1, it was observed that in 2021, 21.9 % of the total deaths caused by CVD were a result of chronic ischaemic heart disease, while 13.3 % were attributed to AMI. Both these conditions are classified as cardiac diseases among CAD. Similarly, the recent data of the German Federal Statistical Office provided in 2023 [11] stated, that in the year 2021, approximately 33.4 thousand women and 41.1 thousand men succumbed to fatal outcomes due to chronic ischaemic heart disease, both as a leading cause of mortality. This reaffirms CAD’s status as the foremost contributor to mortality in Germany.

According to the German Heart Surgery Report for the year 2021, a total of 36,122 CABGs were conducted in Germany. Among these, 27,947 procedures were performed as standalone operations, without being combined with other heart surgeries [12]. When considering the isolated CABGs, 21,280 were on-pump and 6,667 were off-pump surgeries. In terms of gender distribution, it was reported that 23 % of the patients were female, while 77 % were male [13].

1.1.C. Risk Factors of CAD

In current society, there exists several reasons to develop CAD, where some of the main environmental factors include drastic changes in their lifestyles, such as uncontrolled diet in combination with lack of physical activity and excessive consumption of alcohol and nicotine that further links to the development of comorbidity among ageing society, as all these are considered to be the major risk factors for the development and progression of CAD. The risk factors of CAD can be distinguished into (a) modifiable risk factors and (b) non-modifiable risk factors [14]. Risk factors that can be controlled (modifiable) include, hypertension; dyslipidaemia; hyperhomocysteinaemia, nicotine consumption; diabetes mellitus; overweight or obesity; lack of physical activity; unhealthy diet and stress. The risk factors that cannot be controlled (non-modifiable) include, age, sex (with men at higher risk), family history with genetic disposition, and race.

As stated by Simon et al.[16], CAD is a multifactorial process that appears to be caused by the interaction of environmental risk factors with multiple predisposing genes and lifestyle of an individual. The family history in terms of genetic susceptibility impacts the manifestation of CAD, where poly-genetic effects involving more than 250 genes may play a role in CAD [16]. The molecular basis of CAD including high oxidative stress, low antioxidant status and increased DNA damage can indeed contribute to its progression [16]. Rising affluence, rapid modernization associated with sedentary and stressful lifestyle are suggested to be the additional risk factors for CAD [16].

Accordingly, a combination of interventions and the right action at right time are defined as targets for the prevention of cardiovascular disease by the German Association of Cardiology (Deutsche Gesellschaft Kardiologie, DGK), [15], in order to minimize and thereby, manage CAD progression (Figure 1.2).

Smoking	Seccession of tabaco consume of any kind
Diet	Low intake of saturated fats; high intake of wholemeal products, vegetables, fruits and fish
Physical activity	Min. 150 min/week moderate aerobic fitness training; 75 min of high-intensity aerobic fitness training, or combination
Body weight	BMI 20-25 kg/m ² , waist circumference: man < 94 cm, women < 80 cm
Arterial blood pressure	< 140/90 mmHg
Blood lipids	
• LDL (primary marker)	• Extreme high risk: < 1.8mmol/l high risk: < 2.6 mmol/l medium-low risk: < 3 mmol/l
• HDL	• > 1 mmol in men, > 1. 2mmol/l in woman
• TAG	• < 1.7 mmol/l
Diabetes mellitus	• HbA1c < 7%

Figure 1.2. Prevention of CAD:

Management of the risk factors according to German Association of Cardiology (DGK)[15]

1.1.D. Pathogenesis of CAD

Response to Injury Hypothesis

A commonly accepted model for the development of atherosclerosis is the response-to-injury-hypothesis, which was initially postulated by Ross in 1977 [17], where initial endothelial injury related dysfunction occurs that slowly develops into a chronic state of inflammation [18]. The endothelial injury leads to an inflammatory response in which lymphocytes, primarily monocytes, migrate to the area of injury and transform into macrophages that ingest lipids, particularly oxidized low density lipoprotein (LDL) [19]. The macrophages then become foam cells, which accumulate in the artery wall and form fatty streaks. Over time, the fatty streaks can progress to more advanced lesions, such as fibrous plaques and complex lesions. The response to injury hypothesis emphasizes the role of inflammation in the development of atherosclerosis and suggests that reducing inflammation may be an effective strategy for preventing or treating the disease.

1. **Initial Lesion:** The initial event in the atherogenesis is injury to the endothelium, the inner lining of the arteries. This injury can be caused by various factors, including some above described risk factors of atherosclerosis like nicotine consumption and elevated levels of LDL cholesterol, which act as chemical disturbing factors, as well, as physical trauma or turbulent blood flow.
2. **Inflammatory Phase:** Following endothelial cell injury, lipids, particularly cholesterol, start to accumulate in the arterial wall. These lipids become trapped in the inner layer of the artery called the intima, forming fatty deposits known as plaques. Leukocytes, primarily monocytes, migrate to the area of injury. This process is initiated as the blood monocytes start to roll on the dysfunctional endothelium and tether in a loose connection, e.g. via E-selectin [20]. In line with this, ox-LDL induces the expression of adhesion molecules (including intercellular adhesion molecule-1 (ICAM-1), vascular cell adhesion molecule-1 (VCAM-1), monocytes chemoattractant protein-1 (MCP-1) (chemokine ligand type 2 (CCL2)), and E-selectin) on activated endothelial cells, arresting the monocytes [21, 22, 23]. The process of monocyte extravasation is explained in section 1.2.A. In the sub-endothelial space, those recruited blood monocytes differentiate into macrophages via macrophage colony stimulating factor (M-CSF) [24]. Subsequently macrophages ingest oxidized (LDL) via scavenger receptors, forming foam cells [21]. Those scavenger receptors include CD36, which is a class B scavenger receptor that is expressed on macrophages and other cell types [25]. It has been shown to play a major role in the binding of oxi-

dized phospholipids, which are present in oxidized LDL and also in the membrane of apoptotic cells. The process of recognition and uptake of ox-LDL via scavenger receptors, activates the nuclear factor kappa B (NF- κ B) signalling pathway that in turn induces the production of pro-inflammatory cytokines such as interleukin-1 beta (IL-1 β) and TNF- α [20].

3. **Formation of fibrous plaques:** The accumulation of lipid-laden foam cells in the intimal layer of the artery leads to the formation of fatty streaks [26]. Here, recruited blood monocytes secrete cytokines (e.g. PDGF) and other growth factors, which in turn activate the proliferation and migration of smooth muscle cells, which alter their phenotype from contractile to secretory [18]. In this state, secretory smooth muscle cells secrete various molecules that escalate the production of extracellular matrix (collagen and proteoglycans) along with other inflammatory signal leading to a maturation of the plaque (fibroatheroma). Moreover, monocytes being antigen presenting cells link further recruitment of immune and adaptive immunity, where T-cells and B-cells infiltrate plaques. Chronic inflammation arises by those processes and local inflammation slowly turns into systemic inflammation [18, 27].
4. **Complex Lesion:** In advanced plaques, macrophages, foam cells and smooth muscle cells undergo apoptosis and necrosis, liberating extracellular lipids and debris into the intima and thus forming a necrotic core [18, 27]. As the disease progresses, smooth muscle cells in the arterial wall continue to proliferate and migrate to the intima. They contribute to the formation of a fibrous cap over the fibroatheroma [27]. As long as the necrotic core is enveloped by this fibrous cap, the atheroma remains in a stable state [18]. But the advanced plaque can become unstable and prone to rupture. In fact, monocytes also promote destabilization of the fibrous cap [21].
5. **Complications:** The clinical manifestations of atherosclerosis occur late in the disease process. The complications of atherosclerosis include stenosis and rupture of the plaque causing thrombus formation or downstream embolism, all of which lead to reduced blood flow to vital organs, causing ischaemia [21]. These complications can lead to various cardiovascular diseases, such as CAD, along with life-threatening events, such as AMI, stroke, and peripheral artery disease.

1.2. Immunological Aspects

The immune system consists of two parts, the innate and the adaptive immune system. While the innate system is known to be non-specific and considered to be the first line defence; the adaptive system is known to be specific for certain pathogen/antigens that usually arises after innate immunity. The innate system is mainly composed of the myeloid lineage, including monocytes, macrophages, dendritic cells, granulocytes, mast cells and natural killer cells. Adaptive immunity is composed of T-cells and B-cells, which produce antibodies. Once innate immune cells such as macrophages and dendritic cells have phagocytosed the pathogen, they present these antigens to the cells of the adaptive immune system, leading to a specific immune response. These activated cells tend to secrete cytokines, which further induces a cascade of pro-inflammatory events. Both the systems play a pivotal role in the onset and progression of atherosclerosis, where monocytes play key role in propagating the atherogenesis progression [20].

1.2.A. Blood Monocytes and Monocyte Subpopulations

The Mononuclear Phagocyte System (MPS) comprises blood circulating monocytes, monocyte-derived dendritic cells, macrophages and tissue-resident macrophages [20]. In the blood stream, about 3-8% of the leucocytes represent circulating monocytes [21]. The function of monocytes are diverse in nature, including immune defence, inflammation, pathogen and dead cell clearance, bridging adaptive immunity, serving as progenitor cells for inflammatory dendritic cells or macrophages and also tissue repair and regeneration during heart disease [28, 29]. In atherosclerosis, they promote leukocyte recruitment to the plaque area, thereby exaggerating inflammation via downstream signalling pathways, including NF- κ B [21]. Monocytes exhibit a high level of plasticity [28], as it is evident that monocytes are rapidly recruited to the tissue site, where they leave the blood stream to enter tissue and differentiate into tissue macrophages or dendritic cells during tissue damage or infection [30]. Of note, these leucocytes possess a unique program to leave the blood stream to the side of inflammation. This process is known as extravasation (targeted migration) and consists of four steps, as described in the textbook Janeway Immunology [31]: First, the Sialyl-Lewis^x unit on monocytes and macrophages interacts with P- and E-selectins, where the expressions are induced by TNF- α and lipopolysaccharides (LPS). These cells attach reversibly to the vessel wall and begin to roll along the endothelium. Second, a tighter attachment is facilitated through the interaction of integrin (e.g. LAF-1) and adhesion molecules, such as ICAM-1 and VCAM-1, where these expressions are

also triggered by $TNF-\alpha$. Monocytes also get arrested by interaction of Chemokine C-X3-C motif receptor 1 (CX_3CR_1)/chemokine C-X3-C motif ligand 1 (CX_3CL_1) and C-C chemokine receptor type 2 ($CCR2$)/ $CCL2$ axis [32]. Third and fourth, diapedesis and migration also known as leukotaxis of the leucocytes to the focus of inflammation is triggered by specific chemokines. After monocytes cross the endothelial surface (diapedesis), they differentiate into macrophages in the subendothelial space. These monocyte differentiated macrophages further ingest circulating oxidized LDL via scavenger receptors to form numerous foam cells (as described in section 1.1.D).

Monocyte Subsets	Identifying Markers	Migration Markers	Frequency	Function
M1: Classical	$CD14^{++} CD16^{-}$	$CCR2^{++}$ $CX_3CR_1^{-}$	80-90%	Proinflammatory Phagocytosis
M2: Intermediate	$CD14^{++} CD16^{+}$	$CCR2^{+}$ $CX_3CR_1^{+}$	2-11%	Proinflammatory
M3: Non-Classical	$CD14^{+} CD16^{++}$	$CCR2^{-}$ $CX_3CR_1^{++}$	2-8%	Proinflammatory or Anti-inflammatory: - Patrolling - Remodeling

Figure 1.3. Monocytes Subsets:

The subsets of human blood monocytes are identified by certain surface markers (CD14 and CD16). The typical migration markers, the frequency of distribution in the human blood and possible functions are displayed.

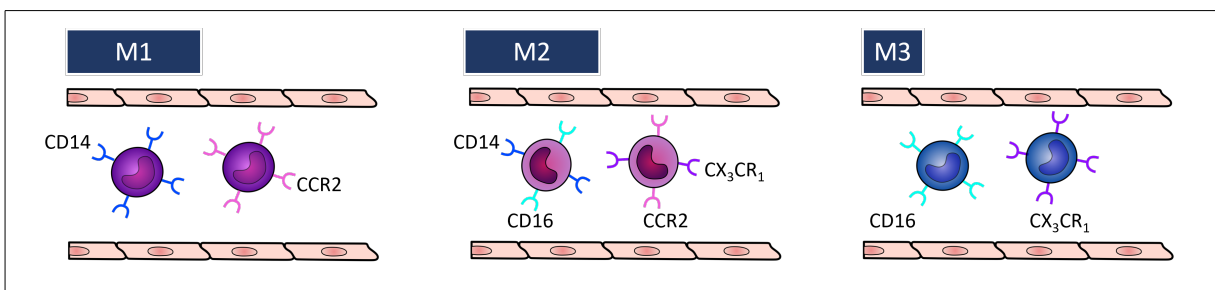


Figure 1.4. Classification of Monocyte Subsets

Classical monocytes (M1): $CD14^{++} CD16^{-} CCR2^{++} CX_3CR_1^{-}$;
Intermediate monocytes (M2): $CD14^{++} CD16^{+} CCR2^{+} CX_3CR_1^{+}$;
Non-classical monocytes (M3): $CD14^{+} CD16^{++} CCR2^{-} CX_3CR_1^{++}$

Human monocytes are distinguished into three subsets, as shown in Figure 1.3 and Figure 1.4, based on the expression of CD14 and CD16 markers in classical monocytes, intermediate monocytes and non-classical monocytes, reflecting defined classification in the mouse model [30]. This was acknowledged in 2010 by the Nomenclature Committee of the International Union of Immunologic Societies [33, 34]. However, the function concerning pro- and anti-inflammatory properties remains controversial [28]. Classical monocytes (M1) give rise to both intermediate monocytes (M2) and non-classical monocytes (M3) monocytes and under inflammatory conditions, where classical monocytes (M1) monocytes are released more rapidly from the bone marrow and go through subset differentiation in a shorter period compared to their differentiation during homeostasis [33]. The greatest fraction of monocyte subsets are **classical monocytes (M1)** CD14⁺⁺ CD16⁻ (equivalent Ly6C^{high} in mouse), which express a high level of CCR2. They invade the site of infection or inflammation via the CCR2/CCL2 axis and their proportion is described between 80-90% [28, 21] to above 92% [35] of circulating human monocytes. Of note, blood circulating M1 monocytes are also considered as inflammatory monocytes, as they enter the inflammatory site and thereby differentiate into macrophages or dendritic cells. At the recruited site, these inflammatory monocyte subset produce pro-inflammatory cytokines (IL-1 β , IL-6 and TNF- α) and reactive oxygen species (ROS), leading to further activation of the immune system [36, 28]. Furthermore, M1 monocytes are more prone to differentiate into inflammatory M1-macrophages, which produce TNF- α as well as IL-6 cytokines [30]. Contradicting this, certain research [30] outlines distinct functional properties that disguise the inflammatory role of human M1 monocytes, particularly in terms of cytokine production patterns. This paper indicate next to their significant phagocytic potential, a heightened peroxidase activity and notable IL-10 secretion in response to LPS, and limited TNF- α generation. Furthermore, analysis of gene expression profiling revealed that human M1 monocytes exhibit a preference for genes expression associated with angiogenesis, wound healing, and coagulation [30, 37]. Zawada et al. confirmed that M1 monocytes exhibit the highest potential for phagocytosis, as their expression of proteins involved in phagocytosis are the highest compared to the other monocyte subsets [38]. The most abundant monocyte subset in the plaque are M1 monocytes, but also M2 monocytes and M3 monocytes are reported to be present [20]. However, a high count of M1 monocytes are associated with poor myocardial recovery and worse outcome after AMI with reduced left ventricular ejection fraction [39]. **Intermediate monocytes (M2)** CD14⁺⁺CD16⁺ (equivalent Ly6C^{high} in mouse) are in the differentiation steps from classical toward non-classical, as the name suggests that they are at their intermediate stage [30, 37]. These M2 monocytes subsets also express CCR2 and exhibit phagocytic

functions to remove apoptotic cells, an important function in pathological conditions such as removal of apoptotic cells after myocardial infarction [35]. Both M1 monocytes and M2 monocytes may invade the site of inflammation via the CCR2/CCL2 axis [30]. They are known to secrete pro-inflammatory mediators such as ROS, TNF- α , IL-1 β , while others accredit IL-10 in response to LPS to M2 monocytes [35].

Non-classical monocytes (M3) CD14⁺CD16⁺⁺ (equivalent to Ly6C^{low} in mouse) represents the smallest proportion of monocytes and are a patrolling type of cell [35, 30], where they invade the tissue through CX₃CR₁/CX₃CL1 axis in a LAF-1/ICAM-1-dependent manner and either lack or have very minimal expression of CCR2 [30]. Possibly, M3 monocytes could exhibit both pro- and an anti-inflammatory functions [36]. On the one hand, according to Yang et al. [30], M3 monocytes have been identified as a subset with inflammatory characteristics in the context of human immune responses. There is an indication that CD16⁺ monocytes show a correlation with atherosclerosis and CAD in patients, signifying an inflammatory phenotype [30]. In fact, there exists a positive correlation between circulating M2 and M3 monocyte levels and the levels of atherogenic lipids and plaque vulnerability [30, 40]. Increased quantities of these monocytes have been linked to various inflammatory diseases, including rheumatoid arthritis, CAD, atherosclerosis, hemophagocytic syndrome, and Crohn's disease [30, 40]. In line, a study published in the European Heart Journal found a significant association between CD16⁺ monocytes and both obesity and subclinical atherosclerosis in low-risk individuals [41]. Moreover, this specific subset is reported to release IL-1 β and TNF- α [30, 42]. Interestingly, they trigger the recruitment of activated neutrophils that damage the endothelium [36]. These findings imply that monocyte subsets display inflammatory properties and could serve as valuable biomarkers for inflammatory conditions, including cardiovascular diseases. On the other hand, some reports propose, that M3 monocytes express anti-inflammatory potential and patrol the endothelium, capable to remove debris from the vasculature (reparative monocytes), thus contributing to both wound healing and the resolution of inflammation in the endothelium [28, 35, 43]. In contrast to M1 monocytes, murine M3 monocytes are more prone to differentiate into alternative M2-macrophages, which are involved in secreting anti-inflammatory cytokines and thereby subsequently contributing to the tissue repair [30]. Apart, some studies have shown that they also possess the tendency to remove lipids from the blood in atherosclerotic disease (cholesterol transporter in hypercholesterolemia) [44, 35].

1.2.B. Monocyte Migration Markers

The key function of migration markers is monocyte migration to the site of inflammation or infection that includes the process of chemotaxis and invasion. This part of the doctoral thesis outlines the migration markers that were investigated. Additionally, the information provided about these migration markers in section 1.2.A in relation to distinct functions and connections with CAD, atherosclerosis, and other chronic inflammatory diseases should be taken into considerations.

- **CD14** is a membrane bound glycoprotein, which serves as a co-receptor for LPS and is mainly expressed on monocytes and macrophages. It is involved in opsonization of pathogens/foreign particles via toll-like receptor 4 (TLR4)-LPS: TLR4 is a transmembrane protein, which belongs to the pattern recognition receptor (PRR) family and is activated by LPS of gram-negative bacteria, where its CD14-dependent activation leads to endocytosis of TLR4, which in turn activates one of two unique intracellular signalling pathways, MyD88-dependent and MyD88-independent [45]. Both regulate the expression of pro-inflammatory cytokines, such as NF- κ B, TNF- α , IL-1 β and IL-6 [45]. It has been reported that TLR4 can also be activated by endogenous compounds called damage-associated molecular patterns (DAMPs) [45]. A study published in the Journal of the American Heart Association found that soluble CD14 (sCD14) may be a race-specific risk marker, as higher levels of sCD14 were associated with an increased risk of incident CAD, stroke, and heart failure [46].
- **CD16** is a transmembrane glycoprotein belonging to the immunoglobulin superfamily and is also known as Fc γ III. It is mainly found on monocytes, macrophages and natural killer cells, mast cells and neutrophils [47]. CD16 plays a crucial role in antibody-dependent cellular cytotoxicity (ADCC) by activating natural killer cells to lyse IgG-labelled target cells [48]. Here, CD16 binds to the Fc portion of IgG immunoglobulin on the surface of target cells. This interaction activates the natural killer cell's lytic mechanism and induces the production and release of cytotoxic granules by the activated cells to lyse the IgG-labelled target cells [48]. These granules subsequently initiate apoptosis in the targeted cell [48].
- **C-C chemokine receptor type 2:** The chemokine MCP-1, also known as CCL2, is a chemoattractant that is involved in the chemotaxis of monocytes to the inflammatory site [35, 49]. It exerts multiple effects on a variety of cells, including monocytes, macrophages, dendritic cells, and endothelial cells and is involved in a diverse range of chronic and acute diseases [50]. Both M1 monocytes and M2 mono-

cytes may invade the site of inflammation via the CCR2/CCL2 axis [30], whereas M3 monocytes are CCR2⁻ subsets [34]. In atherosclerosis, oxidized LDL deposition at plaque region activates the endothelial cells and stimulates expression of CCL2 and smooth muscle cells [32], thereby recruiting CCR2 expressing blood monocytes to the site. Here, NF- κ B is involved in the expression of CCL2 [51]. Interestingly, it has been reported that CCR2 depletion diminishes diet-induced atherosclerosis [32].

- **Chemokine C-X3-C motif receptor 1:** Fractalkine CX₃CL₁ is a transmembrane protein that belongs to the CX₃C chemokine subfamily. It is known to be widely expressed by non-immune and immune human cells, such as monocytes and T-cells [49, 52]. It has been shown that the murine M3 monocytes are recruited into normal tissue by interaction of complementary pair CX₃CR₁/chemokine ligand type 3 (CCL3) via a VCAM-1-dependent manner to become tissue resident macrophages [30]. Likewise, human M3 monocytes also depend on CX₃CL₁ for migration and recruitment at endothelial cell surfaces [21]. During inflammatory processes, there is a significant increase in the expression of CX₃CL₁ in both human arterial and venous endothelial cells [49]. In accordance with research findings, the levels of circulating CX₃CR₁⁺ M2 monocytes are significantly heightened in individuals experiencing AMI, exhibiting a direct association with the increase of cardiac-specific and acute phase indicators [53].
- **C-C chemokine receptor type 5** is a chemokine receptor mainly expressed on lymphocytes in a steady state and have an important role in inflammatory diseases, but is also found on neutrophils and inflammatory monocytes in different inflammatory conditions [54]. C-C chemokine receptor type 5 (CCR5) binds to several ligands, including CCL3, chemokine ligand type 4 (CCL4) and chemokine ligand type 5 (CCL5), a chemotactic cytokine that is also known as RANTES [48]. Both M1 and M2 monocytes are tethered and invade tissue during inflammation not only via the CCR2/CCL2 axis but also through the CCR5/CCL5 axis [30]. In fact, CCR5 is expressed on murine M1 monocytes (Ly6C^{high}) during sepsis, exerting migration of these cells to the infectious zone [54]. Furthermore, it is a well-known co-receptor during HIV (Human Immunodeficiency Virus) infection, where HIV engages CCR5 to enter into macrophages [48]. Humans with a mutation in the allele encoding CCR5 gene results in a non-functioning variant and are less prone to the infectious disease [31]. Nevertheless, the outcome of CCR5 depletion in several mouse studies were controversial. While some studies show protection against diet

induced atherosclerosis in CCR5 knock out mice with more stable plaque phenotype and reduced mononuclear cell infiltration [55], other studies suggest that CCR5 depletion in mice did not affect the mean atherosclerotic lesion area [56].

- **C-C chemokine receptor type 1 (CCR1):** CCR1 can bind to CCL3, which is present in arterial plaque [55], CCL5 (RANTES), chemokine ligand type 7 (CCL7) and chemokine ligand type (CCL23) [48]. CCR1 is expressed on various cell types implicated in atherosclerosis, such as monocytes or macrophages and T-lymphocytes. These cells mediate arrest and transendothelial diapedesis via the RANTES axis [55]. Furthermore, Shi et al. [57], has stated that CCR1 mediates shear-resistant arrest of monocytes using *in-vitro* transmigration assays. Interestingly, analogous to the CCR2/CCL2 axis, the chemokine CCL3 produced at osteoarthritic knees attracted the circulating classical monocytes to the inflamed synovium, which is mediated by CCR1 [58].

1.2.C. Selenium

Selenium is a micronutrient that is necessary for the regulatory and metabolic function of a human body [59]. Sources of vegetarian food that are rich in selenium are cabbage, onions, cereals, and Brazil nuts [59]. Of note, the concentration of selenium highly depends on the soil and water, where the vegetables are being cultivated. Since Europe has a fairly low natural selenium concentration, the intake of selenium rich foods are compensated with animal products, such as beef liver, poultry, shellfish, tuna fish and eggs [59]. The German Nutrition Society (Deutsche Gesellschaft für Ernährung, DGE), [60], recommends a daily intake of 60 μg selenium for female and 70 μg selenium for male adults. While the normal range for plasma selenium is about 60–150 $\mu\text{g}/\text{l}$ [61], an appropriate amount around 80 to 90 $\mu\text{g}/\text{l}$ of selenium is sufficient for the synthesis and activation of selenoproteins (SeP) [62]. However, acute or chronic ingestion of selenium in higher concentration could be detrimental in causing adverse effects like nausea, nail discolouration, hair loss and bad breath [63], especially when exceeding 200 $\mu\text{g}/\text{l}$ [62]. The serum concentration for selenium deficiency is less than 40 $\mu\text{g}/\text{mL}$ [61]. In fact, the first reported disease associated with selenium deficiency is Keshan disease, which spontaneously leads to endemic and highly lethal cardiomyopathy. This disease particularly exists in selenium deficient areas of China and West Africa and is therefore treated with selenium supplementation, both prophylactically and therapeutically [64].

Selenium is present as selenoproteins in the form of selenocysteine (Secys) and the key functions are to regulate the inflammatory process and to reduce oxidative stress [62]. At present, 25 selenoproteins have been identified in humans, out of which 13 selenoproteins have well-known functions, including glutathione peroxidases (GPX)1-4 and 6, thioredoxin reductases (TrxR1-3), iodothyronine deiodinases (DIO1-3) and selenophosphate synthetase 2 (SPS2) [65]. The family of selenium dependent GPXs have several functions, including mitigation of oxidative damage caused by hydrogen peroxide (H_2O_2), damaging lipids and phospholipid hydroperoxides by reducing those compounds to harmless products such as water and alcohols [65]. Further, it has been shown that the selenium-dependent thioredoxin reductase system contributes in ascorbate (vitamin C) regeneration [64].

Compelling evidence has shown the anti-inflammatory role of selenium in regulating NF- κ B activity, a transcription factor that is activated by ROS, pro-inflammatory cytokines like TNF- α [62] as well as in regulating endotoxin LPS/CD14/TLR4 induced MAP Kinase signalling pathway [66, 62]. Of note, in steady state conditions, the activity of NF- κ B is tightly regulated by its inhibitor I κ -B α (NF-kappa-B inhibitor alpha). It is a

master regulator of the NF- κ B proteins, and thereby retains inactive NF- κ B in the cytosol of unstimulated cells [67]. When these cells perceive activation signals (proinflammatory cytokines, ROS), the kinase that phosphorylates I κ -B α , namely, the I κ -B kinase, further liberates NF- κ B proteins to translocate into the nucleus causing transcriptional expression of pro-inflammatory cytokine (e.g. TNF- α), which indeed accelerates the process of inflammation [62]. It has already been reported that selenium mediates an anti-inflammatory action on NF- κ B cascade, where selenium prevents the binding of NF- κ B to the promoter region of pro-inflammatory genes inside the nucleus [62]. It thereby suppresses the production of TNF- α and IL-6 as well as adhesion molecules like VCAM-1, E-selectin, ICAM-1, and chemokine MCP-1 (CCL2) and further aids in reducing monocyte recruitment [62, 68, 69, 66]. Since atherosclerosis is also caused by the peroxidation of endothelial cell membrane lipids, deficit in selenium causes reduced activity of antioxidant enzymes, such as GPX, and thereby resulting in the aggravation of atherosclerosis [70]. Interestingly, in a prospective study involving 636 patients who had previously experienced cardiovascular diseases, it was observed that individuals exhibiting reduced erythrocyte GPX1 activities had a heightened likelihood of recurrent cardiovascular events [65]. This finding suggests that the initial erythrocyte GPX1 activity level could serve as a robust predictor for the occurrence of future cardiovascular events [65]. Hence, the qualities of decreased ROS production, decreased adhesion molecule expression on monocytes and reduced pro-inflammatory cytokine production implies potent anti-inflammatory functions of selenium in inflammatory diseases, including atherosclerosis.

Further, selenium supplementation exhibited a better outcome in treating acute inflammatory diseases, like sepsis and systemic inflammatory response syndrome (SIRS), by reducing the mortality rate [71, 72]. Noteworthy, the SUSTAIN-CSXTM study [73], a prospective, randomized, double-blind, multicentre controlled multinational trial investigated the effect of perioperative high-dose sodium selenite supplementation on the persistence of organ dysfunction in approximately 1,400 high-risk cardiac surgical patients. It showed, that cardiac surgery using cardiopulmonary bypass resulted in a profound intraoperative decrease of antioxidant trace elements in the whole blood levels. According to Stoppe et al., low selenium concentrations at the end of surgery were independent predictors for the postoperative development of multiorgan failure. Therefore, these above listed beneficial functionalities of selenium in attenuating anti-oxidative and anti-inflammatory properties might be regarded as a therapeutic option for CAD.

1.2.D. IL-6-STAT-3-Pathway

The Janus kinase (JAK)-signal transducer and activator of transcription (STAT) pathway occurs intracellularly and plays essential roles in orchestrating the immune system, especially via cytokine receptors to modulate T-cell polarization [31]. Here, the protein STAT is a cytoplasmic transcription factor that is translocated into the nucleus upon activation by cytokines and growth factors [31] and is involved in many cellular processes like development, proliferation, or differentiation and homeostasis of numerous cell types [23]. STAT-3 was first described as an oncogene, as it triggers cell proliferation, cell differentiation, cell survival, angiogenesis, and immunity [23]. STAT-3 activity is indicated by the proportion of phosphorylated signal transducer and activator of transcription type 3 (pSTAT-3), representing the active state, in relation to total STAT-3 [70].

However, recent studies demonstrated the involvement of STAT-3 in the genesis of atherosclerosis. There are four isotopes of STAT-3 known: STAT-3 α , β , γ and δ , partially with contrary functions. While STAT-3 α seems to be activated by IL-6 to develop pro-inflammatory immune responses, STAT-3 β inhibits the production of cytokines and even promotes expression of some anti-inflammatory genes [23].

The proinflammatory cytokine, IL-6 plays a critical role in innate immune response, by binding to its receptor, which is a complex build by a IL-6 specific chain gp80 (CD126) and gp130 (CD130) [74, 23]. It further activates JAK-2 and STAT-3 by dimerization and phosphorylation. Subsequently, pSTAT-3 translocates into the nucleus and promotes transcriptional expression of its target genes by binding to their promotor regions, including acute phase proteins and IL-6 [74, 75]. Here, the ability of pSTAT-3 to promote IL-6 synthesis leads to an autocrine feedback loop to propagate inflammatory reactions. Further, these produced IL-6 cytokine up-regulates MCP-1 (CCL2), ICAM-1 and the VCAM-1 [23], that are required for monocyte migration and recruitment to the atherosclerotic zone, as described in section 1.1.D. There have been several studies performed to investigate the anti-inflammatory effect of STAT-3 inhibition. One has indicated that the JAK2 inhibitor, ruxolitinib, can reduce the development of aortic atherosclerotic plaques [76]. Similar findings are seen in research demonstrating, how metformin, an inhibitor of STAT-3 activity, effectively suppresses inflammation and the differentiation of monocytes into macrophages [77].

Therefore, the inhibition of STAT-3 signalling pathway with selenium is in the focus of this study as a potential treatment strategy for underlying atherosclerosis in CAD.

1.3. Chronic Inflammation and the Combined Impact of Monocytes and IL-6-STAT-3-Pathway in CAD

In Figure 1.5, the illustration presents a comprehensive depiction of chronic inflammation in atherosclerotic lesions. Here, the chronic inflammation serves as the principal driving force behind the progression of atherosclerosis. Monocytes, characterized as a heterogeneous group of cells, are categorized into three distinct subgroups: classical, intermediate, and non-classical monocytes (M1, M2, M3). While M1 and M2 monocytes participate in trans-endothelial chemotaxis by binding through CCR2/CCL2 to infiltrate sites of inflammation, M3 monocytes assume a patrolling role, invading tissues via CX₃CR₁/CX₃CL₁ receptors. Upon encountering tissue damage or infection, monocytes are recruited to the affected area, where they have the ability to differentiate into tissue macrophages or dendritic cells. Particularly noteworthy is the fact that M1 and M2 monocytes differentiate into inflammatory M1-macrophages, known for their lipid uptake, especially in states of hyperlipidemia, ultimately transforming into foam cells. M3 monocytes demonstrate a greater propensity to differentiate into alternative M2 macrophages. In a complex sequence of events, these foam cells progress into advanced plaques with an increased risk of complications, such as stenosis, acute obstruction, ulceration/rupture with haemorrhage, local thrombosis, downstream embolism, and aneurysms, all of which can lead to life-threatening events, including myocardial infarctions. Furthermore, monocytes and macrophages are capable of producing pro-inflammatory cytokines such as TNF- α and IL-6, which, in turn, activate the JAK-STAT3 pathway causing endothelial dysfunction and inflammation, including heightened expression of CCL2 (MCP-1) and adhesion molecules (ICAM and VCAM) next to magnified IL-6 production. It is important to note that M1 and M2 monocytes are the primary sources of these pro-inflammatory cytokines. This sets in motion a vicious cycle, attracting even more monocytes into the inflammatory cascade.

1.3. CHRONIC INFLAMMATION AND THE COMBINED IMPACT OF MONOCYTES AND IL-6-STAT-3-PATHWAY IN CAD

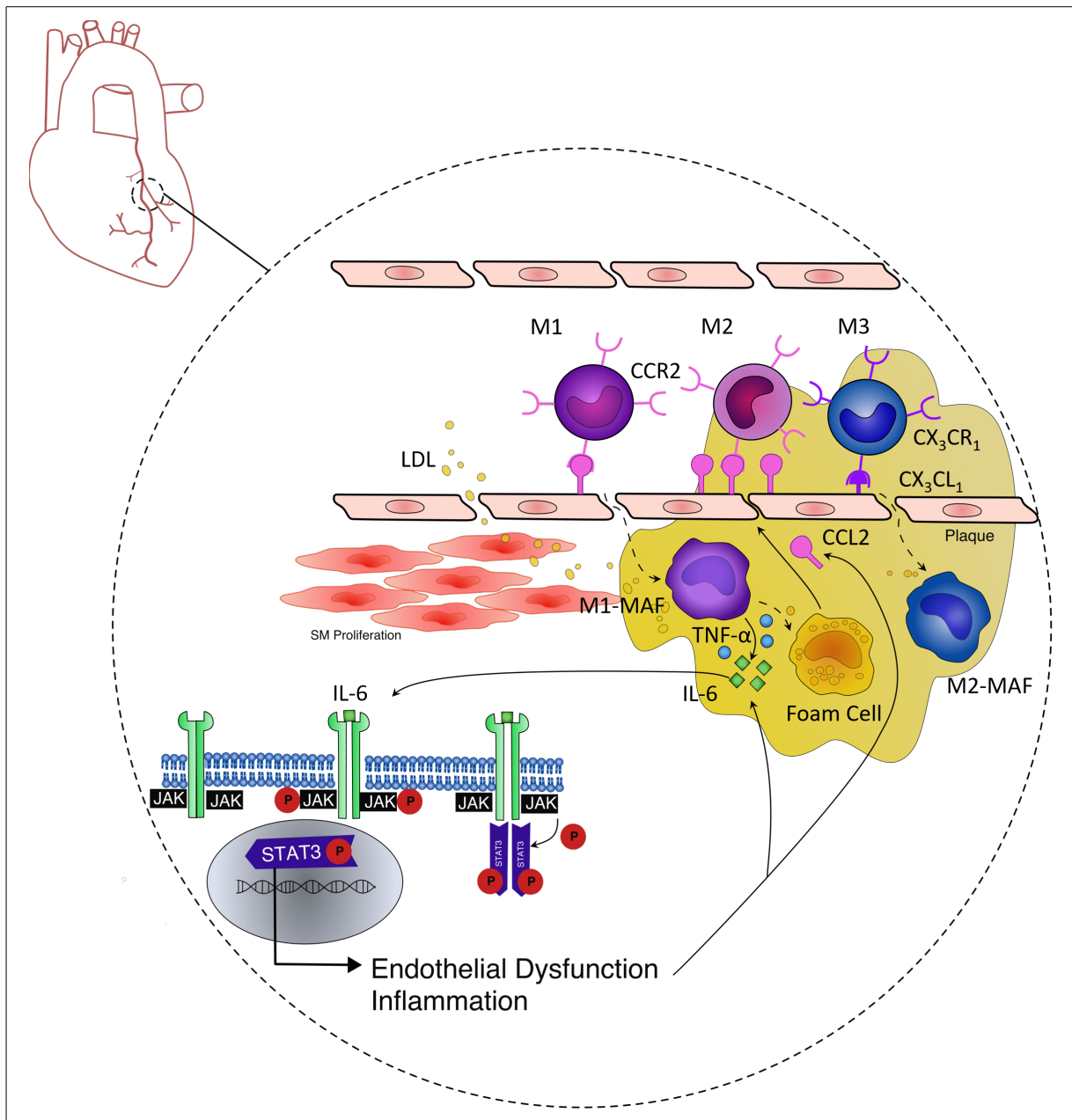


Figure 1.5. Chronic inflammation in atherosclerotic lesions

Chronic inflammation is the main driving force for the progression of atherosclerosis. Monocytes can be divided into three subgroups: classical, intermediate and non-classical monocytes (M1, M2, M3). While M1 and M2 monocytes bind via CCR2/CCL2 to invade the side of inflammation (trans-endothelial chemotaxis), M3 are a patrolling type of cells and invade the tissue via CX₃CR₁/CX₃CL₁. Upon tissue damage or infection, monocytes are rapidly recruited to the tissue, where they can differentiate into tissue macrophages. Especially M1 and M2 monocytes differentiate to inflammatory M1 macrophages, which uptake lipids in the state of hyperlipidaemia, and turn into foam cells. M3 monocytes are more likely to differentiate into alternatives M2 macrophages. Next to others, monocytes and macrophages produce pro-inflammatory cytokines, such as TNF- α and IL-6, which in turn activate the JAK-STAT3-pathway leading to endothelial dysfunction and inflammation, e.g. magnifying CCL2 (MCP-1) expression. Here, M1 and M2 monocytes are the main producer of pro inflammatory cytokines. A vicious cycle occurs, as even more monocytes are attracted.

1.4. Aims and Objectives

This doctoral thesis focuses on three major aims as follows, which are schematically shown in Figure 1.6:

1. The inflammatory status of CAD patients was determined by investigating the frequencies of blood monocyte phenotypes as well as the expression pattern of monocyte migration markers, such as CCR2, CX₃CR₁, CCR5 and CCR1. The results were compared with normal controls.
2. Furthermore, the inflammatory status of CAD patients was determined by quantifying the plasma levels of pro-inflammatory cytokines, such as IL-6 and TNF- α . The results were compared with normal controls.
3. Next, the *in-vitro* therapeutic effects of selenium on mononuclear cells obtained from CAD patients were investigated, according to the three following objectives:
 - a) Selenium impact was evaluated on the frequencies of monocyte subsets and the expression pattern of monocyte migration markers.
 - b) Selenium impact was evaluated on phosphorylation status of STAT-3.
 - c) Selenium impact was evaluated on the cell supernatant concentration of IL-6 and TNF- α cytokines.

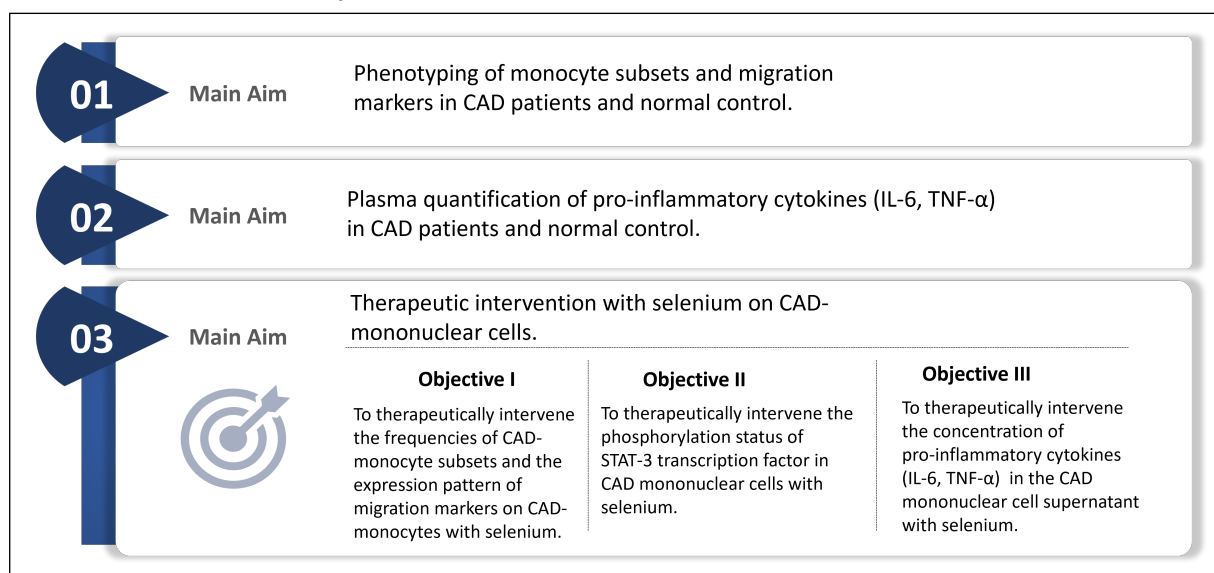


Figure 1.6. Aims and objectives of the doctoral thesis

2. Materials

2.1. Biological Materials and Ethical Approval

To study various aspects of monocytes, a total of 23 CAD patients (15 male, 8 female, median age: 70 years) were recruited postoperative in the time from November 2019 through May 2020 at the Department of Cardiothoracic Surgery at Otto-von-Guericke University Hospital Magdeburg, under the approval of the Institutional Ethics Committee of the medical faculty of Otto-von-Guericke University in Magdeburg (study approval number: 18/19). The obtained peripheral blood mononuclear cells (PBMC) were used in various experiments, including cell culture (section 3.5.B), phenotyping of monocyte subsets (section 3.3) and selenium intervention on the frequencies of monocyte subsets and expression of monocyte migration markers and phosphorylation of STAT-3 transcription factor (section 3.5.C, section 3.5.D). The plasma obtained from the blood samples were used to determine the concentration of proinflammatory cytokines, namely IL-6 and TNF- α (section 3.4, section 3.5.E). Moreover, human leukaemia monocytic cell lines (THP-1) (ACC No.16) (German Collection of Microorganisms and Cell Cultures (DSMZ), Braunschweig, Germany) were used to analyze the anti-inflammatory properties of selenium (section 3.5.A).

2.2. Materials Corresponding to the Methods

2.2.A. FACS

- Cellular Marker Antibodies for FACS

Description	Fluorochrome Laser	Isotype	Cat. No	Company
CD14	FITC	Mouse IgG1 κ	325603	Bio Legend
CD16	APC	Mouse IgG1 κ	302011	Bio Legend
CCR2	PE	Mouse IgG1 κ	357205	Bio Legend
CX ₃ CR ₁	BV421	Rat IgG2b κ	341619	Bio Legend
CCR5	BV711	Rat IgG2b κ	359121	Bio Legend
CCR1	Pe-Cy7	Mouse IgG1 κ	362912	Bio Legend
Zombie Aqua TM	BV510	-	423101	Bio Legend

2.2. MATERIALS CORRESPONDING TO THE METHODS

- Isotype Control Antibodies for FACS

Description	Fluorochrome Laser	Isotope	Cat. No	Company
Mouse IgG1	APC	κ Isotype control	400121	Bio Legend
Mouse IgG1	PE	κ Isotype control	400213	Bio Legend
Rat IgG2b	BV421	κ Isotype control	400639	Bio Legend
Rat IgG2b	BV711	κ Isotype control	400653	Bio Legend
Mouse IgG1	Pe-Cy7	κ Isotype control	400125	Bio Legend

- Chemicals, Media, Buffers and Solutions for FACS

Description	Cat. No.	Company
Human TruStain FcX TM	422302	Bio Legend
BD Comp Beads Anti Rat Ig κ	552845	BD Biosciences
BD Comp Beads Anti Mouse Ig κ	552843	BD Biosciences
PFA 4 %	11762.00500	MORPHISTO
Trypan Blue	4360496	Sigma Aldrich
RBC Lysis Buffer (10X)	420301	Bio Legend

Compensation Beads Preparation: In 1ml of PBS (phosphate buffered saline), 4 drops of positive control beads and 4 drops of negative control beads were added, vortexed and stored in +4 °C, before usage.

2.2.B. ELISA

- Antibodies, Chemicals, Media, Buffers and Solutions for ELISA

Description	Cat. No	Company
ELISA Max™ Deluxe Set Human IL-6	430504	Bio Legend
ELISA Max™ Deluxe Set Human TNF- α	430204	Bio Legend

- Materials provided in Human IL-6 and Human TNF- α kits:
 - Human IL-6 ELISA MAX™ Capture Antibody (200X)
 - Human IL-6 ELISA MAX™ Detection Antibody (200X)
 - Human IL-6 Standard
 - Human TNF- α ELISA MAX™ Capture Antibody (200X)
 - Human TNF- α ELISA MAX™ Detection Antibody (200X)
 - Human TNF- α Standard
 - Avidin-HRP (1000X)
 - Substrate Solution A
 - Substrate Solution B
 - Coating Buffer A (5X)
 - Assay Diluent A (5X)
- Preparation of 1X Reagent for 1 Plate

Solutions	Diluted to 1X working concentration
2.4 mL of Coating Buffer A (5X)	9.6 mL of Deionised Water
60 L of Capture Antibody (200X)	12 mL of 1X Coating Buffer A
12 mL of Assay Diluent A (5X)	48 mL of PBS
60 L of Detection Antibody (200X)	12 mL of 1X Assay Diluent A
12 L of Avidin-HRP (1,000X)	12 mL of 1X Assay Diluent A

2.2.C. RT-PCR

- Primers for real-time polymerase chain reaction (RT-PCR):

The sequences of the primers used were (i) TNF- α (forward: CAGCCTCTTCTCCTTCCTGAT and reverse: GCCAGAGGGCTGATTAGAGA, custom-made by Eurofins), (ii) IL-1 β (forward: TACCTGTCCTGCGTGTTGAA and reverse: TCTTTGGGTAATTTTGGGATCT, Maxima first strand cDNA synthesis kit with dsDNase, Cat.No K1671, Thermo Fischer Scientific) and (iii) β 2-microglobulin (B2M) (forward: TTCTGGCCTGGAGGCTATC and reverse: TCAGGAAATTTGACTTTCCATTC, custom-made by Eurofins).

- Chemicals, Media and Buffers for RT-PCR:

Description	Cat. No	Company
Maxima First Strand cDNA Synthesis Kit for RT-PCR, with dsDNase	K1671	Thermo Fischer Scientific
PowerUp TM SYBR TM Green Master Mix 5x1ml	A25780	Thermo Fischer Scientific
Thermo Scientifi TM Wasser, nukleasefrei	11893933	Thermo Fischer Scientific
PCR Master Mix (2X)	K0171	Thermo Fischer Scientific
RNeasy Micro Kit (50)	74004	Qiagen
DNase	79254	Qiagen
LPA (Ambion TM Linear Acrylamide)	AM9520	Invitrogen
7.5M Ammoniumacetat (NH ₄ OAc)	A2706	Sigma-Aldrich
Ethanol	A3678	AppliChem
DEPC water	46-2224	Invitrogen

2.2.D. Cell Culture and Selenium Treatment

Description	Cat. No	Company
Sodium selenite (stock conc. 3 mM)	S5261	Sigma Aldrich
Recombinant human IL-6 (rIL-6)	R200-06	Peprotech
LPS (lipopolysaccharide)	L2654	Sigma Aldrich
TrypLE™ Gibco	12604021	Thermo Fisher Scientific
RPMI (Roswell Park Memorial Institute) 1640 Gibco	21875034	Gibco
FBS superior stabil®	FBS.S0615	Bio & Sell
L-glutamine (200 mM)	25030081	Thermo Fischer Scientific
Roti® -CELL Pyruvate solution (Sodium- Pyruvate)	9182.1	Roth
RLT-buffer	79216	Qiagen

- **RPMI for cell culture:** 500 ml RPMI + 10 % FBS (50 ml) + 1 % PIS (5 ml) + 1 % Glutamine (5 ml) + 1 % Sodium Pyruvate (5 ml)

2.2.E. WB

- Antibodies for Western Blot (WB)

Description	Cat. No	Company
Phospho-STAT-3 (Tyr 705, D3A7) XP rabbit mAb *	9145	Cell Signalling Technology
STAT (D3Z2G) rabbit mAb *	12640	Cell Signalling Technology
α -Tubulin (11H10) rabbit mAb *	2125	Cell Signalling Technology
anti rabbit IgG, HRP-linked Antibody **	9145	Cell Signalling Technology

* : Primary antibody ** : Secondary antibody

2.2. MATERIALS CORRESPONDING TO THE METHODS

- Chemicals, Media, Buffers and Solutions for WB

Description	Cat. No	Company
10 % SDS (sodium dodecyl sulfate)	1610302	Bio Rad
Acryl- /Bisacrylamid 30 % (37.5:1)	10688.01	Serva
Ammonium persulphate (APS)	161-0700	Bio Rad
Aprotinin	A2131	PanReac AppliChem
β -2- Mercaptoethanol	M6250	Sigma Aldrich
Bromphenolblau	114391-25 g	Sigma Aldrich
Chymostatin	A2144,0010	PanReac AppliChem
Dimethylsulfoxid	D8418	Sigma Aldrich
EDTA (ethylenediaminetetra- acetic acid)	3690	Sigma Aldrich
Ethanol	22065000	Chemo Solute
Glycerin	7530.1	Roth
Glycine	A1067,5000	PanReac AppliChem
Kaliumchlorid (KCl)	6781.3	Roth
Leupeptin	A2183 ,0010	PanReac AppliChem
Milk powder	T145.2	Roth
Methanol 99.9 %	0082	Roth
Natriumazid (sodium azide)	S2002-25 g	Sigma Aldrich
Natriumchlorid (NaCl)	9265.2	Roth
PageRuler™ Prestained Protein Ladder	26616	Thermo Fisher Scientific
Pepstatin A	A2205,0010	PanReac AppliChem
Phenyl Red Dye	P3532	Sigma Aldrich
Phenylmethylylsulfonylfluorid (PMSF)	P7626	Sigma Aldrich
Pierce™ ECL Western, Blot- ting Substrate	32106	Thermo Fisher Scientific
Pierce™ ECL Western, Super- Signal™ West Femto	34094	Thermo Fisher Scientific
Pierce™ BCA Protein Assay Kit	23225	Thermo Fisher Scientific
Ponceau S Dye	A2935	PanReac AppliChem
Sodium orthovanadate (Na ₃ VO ₄)	S6508	Sigma Aldrich
Tetramethylethylenediamine (TEMED)	161-0801	Bio Rad

Continued on next page

Table 2.1 – continued from previous page

Description	Cat. No	Company
Tris Base	161-0719	Bio Rad
Trizma Base	T1503	Sigma Aldrich
Tween 20	A4974,0250	Appllichem

- Preparation of WB Solutions

- **10x TBS (tris-buffered saline) buffer:** The 10x TBS buffer is used for the washing steps and as solvent for other solutions. For its preparation, 80 g Sodium Chloride (NaCl, M 58.44 g/mol), 2 g Potassium Chloride (KCl, M 74.56 g/mol), 30 g TRIS and 1 L H₂O were blended and adjusted at pH 7.4. It was stored at room temperature. For blotting purpose, 1x TBS was prepared by mixing 100 ml of 10x TBS in 900 ml ddH₂O (double distilled water).
- **1x TBS-Tween:** The 10x TBS buffer was diluted to 1:10 with ddH₂O and 0.1 % Tween-20 (1 ml Tween-20 + 1 L 1x TBS Buffer) was added. It was then mixed with a magnetic stirrer for 30 min.
- **10x Running Buffer:** To prepare the 10x running buffer, 144 g glycine (192 mM), 30 g TRIS Base (25 mM), 10 g SDS (sodium dodecyl sulfate) and 1 L of ddH₂O were mixed. 1x Running Buffer is required for SDS Page in Western Blotting.
- **10x Transfer Buffer:** Here, 288 g glycine (192 mM), 60.4 g TRIS Base (25 mM) and 2 L ddH₂O were mixed. 1x transfer buffer is required for transfer steps and was prepared by mixing 100 ml 10x transfer buffer, 200 ml methanol and 600 ml ddH₂O.
- **TRIS Buffer 1.5 M:** TRIS buffer 1.5 M is required for the preparation of the 10 % running polyacrylamide gel. For this, 181.7 g TRIS Base, 4 g SDS were mixed in 1 L ddH₂O and adjusted at the pH 8.8.
- **TRIS Buffer 0.5 M** TRIS buffer 0.5 M is required for the preparation of the 10 % polyacrylamide stacking gel. For this, 30.3 g TRIS Base, 2 g SDS were mixed in 0.5 L ddH₂O and adjusted at the pH 6.8.
- **APS:** 1 g of ammoniumpersulfat was diluted in 10 ml dd H₂O. It is required for preparation of the 10 % polyacrylamide gel.
- **Reducing Sample Buffer:** The reducing sample buffer is required for preparation of the samples. To prepare, 50 ml glycerine (50 %), 10 g SDS (10 %), 25 ml β -2-mercaptoethanol (25 %), 5 ml TRIS (pH 6.8; 50 mM), 25 mg

bromophenol blue (0.0025 %) were used.

- **TPNE Lysis Buffer:** Since protein lysis is an essential step in preparing the biological samples for SDS Page, TPNE Lysis buffer is needed. For this 50 ml of 10x PBS (1x), 30 ml 5 M NaCl (300 mM), 1 ml 0.5 M EDTA (1 mM) and 50 ml 10 % Triton X100 (1 %) were mixed.
- **100x SPI (per 50 ml H₂O):** SPI (Sodium Phosphate Buffer with Iodide) is also used for protein lysis. For this, 5 mg aprotinin in 5 ml H₂O and 5 mg leupeptin in 5 ml H₂O and 5 mg pepstatin A were mixed in 5 ml DMSO (dimethyl sulfoxide) and 5 mg chymostatin. It was stored in aliquot portions at -20 °C.
- **Phenylmethylsulfonylfluorid (PMSF):** PMSF is also used for protein lysis. For this 0.87 g PMSF was mixed in 50 ml 100 % EtOH and stored in -20 °C.
- **5 % Milk TBST (tris-buffered saline with Tween20):** Here, 5 g milk powder was mixed with 100 ml TBST with a magnetic stirrer for 30 min. The milk is required for blocking and as medium for the secondary antibodies in Western Blotting.
- **5 % Milk TBSTA (tris-buffered saline with Tween20 and sodium azide):** Here, 5 g milk powder was mixed with 100 ml TBST and 0.01 % sodium azide (100 μ l of 10 % sodium azide in 100 ml TBST) with a magnetic stirrer for 30 min. The milk is required as a medium for the primary antibodies in Western Blotting.
- **Stripping Buffer:** To detect more than one protein on the same membrane, the protein must be stripped from the membrane in order to stain another protein. For this, the membrane must be incubated with 1.5 % sodium azide for 20 min (1.5 ml 10 % sodium azide was diluted in 8.5ml TBS).

2.3. General Lab Materials

2.3.A. General Chemicals, Media, Buffers and Solutions

Description	Cat. No	Company
Ficoll-Paque TM PLUS	17144002	Sigma Aldrich
PBS Gibco TM PBS-tablets	18912014	Thermo Fischer Scientific

- PBS

The PBS solution contains: sodium chloride (140 mmol/L), potassium chloride (2.7 mmol/L), sodium dihydrogen phosphate (7.2 mmol/L) as well as potassium hydrogen phosphate (1.5 mmol/L).

2.3.B. Consumables

Description	Cat. No	Company
24-well plate	662160	Cell Star
6-well plate: Nucleon Delta surface	140675	Thermo Fischer Scientific
96 well plate without Lid SH	162376	Thermo Fisher Scientific
Silver foil	-	-
Eppendorf tubes: Safe Lock tubes 0.5ml	diverse	-
Eppendorf tubes: Safe Lock tubes 1.5ml	diverse	-
Falcon [®] 5mL Round Bottom Polystyrene Test Tube	352052	Corning [®]
Falcon tubes 50 ml, Greiner Bio- One CELLSTAR [®]	10480623	Fisher Scientific
Ficoll tubes 15 ml, Greiner Bio- One CELLSTAR [®]	10384601	Fisher Scientific
Glass pipette	-	Schuett Biotec
BD Vacutainer [®] Plasmaanalyse	367378	BD
Vasco Nitril white, Nitril Untersuchungshandschuhe, M	9207929	B.Braun
M μ ltiFlex Tips Pipettenspitzen 1 - 200 μ l	Y419.1	Carl Roth GmbH
Bemis [®] Curwood Parafilm [®] M Labor-Verpackungsfolie	11693119	Fisher Scientific
Pasteur Pipettes	diverse	-
epT.I.P.S. Eppendorf Quality [™] , 0.1-10 μ l, 34 mm, dunkelgrau, farblose Spitzen,	0030073363	Fisher Scientific
epT.I.P.S. Eppendorf Quality [™] , 2-200 μ l, 53 mm, gelb, farblose Spitze	0030073460	Fisher Scientific
epT.I.P.S. Eppendorf Quality [™] , 50-1.000 μ l, 71 mm, blau, farblose Spitzen	0030073460	Fisher Scientific
Amersham [™] Hybond [™] 0.2 μ m PVDF	A24040268	GE Health Care Life Science
Stripette 10 ml	4488	Corstar [™]
zetBox – Labor- und Hygienetücher, weiß	16515-00	ZVG-Troisdorf

2.3.C. Laboratory Materials

Description	Cat. No	Company
Test tube rack	-	diverse
Glas bottles 100, 250, 1000 ml	-	Schott/ SIMAX
Hand counter	-	-
Cold protective gloves	-	-
Isolation box	-	-
Tweezers	-	-
Measuring cylinder 1000 ml	-	Hirschmann
Brand [®] Measuring cylinder 250 ml	12075322	Fisher Scientific
Counting chamber Marienfeld Superior	0640010	Neubauer
Spray flask	-	-
Stirring fish	-	PTFE Stirrers
Sample Loading Guide	1653146	Bio Rad
Mini-PROTEAN Comb, 10-well, 30 μ l	4560013	Bio-Rad
Gel Releasers	1653320	Bio-Rad
Pipettes	diverse	Eppendorf Research Plus
Pipetus	-	Hirschmann

2.3.D. Laboratory Devices and Software

- Laboratory Devices

Laboratory Devices	Company
Milli-Q [®] Reference Reinstwasser (Typ 1)	Merck
Vakuum Controller CVC 3000	Vacuubrand [®]
Autoclave	SHP Laboklav
Bench Herasafe KS	Thermo Fisher Scientific
Incubator 37°C - 5 % Co2	Panasonic Healthcare Co
Tumbler SU 1402	sunlab [®]
Freezer	-80°C and -10°C
Ice cube machine S-No: 105587	Ziegra
Miele Professional G 7835 CD	Miele
Microscope Scientific Evos XL core	Thermo Fisher Scientific
ECL ChemoStar	INTAS
Laboratory shaker KS 501 digital	IKA
ThermoCell MixingBlock	Bioer
Continued on next page	

Table 2.2 – continued from previous page

Laboratory Devices	Company
Laboratory fume hood	Wesemann
Water bath	GFL 1083
Mini Vortexer 120567	Heathrow Scientific
Hettrich Rotina 420 R	Hettrich
Pipetting Aid	Hirschmann
Mini Protean [®] Tetra Cell Kit	BIO rad
Mini Trans-Blot [®] Electrophoretic Transfer Cell Kit	BIO Rad
BD LSR Fortessa [™]	BD Sciences
Ista ChemoStar Imager	INTAS Science Imaging
Tecan Infinite [®] Spectrometer	Tecan
Applied Biosystems StepOnePlus System Real-time PCR system	Thermo Fisher Scientific

- Software

Software	Description	Developer
Excel	Table calculation	Microsoft
Word	Text editing	Microsoft
PowerPoint	Illustrations	Microsoft
Graph Pad Prism V8.0.1.	Illustrations	-
Tecan Megelan	Spectrometer Protein Assay	Tecan
Flow Jo V9.9.6	FACS data analysis	Tree star
FACS Diva software V6.1.3	FACS data acquisition	BD Biosciences
StepOne Software V2.1	RT-PCR data acquisition	Thermo Fisher Scientific
Zotero V6.0.26	Literature administration	Corporation for Digital Scholarship
Visual Studio Code V1.81.0	Text editing	Microsoft
Vectornator V4.13.7	Drawings and Illustrations	-

3. Methods

3.1. Collection of Subjects: CAD Patients and Normal Controls

A total of 23 CAD patients (15 men, 8 women, median age: 70 years) were recruited at the Department of Cardiothoracic Surgery at Otto-von-Guericke University Hospital Magdeburg. These patients were diagnosed with coronary artery disease through angiography and were referred for CABG surgery following the decision of the local heart team. To be more specific, the patients had suffered from NSTEMI with the occurrence being either within a week or less on average (other categories included: STEMI \leq one week, STEMI $>$ one week and NSTEMI $>$ one week). In terms of severity of significant CAD, the majority of cases were characterized by TVD, affecting nearly all patients except for one individual who had DVD. None of the patients exhibited SVD. The exclusion criteria encompassed patients with CAD who had known infections such as hepatitis and HIV, those with cancer diagnoses, individuals experiencing hemodynamic instability, and those with anaemia. Following the CABG surgery (between day 1 and day 3 post CABG surgery), blood samples were collected from every participant enrolled in the research in a sterile manner using a heparin blood sample tube (BD Vacutaner[®] Heparin) at the regular care unit. The collected blood samples were immediately transferred to the research laboratory and the cells were processed. Furthermore, 10 normal controls were recruited in the study: Out of ten controls, five were younger (≤ 30 years) and five were older (≥ 50 years). The reason for recruiting younger control is that the onset of atherosclerosis and the corresponding inflammation is also described to manifest during adulthood.

3.2. Sample Preparation: Isolation of PBMC

To study the frequencies of blood monocytes and intensities of monocyte migration markers, PBMC, were isolated using the ficoll-paque gradient technique. Ficoll is an uncharged sucrose polymer with a specific density (1.077 g/mL), that will sort the cells in gradient centrifugation into the different phases, as shown

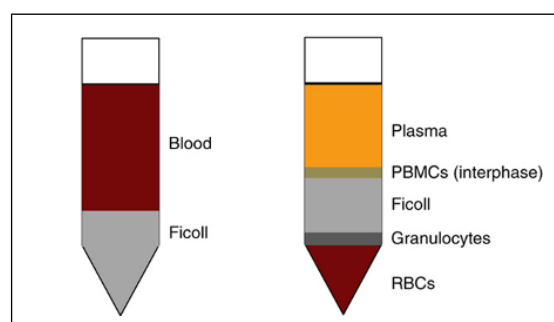


Figure 3.1. Ficoll gradient centrifugation [78]

in Figure 3.1. These PBMC contains B- and T-lymphocytes, natural killer cells and monocytes. After centrifugation, they will appear as an interphase (blurry white ring). The obtained heparinised blood samples (CAD patient or normal controls), were diluted at the ratio of 1:1 with PBS. In a 15 ml ficoll tube, 7 ml of the diluted blood was then layered on-top of 3 ml Ficoll-Paque[®] PLUS. Subsequently, the ficoll tubes were centrifuged with 1200 revolutions per minute (rpm) for 20 minutes at room temperature, especially with break-off during ficoll-paque gradient step. The cloudy interphase was then collected into a fresh ficoll tube, washed with PBS by centrifugation at 1200 rpm for 10 minutes at +4 °C. Upon centrifugation, the supernatant was discarded and the cell pellet was resuspended in 1 ml PBS. If the cell pellet contained red blood cells (RBC), lysis of the erythrocytes were performed using 1 ml 1x RBC lysis buffer for 2 minutes (10x Biolegend[®] RBC Lysis Buffer was diluted with ddH₂O to achieve 1 X RBC lysis buffer), and washed by centrifugation. To ensure equal numbers of cell distribution, these PBMC were counted using a Neubauer counting chamber. Based on cell requirement for different experimental setups, diluted PBMC was then further diluted. Mostly, the concentration of 1 million cells/200 μ l was utilized.

3.3. Phenotyping of Monocyte Subsets and Migration Markers by FACS

According to the first aim (section 1.4), the inflammatory condition between CAD patients and normal controls were compared by phenotyping the blood monocytes. To assess their migration capability, the markers CCR2, CX₃CR₁, CCR5, and CCR1 were also phenotyped. Here, blood monocytes were identified using the markers CD14 and CD16. Furthermore, CCR2 and CX₃CR₁ markers were stained to differentiate the various subsets of monocytes, as explained in section 1.2.A. In addition, CCR5 and CCR1 markers were also stained.

FACS Extra Cellular Staining Procedure

The FACS staining solutions were prepared as shown in Figure 3.2:

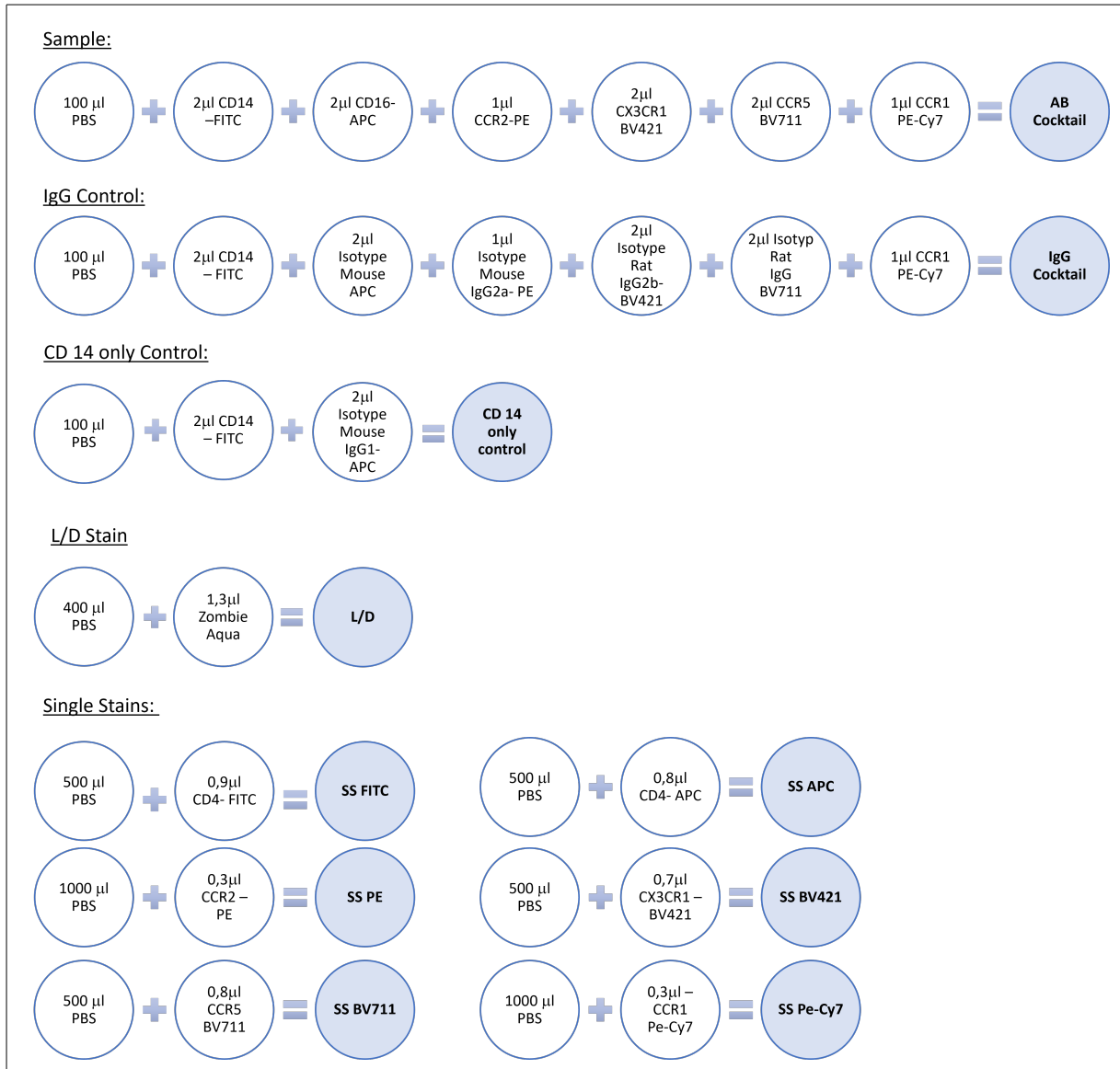


Figure 3.2. Migration Marker Stain

Composition of the different staining solution for the sample (antibody cocktail), IgG-Control (IgG cocktail), CD-14 only control, life/dead (L/D) and single stains (SS) including FITC, PE, BV711, APC, BV421, Pe-Cy7.

3.3. PHENOTYPING OF MONOCYTE SUBSETS AND MIGRATION MARKERS BY FACS

The isolated PBMC were utilized for FACS staining. Here, FACS tubes containing one million PBMC (1 Mil cells/200 μ l) were washed with 1 ml of PBS and centrifuged at 1200 rpm for 10 minutes at 4 °C, and the supernatant was removed. The cells were mixed with 100 μ l/well of L/D stain (Figure 3.2) and 4 μ l/well of human FcR block (diluted at a ratio of 1:25) and thereafter incubated in the dark at room temperature for 20 minutes. Here, Zombie Aqua TM was used as LD stain, which is an amine-reactive fluorescent dye. It binds only to compromised membranes of deceased cells, allowing to distinguish between live and dead cells. This method provides a means to determine the (%) of viable cells. The presence of Fc receptors (FcXs) on monocytes can lead to erroneous outcomes in immunofluorescent staining, as they can cause false positive or false negative results by binding to immunoglobulin (Ig) Fc regions. To mitigate this issue, the FcX Block is employed. The IgG isotype control serves as a negative control to detect any of these non-specific background signals by fluorochrome. These IgG isotype control antibodies belong to the same class and type as the experimental antibodies, but they do not specifically target the intended molecule or antigen. Thereafter, 100 μ l of mouse beads were added into the labelled FACS tubes for CD4-FITC, CD4-APC, CCR2-Pe, CCR1-Pe-Cy7 and 100 μ l rat beads into CX₃CR₁-BV421 and CCR5-BV711-tubes. As the next step, the antibody cocktail, IgG control, CD14-only control and the single stains were given into the respective tubes (see Panel Layout Figure 3.2) and incubated at 4 °C in the dark with subsequent washing and centrifugation. Following this, the cells were fixed using a 1.5 % paraformaldehyde (PFA) solution, washed, and centrifuged. The samples, including the single stains, unstained samples, L/D stain, IgG control, and CD14-only control, were measured using the FACS BD Fortessa immediately.

BD Fortessa FACS Acquisition and FlowJo Analysis

Flow cytometry, also referred to as fluorescence-activated cell sorting (FACS), is a technique used to count and analyse cells in a liquid sample by simultaneously assessing their physical and molecular characteristics. When the laser beam of the device interacts with the cells, they exhibit distinct scatter patterns based on their size and cellular complexity (like granularity). This scatter can be divided into two components: forward scatter (FSC) and sideward scatter (SSC). The FSC results from light diffraction on the cell surface, while the SSC arises from the diffraction of the cell membrane and vesicles. Consequently, the FSC provides information about the cell's size, while the SSC indicates its granularity. Moreover, cells are distinguished based on the presence of specific surface antigens through immunofluorescent staining. In this method, antibodies specific to the surface antigens of interest are labelled with fluorescent markers. These fluorescent markers emit light of a particular wavelength when excited by a laser. The FACS machine is equipped with detectors that can detect and measure the emitted fluorescent light. In the experimental setup, the BD LSR II FortessaTM Cell Analyser (BD Bioscience) installed with FACS DIVA software (version 6.1.3) was used. For optimizing the voltage settings, unstained cells were utilized. Based on the literature, it is known that monocytes exhibit higher FSC and SSC values compared to lymphocytes [28]. To obtain more accurate data only singlet cells were included during the acquisition. Next, 30,000 beads of the different single stains were run: FITC, APC, PE, BV421, BV711 and Pe-Cy7. Subsequently, 1 million cells from each sample, including LD stain, IgG-control and the sample, were acquired. Further, analysis was performed using FlowJo version 9.9.6. The gating strategy for phenotyping human monocyte subsets involves several steps, as shown in Figure 3.3. After identifying and labelling monocytes based on their size according to the FSC and SSC, only singlet cells were included in the analysis. To ensure that only viable cells were studied, the LD stain was employed. With this setup, the monocyte subpopulation, consisting of M1, M2, and M3 monocytes, could be distinguished using markers such as CD14 and CD16 [33]. Here, CD14 only stain was included in the study in order to find the correct gate between CD14 and CD16 positive monocytes to distinguish M1 and M2 monocytes. Additionally, in this study a combination of the rectangular gating approach and a zebra plot was utilized to provide additional visual cues for more precise and objective differentiation of each subset [33]. The zebra plot displays the median, allowing for symmetrical gating of monocytes, resulting in an even distribution of cells around the median population [33]. Subsequently, the subpopulations were also assessed for the expression of various migration markers (CCR2, CX₃CR₁, CCR5, CCR1).

3.3. PHENOTYPING OF MONOCYTE SUBSETS AND MIGRATION MARKERS BY FACS

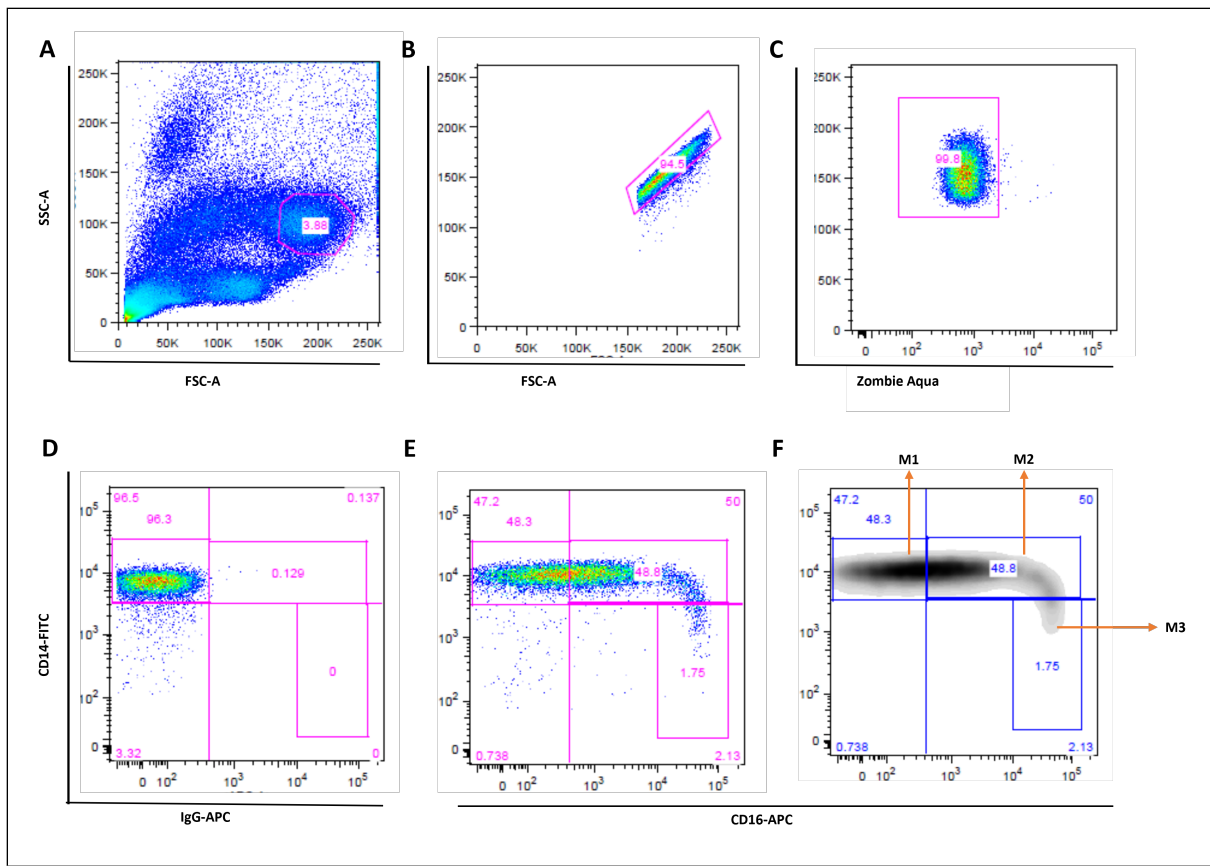


Figure 3.3. FACS Analysis with Flow Jo

Gating strategy for phenotyping human monocyte subsets, including **A**: size discrimination, **B**: doublet exclusion, **C**: selection of living cells, **D**: gating according to the expression of CD14 only (differentiation M1 and M2), **E and F**: gating according to the expression of CD14 and CD16 in combination of the rectangular gating approach and data displayed in a zebra plot (differentiation M2 and M3).

3.4. Plasma Quantification of Pro-inflammatory Cytokines in CAD and Normal Control

The plasma levels of pro-inflammatory cytokines IL-6 and TNF- α were measured in both CAD patients and normal controls, as well as in cell supernatants from selenium cultivation. This was accomplished using the ELISA MAXTM Deluxe Set from BioLegend, which is a sandwich Enzyme-linked immunosorbent assay (ELISA) technique. According to the manufactures instruction, the ELISA (96 well) plate is coated with capture antibody diluted in 1X coating buffer as described in Table 2.2.B Preparation of 1X Reagent for 1 Plate (p.23) and refrigerated. After an overnight (16-18 hrs) incubation in the fridge, the wells were washed and blocked with 200 μ l/well 1X assay diluent to block nonspecific binding and to reduce background. The plate was incubated at room temperature for 1 hour on a plate shaker (500 rpm). Upon washing, 100 μ l/well of standards or samples were added to the corresponding wells and the plate was incubated for 2 hours at room temperature on a plate shaker (500 rpm). During this step, TNF- α or IL-6 binds to the immobilised capture antibody. The plate was washed and 100 μ l/well detection antibodies were added, which produces an antibody-antigen-antibody-sandwich like complex and it was incubated at room temperature for 1 hour on a plate shaker (500 rpm). Upon washing, 100 μ l/well of avidin-horseradish peroxidase was added and incubated for 30 min at room temperature on a plate shaker (500 rpm), followed by adding freshly mixed 100 μ l TMB substrate solution and incubation for 15 min in the dark, producing a blue colour in proportion to the concentration of TNF- α /IL-6 present in the sample. Finally, 100 μ l stop solution was added to stop the reaction where the produced blue colour was changed to yellow. The absorbance was read at 450 nm within 15 minutes with the Tecan Infinite[®] Spectrometer using the Tecan Magellan software. After each incubation step, the plate was washed 4 times with 300 μ l wash buffer per well and the residual buffer was drained by firmly tapping the plate on absorbent paper. After adding avidin-HRP reagent, treatment, a 5th washing step was followed, where the washing buffer was soaked inside the well for 30 sec. All samples were run in duplicates and a standard curve was calculated on log-log axis graph paper, with the x-axis representing analyte concentration and the y-axis representing absorbance for each assay. Prior to use, all reagents were brought to room temperature.

3.5. Therapeutic Intervention with Selenium on CAD Mononuclear Cells

3.5.A. Pharmacokinetic Selenium Dose Evaluation by RT-PCR

The objective of this study is to determine the interventional dosage of selenium for *in-vitro* experiments. To achieve this goal, the ideal concentration and incubation time (6 and 24 hours) that effectively inhibits pro-inflammatory cytokine genes, namely IL-1 β , TNF- α was identified with β 2-microglobulin (B2M) serving as a stable reference gene for normalization. No template control (NTC) was employed as negative controls.

- **Selenium Stock Concentration:** To generate the stock concentration of 3 mM sodium selenite, 0.58 mg of sodium selenite was dissolved in 1000 μ l of MQ water. To meet the working concentration mentioned below table from No. 1 to 8, 15 ml complete RPMI was diluted with the sodium selenite from stock (3 nM) in the concentration shown below.

No.	concentration	dilution from stock
1	50 nM	0.25 μ l sodium selenite
2	100 nM	0.5 μ l sodium selenite
3	500 nM	2.5 μ l sodium selenite
4	1000 nM	5 μ l sodium selenite
5	5 μ M	25 μ l sodium selenite
6	10 μ M	50 μ l sodium selenite
7	20 μ M	100 μ l sodium selenite
8	50 μ M	250 μ l sodium selenite

- **Cell Culture:** THP-1 cell lines were cultured until 85 % confluent in a 6 wells plate. Next, LPS (1 μ g/ml) was added to stimulate pro-inflammatory genes. Subsequently, eight different concentrations of sodium selenite were added to the cells, including (i) 50 nM, (ii) 100 nM, (iii) 500 nM, (iv) 1000 nM, (v) 5 μ M, (vi) 10 μ M, (vii) 20 μ M, (viii) 50 μ M and (ix) LPS alone in duplicates with an incubation time for each 6 hours and 24 hours. After incubation, the cells were centrifuged at 1200 rpm at 4 °C for 10 minutes. The cell pellet was resuspended in RLT buffer with (1%- β -mercaptoethanol) and stored at -80 °C.

- **RNA Isolation and cDNA Synthesis:** The cell pellet was brought to room temperature, and an equal amount of 70-75 % ethanol was added to the tube. The mixture was gently combined using a pipette. Subsequently, the solution was added on the top of the RNA-kit mini columns. Centrifugation was performed at 10,000 rpm for 15 seconds, with a repeat if necessary. The flow-through was discarded, and the samples were separated into a separate ficoll tube. Next, 350 μ l of RW1 buffer was added, and another centrifugation step was conducted at 10,000 rpm for 15 seconds. Before centrifugation, the RDD buffer and DNase were prepared, with 70 μ l of RDD buffer and 10 μ l of DNase. After centrifugation, 80 μ l of RDD buffer and DNase mix were added to each sample, and the samples were incubated for 15 minutes at room temperature. Following this, 350 μ l of RW1 was added, and another centrifugation step was performed at 10,000 rpm for 15 seconds subsequently discarding the flow-through. The columns were transferred to new collection tubes provided in the kit. Then, 500 μ l of RPE buffer was added, and centrifugation was performed at 10,000 rpm for 15 seconds. The flow-through was discarded, and the step was repeated with another 500 μ l of RPE buffer, followed by centrifugation at 10,000 rpm for 2 minutes. The flow-through along with the collection tube was discarded. The columns were then placed in sterilized 1.5 ml Eppendorf tubes. Subsequently, 50 μ l of RNase-free water was added over the filter, and incubated for 3 minutes, followed by centrifugation at 10,000 rpm for 1 minute. This step was repeated. Here, the flow-through obtained contained the RNA and was not discarded. The columns (filters) were discarded, and 1 ml of LPA (linear polyacrylamide, AmbionTM) was added. Additionally, 50 μ l of 7.5M NH₄OAc and 375 μ l of -20 °C stored absolute (100 %) ethanol (2.5 vol) were mixed gently with the sample. The mixture was then incubated for 30 minutes to 1 hour at -80 °C or overnight at -20 °C. The next day, the centrifuge was pre-cooled to 4 °C, and the samples were centrifuged at 1,350 rpm for 45 minutes at 4 °C. The supernatant was carefully removed. Subsequently, 500 μ l of 80 % ethanol (stored at -20 °C) was added, and the samples were centrifuged at 1,350 rpm for 8 minutes at 4 °C . The supernatant was discarded carefully with a pipette. This step was repeated. The tube was placed in a 37 °C heat box (without shaking) for 10 minutes. Afterward, 12.5 μ l of DEPC water was added and gently mixed. Here, 11 μ l of the RNA samples were required for cDNA synthesis and 1.5 μ l for the RNA concentration measurement using NanoDrop spectrophotometer. The RNA samples were immediately stored in an -80 °C freezer.

- **RT-PCR:** Real-time-PCR, also called quantitative real-time polymerase chain reaction (qPCR), is a molecular biology technique used to amplify and quantify DNA sequences in real-time as the reaction progresses. One popular method of real-time PCR involves using a fluorescent dye called SYBR Green. The cDNA produced during the reverse transcription stage in RNA isolation serves as the template for qPCR amplification. This involves the utilization of specific primers and fluorescent probes to amplify and identify the target gene of interest.

Principle: RT-PCR with SYBR Green is based on the amplification of a specific DNA target using the polymerase chain reaction. SYBR Green is a fluorescent dye that binds to double-stranded DNA. As the DNA amplification progresses there is an increased SYBR Green fluorescence binding, which is directly proportional to the amount of amplified DNA. A DNA sample containing the target sequence is mixed with primers, a short DNA sequences that flank the target region, and a reaction mixture that includes SYBR Green and DNA polymerase. The reaction mixture is placed in a real-time PCR machine, also known as a thermal cycler. The thermal cycler repeatedly heats and cools the reaction mixture, allowing DNA denaturation and primer annealing, followed by DNA extension by the DNA polymerase. As DNA replication proceeds, the DNA target's quantity doubles in each cycle. The real-time PCR machine continuously measures the fluorescence emitted by the SYBR Green dye after each cycle. The machine's software plots the fluorescence data against the cycle number to generate a fluorescence curve. The point at which the fluorescence signal crosses a certain threshold is known as the threshold cycle (Ct). The Ct value is inversely proportional to the initial amount of target DNA in the sample.

Procedure: The Maxima First Strand cDNA Synthesis Kit for RT-PCR was utilized for qPCR purposes. The quantitative PCR reaction mix was prepared with 12.5 μl SYBR Green Master mix, 2 μl Primer mix (forward Primer: 1 μl in 10 μl of nuclease free water; reverse Primer: 1 μl in 10 μl of nuclease free water), 9.5 μl nuclease free water and 1 μl of the cDNA template (diluted to 1:5 in nuclease free water). The reaction mixture was placed in the thermal cycler. The PCR was performed with the following setup and cycler temperature setting: **Step 1:** 95 °C 10 min (1 cycle), **Step 2a:** 95 °C 15 sec, **Step 2b:** 60 °C 30 sec, **Step 2c:** 72 °C 30 sec (40 cycle), **Step 3:** 72 °C 10 min (1 cycle) and **Step 4:** 4 °C 2 hours (1 cycle). The calculation involved the utilization of Ct values, which were derived from the duplicate measurements. The determination of relative expression for a specific target transcript in a particular sample was carried out employing the ΔCt method [79].

3.5.B. Cell Culture and Selenium Treatment

The isolated PBMC were seeded at the concentration of 1×10^6 cells/well in a 24 wells plate, as shown in Figure 3.4. These cells were used for evaluating monocyte phenotype markers by FACS, and the cell supernatant was aliquoted and the cytokine concentrations (IL-6 and TNF- α) was measured by ELISA. These cells were treated with two different concentrations of selenium (100 nM and 5 μ M) and incubated at 37 °C for 24 hrs. The optimal dose and incubation time that effectively inhibits pro-inflammatory cytokine genes were identified as 100 nM and 5 μ M prior to the cell culture study (section 3.5.A, section 4.2).

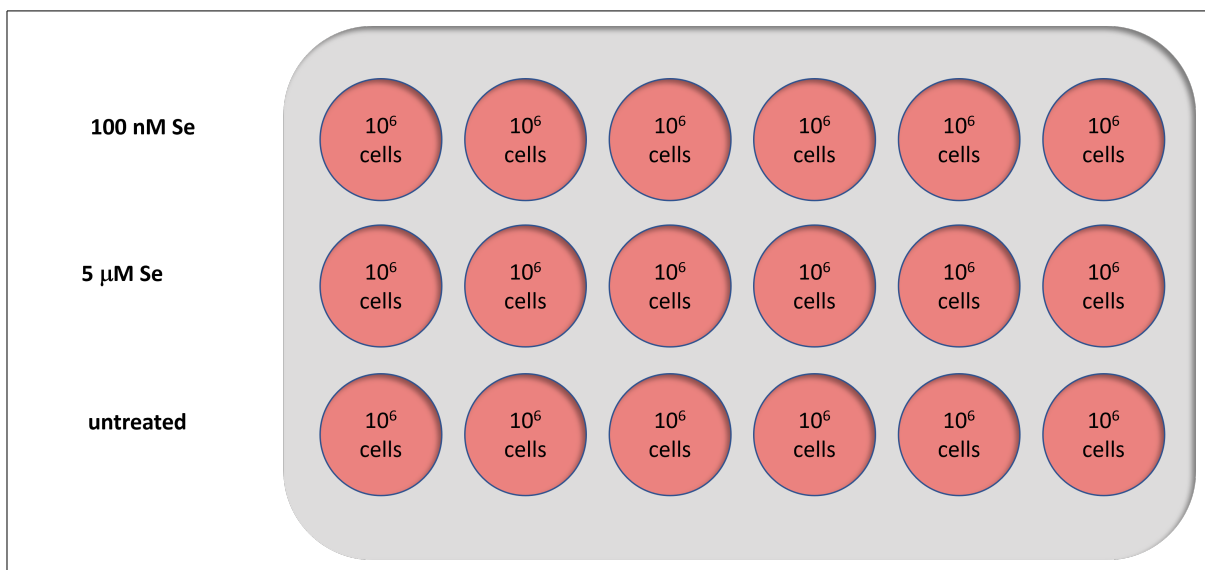


Figure 3.4. Cell Culture: Phenotyping of monocytes upon selenium treatment by FACS

Similarly, PBMC were also seeded at the concentration of 1×10^6 cells/well in a 6-well-plate, shown in Figure 3.5. These cells were used for evaluating STAT-3 activity by WB. These cells were treated with two different concentrations of selenium (100 nM and 5 μ M) and incubated for 24 hrs. In addition, the cells were treated with 1 ml of recombinant IL-6 (100 ng/ml) in the respective conditions for last 30 minutes of 24 hrs of incubation. Upon incubation, the cells were harvested.

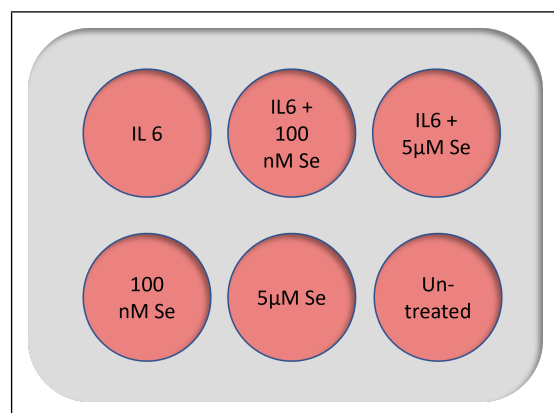


Figure 3.5. Cell Culture: Evaluating STAT-3 activity upon selenium treatment for 24h by WB

In both cell culture set ups, the cells were trypsinized with TrypLE (200 μ l for 24 wells plate and 500 μ l for 6 wells plate) as monocytes usually tend to adhere to the plastic materials [28]. These trypsinized plates were incubated for 4-5 minutes at 37 °C. Upon checking the detached cells under the microscope, 1 ml of RPMI was added to stop the reaction. The cells with the same conditions in different wells were then pooled together and washed by centrifugation at 1200 rpm at 4 °C.

The cell pellets for phenotyping of monocytes were immediately processed for further staining procedure for FACS acquisition (section 3.5.C). The cell supernatant (incubation medium) obtained from different respective conditions was aliquoted and stored at -80 °C to measure the cytokine concentrations (IL-6 and TNF- α) by ELISA (section 3.5.E). The cell pellets for further evaluation of pSTAT-3 by WB technique (section 3.5.D) were stored at -80 °C.

3.5.C. Selenium Intervention on the Frequencies of Monocytes Subsets and Expression of Monocyte Migration Markers in CAD Mononuclear Cells

Following the selenium treatment, the 1 Mil cells from each experimental condition including 100 nM and 5 μ M selenium as well, as untreated cells were used as one separate sample. Any remaining cells were then combined from all conditions and utilized for unstained, life/dead (L/D), IgG control, and CD-14 only control samples. The staining procedure followed the instructions outlined in the FACS fresh stain protocol (section 3.3). Acquisition of data was conducted immediately after the staining process. Both the acquisition and analysis procedures were performed as described in FACS fresh stain protocol (section 3.3).

3.5.D. Selenium Intervention on Phosphorylation of STAT-3 Transcription Factor in CAD Mononuclear Cells

The WB technique is employed to detect specific proteins within a protein mixture. The WB process consists of several steps. First, the sample is prepared by lysing cells and performing a protein assay. Next, SDS-PAGE is conducted, which involves separating proteins based on their size. Subsequently, the proteins are transferred onto a PVDF (polyvinylidene fluoride) blotting membrane to enable antibody detection of the specific

3.5. THERAPEUTIC INTERVENTION WITH SELENIUM ON CAD MONONUCLEAR CELLS

proteins of interest. In this study, the target proteins are pSTAT-3 and STAT-3, whereas α -Tubulin is used as a loading protein. The experiment involves treatment with different conditions, including (i) rIL-6, (ii) rIL-6 + 100 nM Se, (iii) rIL-6 + 5 μ M Se, (iv) 100 nM Se, (v) 5 μ M Se, and (vi) untreated as described in section 3.5.B.

- **Preparation of the sample - Cell Lysis:** 120 μ l lysis buffer was added to treat 2 million cells (150 μ l per 3 million cells). The pellet was resuspended gently, to fully dissolve the pellet. After incubation for 30 min on ice, the cells were centrifuged at 4 °C, 1350 rpm for 15 min. The supernatant was transferred into 1.5 ml Eppendorf tubes and stored at -20 °C until further utilization.
- **Protein Assay:** Pierce™ BCA Protein Assay Kit was used to measure the exact protein concentration of the samples, to ensure the samples loading volume contained an equal amount of proteins.

Principle: This method allows the photometric quantification of proteins in the samples. Colorimetric determination and quantification of the total amount of proteins is achieved through the interaction of proteins with copper. In an alkaline medium, proteins reduce Cu^{2+} to Cu^{1+} . The reduced cation Cu^{1+} then reacts with bicinchoninic acid (BCA) creating a BSA/Cu complex with an intense purple colour. The proportion of the violet reaction complex can be detected at 562 nm and is proportional to protein concentrations.

Procedure: The BSA was diluted according to the protocol of Pierce™ BCA Protein Assay Kit (Figure 3.6) to determine the standard curve. The following calculations were performed using Microsoft Excel. The average absorbance of each standard against its concentration in $\mu\text{g}/\text{mL}$ was plotted to create a standard curve. By this method, the protein concentration of each sample was calculated by comparing its absorbance to the standard curve. To correct for any dilutions made during sample preparation, the calculated protein concentration was multiplied by the dilution factor. Consecutively, 10 μ l BSA standard dilution A-H, BSA 0 and 10 μ l of each lysed sample was given on the microtiter plate in duplicates, 200 μ l of working reagent was added (Reagent A+B, 1:50). The microtiter plate was incubated at 37 °C and subsequently measured at 562 nm with the spectrometer (Tecan, Megelan).

Standart BSA dilution A: 1: 2000
Standart BSA dilution B: 1:1500
Standart BSA dilution C: 1:1000
Standart BSA dilution D: 1:750
Standart BSA dilution E: 1: 500
Standart BSA dilution F: 1:250
Standart BSA dilution G: 1:125
Standart BSA dilution H: 1:25
Standart BSA O: Blank

Figure 3.6. Pierce™ BCA Protein Assay Kit Standard Dilution

3.5. THERAPEUTIC INTERVENTION WITH SELENIUM ON CAD MONONUCLEAR CELLS

- **Preparation of the gels:** For the preparation of 10 % tris-glycine polyacrylamide gels, the Mini Protean[®] Tetra cell kit (Bio Rad) was used. The gel consists of two parts: the stacking gel and the separating gel. The casting was set up as shown in Figure 3.7.

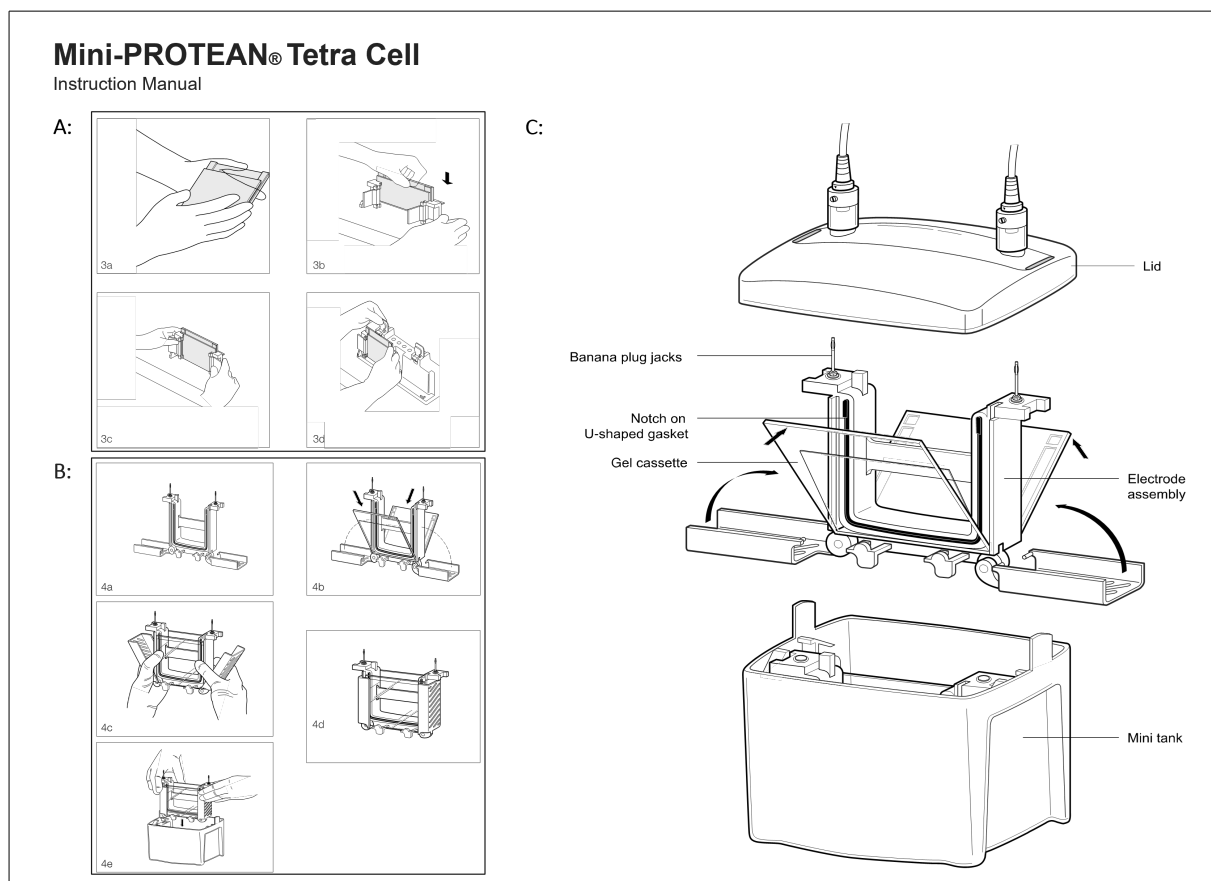


Figure 3.7. Mini Protean Tetra Cell Manuel [80]: **A:** Assembling the Mini-PROTEAN casting stand and frame. **B:** Assembling the Mini-PROTEAN Tetra cell electrophoresis module. **C:** Assembling the Mini-PROTEAN Tetra Cell.

First, the solutions of the separation gels were mixed under a laboratory fume hood (Figure 3.8). APS and TEMED were introduced immediately before being poured into the casting frame to initiate the polymerization process. Approximately 5 ml of the mixture was used per gel and covered with 200 μ l isopropanol. After 30 min, the stacking gel was prepared. A filter paper was placed in the casting stand, to soak up the isopropanol 10 min before. Approximately 4 ml/gel was now poured on top of the polymerised separation gel and a comb was placed to form the gel pockets for sample loading. Again, the gel polymerised for 30 min. The readily prepared gels were stored in the fridge at 4 °C to a maximum of four weeks.

3.5. THERAPEUTIC INTERVENTION WITH SELENIUM ON CAD MONONUCLEAR CELLS

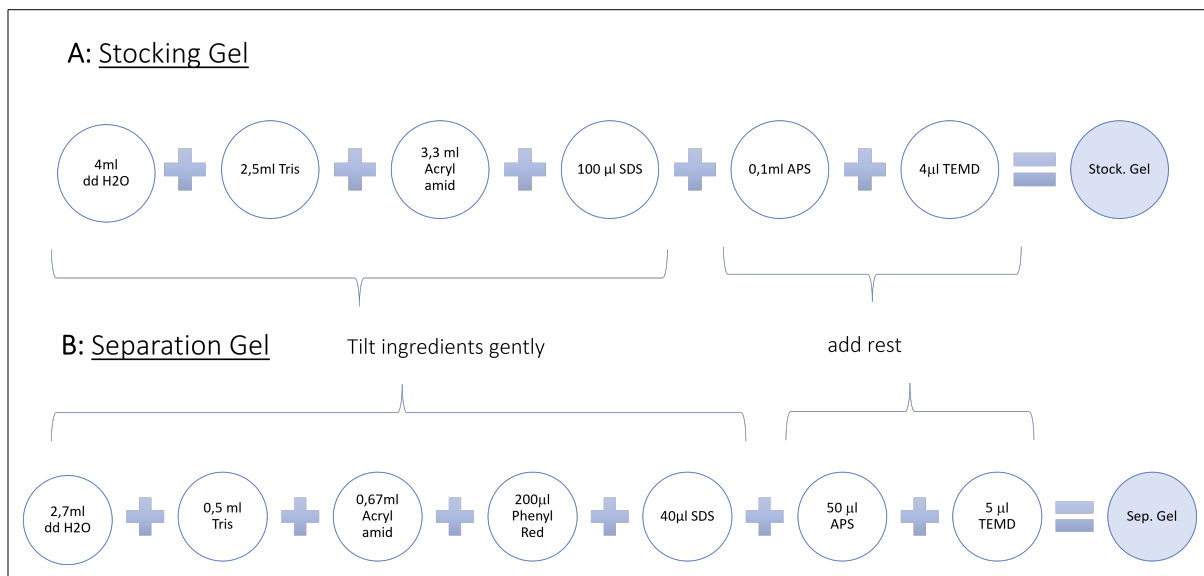


Figure 3.8. Solutions for separation and stocking gel

- **Discontinuous SDS Page:** Sodium dodecyl sulfate polyacrylamide gel electrophoresis (SDS-Page) aims to separate proteins according to their molecular weight when an electrical field is applied. In order to separate the proteins, a Mini Protean[®] Tetra cell kit (Bio Rad) was used.

Principal: The 10 % polyacrylamide gel is composed of the stocking and the separating gel. The two gels differ in pH (stocking gel: neutral pH, separation gel: alkaline pH), size of pores and ionic strength. The pH gradient creates a stacking effect, resulting in better protein separation. The reducing buffer contains SDS, which denaturizes the proteins with a loss of their secondary and tertiary structure, acting as a surfactant and covering the electrical intrinsic charge of the proteins in corresponding charge-to-mass ratios. Also, the proteins get linearized due to the containing thiol (β -2-mercaptoethanol) breaking down the disulphide-bridges by reduction reaction [81]. Nevertheless, the epitopes, required for specific antibody staining are not harmed. An electrical field (85-95 V) is applied and the proteins in the prepared sample move through the gel. The negatively charged proteins are attracted toward the anode. With this, the proteins are separated according to their size, as small proteins (low molecular weight) easily migrate through the gel in contrast to the larger proteins [82].

Procedure: All the steps were accomplished under the laboratory fume hood.

The 1x running buffer was prepared. The assembled gels were placed in the provided tank (Figure 3.7 B) after the comb was removed under aqua dest. Up to the mark

3.5. THERAPEUTIC INTERVENTION WITH SELENIUM ON CAD MONONUCLEAR CELLS

for the respective number of gels used, the tank was filled with 1x running buffer. Prior to loading the samples into the gel, they must be treated with 4x reducing sample buffer (1:1). The mixture was cooked at 95 °C for exactly 5 min. Using the long pipette tip the samples were now loaded into the gel according to the table established in protein assay (section 3.5.D) with the help of a sample loading guide. The first pocket was loaded with 10 μl protein leader (Thermo Fisher Scientific 26616). If there was an empty pocket, it was loaded with 4x reducing buffer only. The electrical field was applied at 85 V until the samples passed the stocking gel and was then raised to 95 V, until the samples reached the bottom of the gel. The ampere was set to a maximum of 200mA.

- **Transfer:**

Principle: In order to make the proteins accessible to specific antibody bindings, they must be transferred from the gel to a membrane. An electric current is applied and the negatively charged proteins are pulled from the gel towards the positively charged anode, and into the membrane maintaining the organization they had within the gel. A PVDF membrane was used [81].

Procedure: Again, all the steps were accomplished under the laboratory fume hood. First, the 1x transfer buffer was prepared and chilled at -20 °C for at least 1 h. The PVDF membrane was activated with ethanol for 3 min. Meanwhile, the gel was gently removed from the glass plates and the

stocking gel was cut out with a scapula (Bio Rad). Everything was prepared to set up the gel-sandwich in the following order and placed in the electrode module as shown in Figure 3.9. After the electrode module was placed in the buffer tank, it was filled with chilled 1x transfer buffer up to the blotting mark and placed in an ice box. Electric current was applied for 115 min 100 V 150 mA.

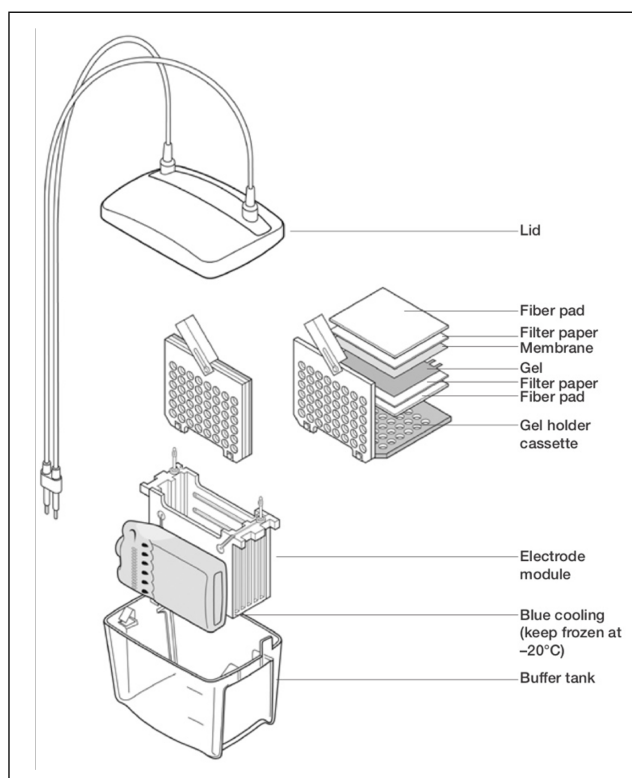


Figure 3.9. Assembly Mini Trans[®] Blot (Bio Rad)

- **Blotting:**

Principle:

- **Ponceau-S Dye:** The PVDF membranes are dyed with Ponceau-S to control if the proteins are transferred successfully from 10 % polyacrylamide gel to the PVDF membrane.
- **Blocking:** The PVDF membrane, which has a high affinity for proteins, is blocked with fat-free dry milk, to prevent non-specific bindings.
- **Blotting/Protein detection:** Detection of specific proteins of interest is achieved in a two-stepped manner. First, the primary antibody (here derived from rabbits), binds to the specific proteins of interest. Second, the HRP-conjugated secondary antibody binds to the primary antibody
- **Development:** Detection of the secondary antibody uses the principle of enhanced chemiluminescence. The luminol-based enhanced chemiluminescent substrate is catalysed by HRP, in the presence of hydrogen peroxide. The excited reaction product changes spontaneously to a stable form during which light is emitted. The ECL ChemoStar Intas consists of a CCD camera (charge-coupled device), which captures a digital image of the signal [83].
- **Stripping:** Stripping allows reusing the same PVDF membrane for more than one protein detection, since all the antibodies, including primary and secondary are removed with a re-blotting reagent (1.5 % sodium azide). The membrane was always stained in the following order: (i) pSTAT-3, (ii) STAT-3 and finally, (iii) α -Tubulin.

Procedure:

- **Ponceau-S:** The membrane was reversible dyed with Ponceau-S for a maximum of 5 min. Afterwards, the dye was washed out with aqua dest.
- **Blocking:** The PVDF membrane was incubated in 5 % non-fat dry milk in TBS-T for 45 min on a tumbler (50 rpm) at room temperature and thereafter washed 3 times with TBST and 1 time with TBS for 10 minutes each.
- **Blotting:** The membrane was incubated overnight with the primary antibody in a 50 ml falcon tube on a tumble at 4 °C in the dark. The primary antibody was dissolved in 3 ml 5 % fat-free dry milk (pSTAT-3: 1:2000, STAT-3 and α -Tubulin: 1:1000). The next day, the membrane was washed with TBST (3 times) and TBS (one time) for 10 min each. Incubation with the secondary antibody was performed in the dark for 1 h on the tumbler at 50 rpm for 1 hour. The antibody dilution used was 1:1500 for the detection of pSTAT-3

3.5. THERAPEUTIC INTERVENTION WITH SELENIUM ON CAD MONONUCLEAR CELLS

antibody and 1:3000 for total STAT-3 and α -Tubulin. Secondary antibodies were dissolved in 10 ml of fat-free dry milk (5 %) in TBST and thereafter washed 3x with TBST and 1x with TBS for 10 minutes each.

– **Development:**

The membrane was treated depending on the signal with Pierce™ ECL Western (α -Tubulin) or Super-Signal™ West Femto (pSTAT-3 and STAT-3), which was prepared just before with reagent A and B (1:1) and incubated for 2 min. Now, it was scanned and pictures were taken at different time points (10-20 min) in the ECL ChemoStar Intas. An example of the scans is given in Figure 3.10.

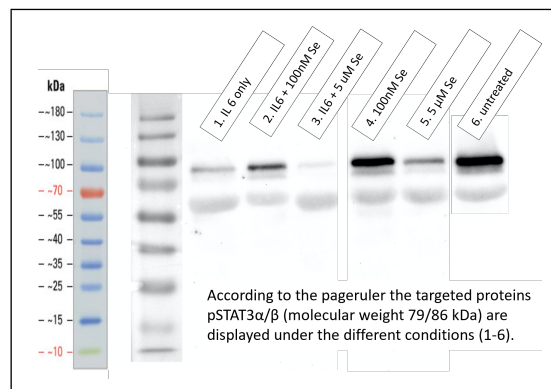


Figure 3.10. Example Scan with ECL ChemoStar Intas

– **Stripping:** The membrane was stripped for 20 min with 10 ml of 1.5 % sodium-azide at room temperature, washed (3x TBST and 1x TBS; 10 min each), blocked and again washed (3x TBST and 1x TBS; 10 min each).

- **LabImage 1D:** The subsequent development of bands was detected using INTAS ECL ChemoStar Imager (INTAS science Imaging) and subsequent quantification of densitometric measurements was performed with the LabImage ID software. Here, the subsequent workflow was applied: selection of the region of interest, labelling of the lanes for each condition, reduction of the background using the rolling ball method (with a radius of 50), and definition of the bands. Consequently, LabImage 1D generated a table displaying the corresponding “band volume”. Subsequently, additional calculations and statistical analyses were performed using this data.

- **Normalisation:**

Normalisation was done using the housekeeping protein:

$$\frac{\text{Band Volume} - \text{Target Protein}}{\text{Band Volume} - \alpha\text{-Tubulin}}$$

- **STAT-3 activity:**

The STAT-3 activity is the quotient from the volume of pSTAT-3 and STAT-3 [70]:

$$\frac{\text{normalised volume pSTAT-3}}{\text{normalised volume STAT-3}}$$

3.5.E. Selenium Intervention on Pro-inflammatory Cytokines in CAD Mononuclear Cells

Peripheral blood mononuclear cells were isolated from CAD patients and were seeded in 24 well plates. Thereafter, two different concentrations of selenium were added to evaluate the therapeutic effect of selenium on the concentration of pro-inflammatory cytokines, such as IL-6 and TNF- α , that were produced from PBMC (section 3.5.B). Untreated cells were used as a control. Upon 24 hours of selenium treatment, the cell culture supernatant was collected and stored at -80 °C for further utilisation. Further, ELISA was used to quantify the concentrations of IL-6 and TNF- α cytokines in the three conditions (untreated, 100 nM and 5 μ M) as described in section 3.4.

3.6. Statistical Analysis

As an outcome, the differences between the monocyte frequencies and intensities of monocyte migration markers and soluble analytes among CAD patients and controls were analysed using the non-parametric Mann-Whitney-U-test. The levels of pro-inflammatory cytokines and phosphorylation of STAT-3 between different *in-vitro* conditions were performed using one way ANOVA non-parametric test. The p-value ($p < 0.05$) was considered significant in the study. Graphical representations were generated using GraphPad Prism version 8.0.1.

4. Results

4.1. Phenotyping of Monocyte Subsets and Migration Markers in CAD Patients and Normal Controls

These findings correspond to the first main of the study. PBMC obtained from 23 CAD patients (15 male, 8 female, median age: 70 years) and 10 normal controls were phenotyped for blood monocyte subsets and the intensities of migration markers by flow cytometry. The experimental set-up is stated in section 3.3. The findings indicate, upon classifying these monocytes into M1, M2 and M3 monocytes subsets, based on the expression of cell surface markers CD14 and CD16 (Figure 3.3), a significant difference in the frequencies of M1 and M3 monocytes, as shown in Figure 4.1. Here, CAD patients exhibited significantly lower levels of M1 monocytes (%) compared to normal controls, whereas CAD patients had significantly higher levels of M3 monocytes (%) compared to normal controls. Also, CAD patient group exhibited increased distribution with outliers.

Subsequently, the mean fluorescent intensities (MFI) of migration markers (CX_3CR_1 , CCR5, CCR2, and CCR1) were evaluated within the various monocyte sub-populations, as depicted in Figure 4.2.

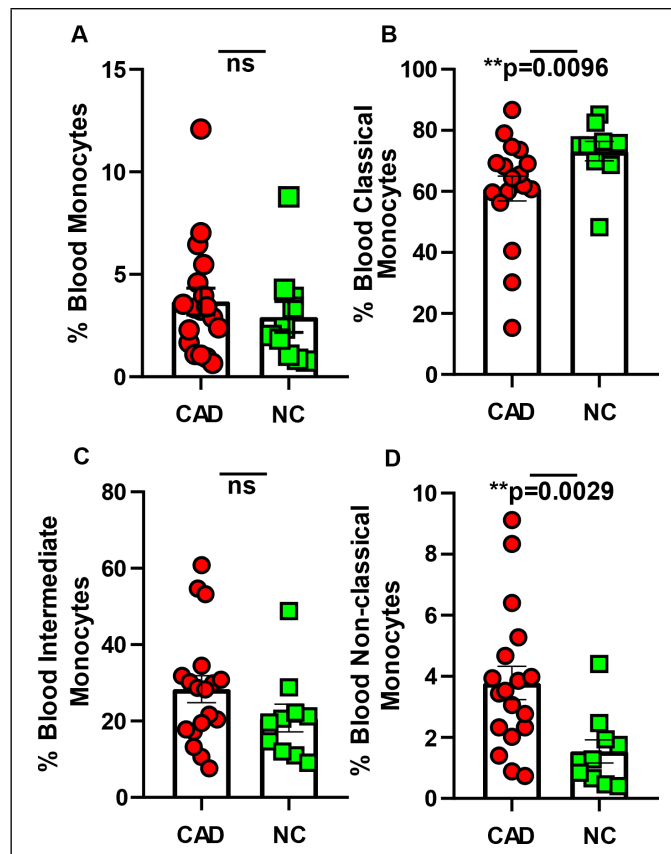


Figure 4.1. Comparison of the frequencies of blood monocytes between CAD patients (red) and normal controls (green) (A). Moreover, the frequencies of M1 (B), M2 (C) and M3 (D) monocytes were compared between CAD patients (red) and normal controls (green). Statistical analyses were performed by a non-parametric Mann-Whitney test. The coloured dot plots represent individual data values. The vertical lines in the scatter dot plot with bar represents the median with range. (* $p \leq 0.05$; ** $p \leq 0.01$; ns: non-significant)

4.1. PHENOTYPING OF MONOCYTE SUBSETS AND MIGRATION MARKERS IN CAD PATIENTS AND NORMAL CONTROLS

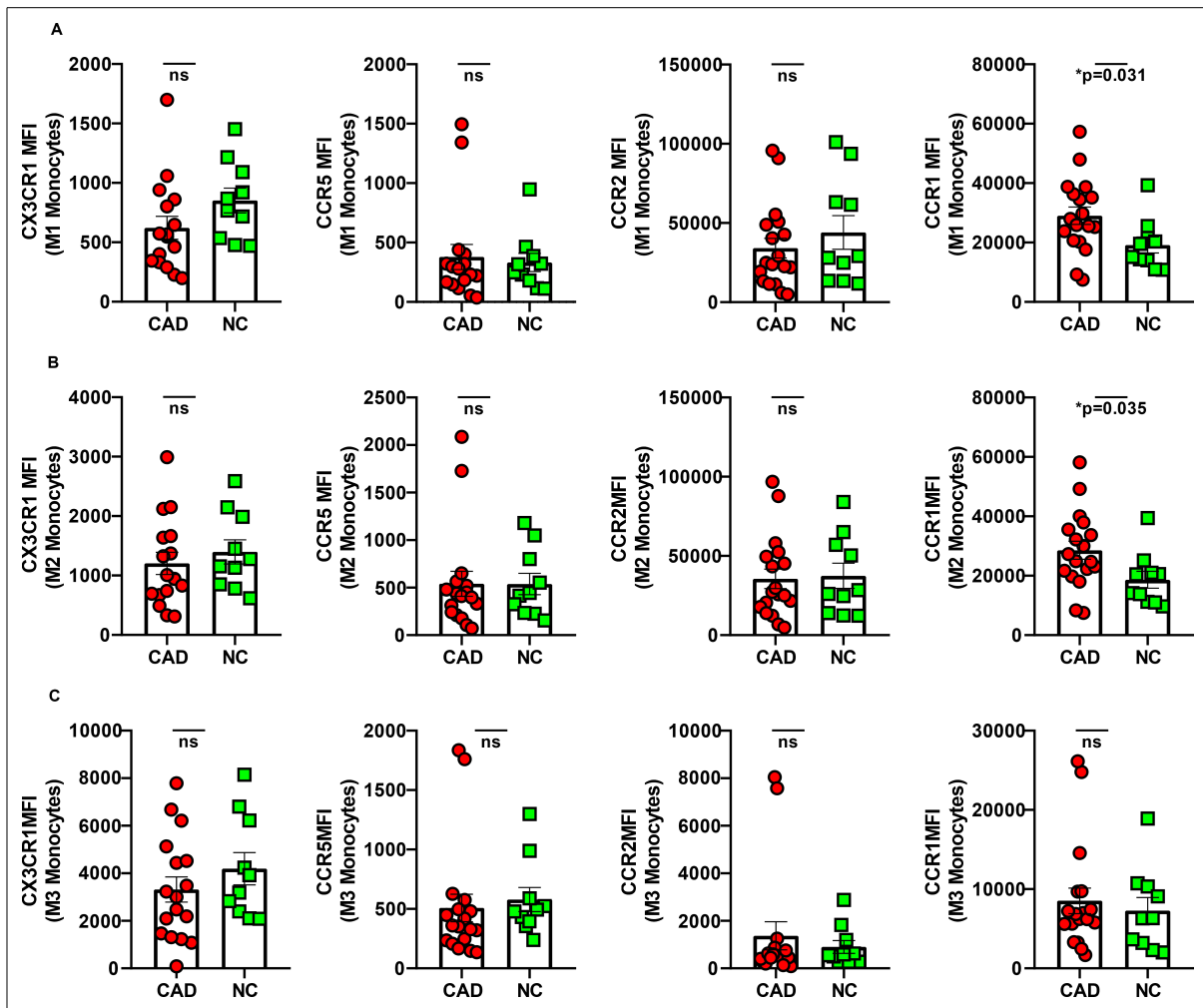


Figure 4.2. Comparison of median fluorescent intensities (MFI) of expressed monocyte migration markers (CX₃CR₁, CCR2, CCR5, and CCR1) in the **A:** classical, **B:** intermediate, and **C:** non-classical monocyte subsets of CAD patients (red) and normal controls (green). Statistical analyses were performed by a non-parametric Mann-Whitney test. The coloured dot plots represent individual data values. The vertical lines in the scatter dot plot with bar represents the median with range. (* $p \leq 0.05$; ns: non-significant)

Strikingly, the findings demonstrated a significant elevation of CCR1 expression specifically in M1 and M2 monocytes. Similarly, noticeable differences were observed in the expression of CCR1 among M3 monocytes, although it did not reach statistical significance in the current study. Conversely, no significant disparities were observed in the expression levels of the remaining migration markers (CX₃CR₁, CCR5, CCR2) across the monocyte subgroups. However, CCR2 intensities were noticeably decreased in M1 monocytes among CAD patients when compared with normal controls.

4.2. Plasma Quantification of Pro-inflammatory Cytokines in CAD Patients and Normal Controls

These findings correspond to the second aim of the study. Here, the measurement of pro-inflammatory cytokines, IL-6 and TNF- α , were performed in the plasma samples of 23 CAD patients and 10 normal controls using ELISA. The experimental set-up is stated in section 3.4. Interestingly, a significant increase in plasma IL-6 levels in CAD patients compared with the normal control were observed Figure 4.3. In contrast, the plasma levels of TNF- α were significantly decreased among CAD patients when compared with controls (Figure 4.3)

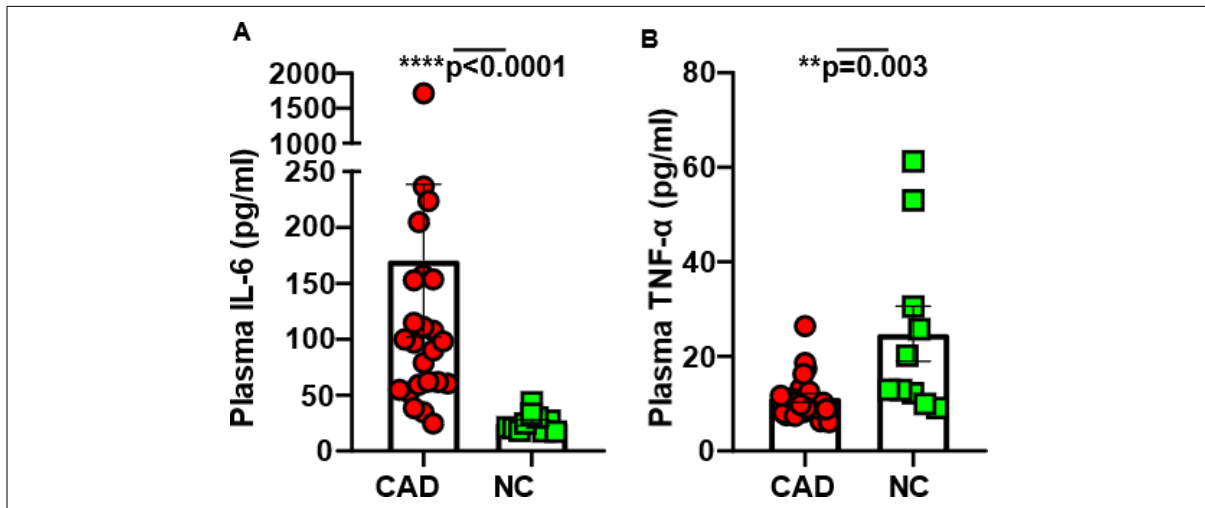


Figure 4.3. Plasma levels of pro-inflammatory cytokines among CAD patients and controls. **A:** Comparison of plasma IL-6 levels between CAD patients (red) and controls (green) **B:** Comparison of plasma TNF- α levels between CAD patients (red) and controls (green). Statistical analyses were performed by a non-parametric Mann-Whitney test. The coloured dot plots represent individual data values. The vertical lines in the scatter dot plot with bar represents the median with range ($*p \leq 0.05$; $**p \leq 0.01$; $***p \leq 0.0001$; ns: non-significant).

4.3. Therapeutic Intervention with Selenium on CAD Mononuclear Cells

4.3.A. Pharmacokinetic Selenium Dose Evaluation Study by Real-Time PCR.

Here, the ideal interventional dosage and incubation time of selenium for *in-vitro* experiments was identified by inhibition of pro-inflammatory cytokine genes, namely IL-1 β and TNF- α . The experimental set-up is stated in section 3.5.A. Selenium concentration of 100 nM and 5 μ M show convincing inhibitory effects after 24 h of selenium incubation under LPS stimulus, especially concerning the IL-1 β gene expression. Hence, 100 nM and 5 μ M were selected as dosages of selenium to be used in the *in-vitro* studies, which align with physiologically therapeutic levels [65].

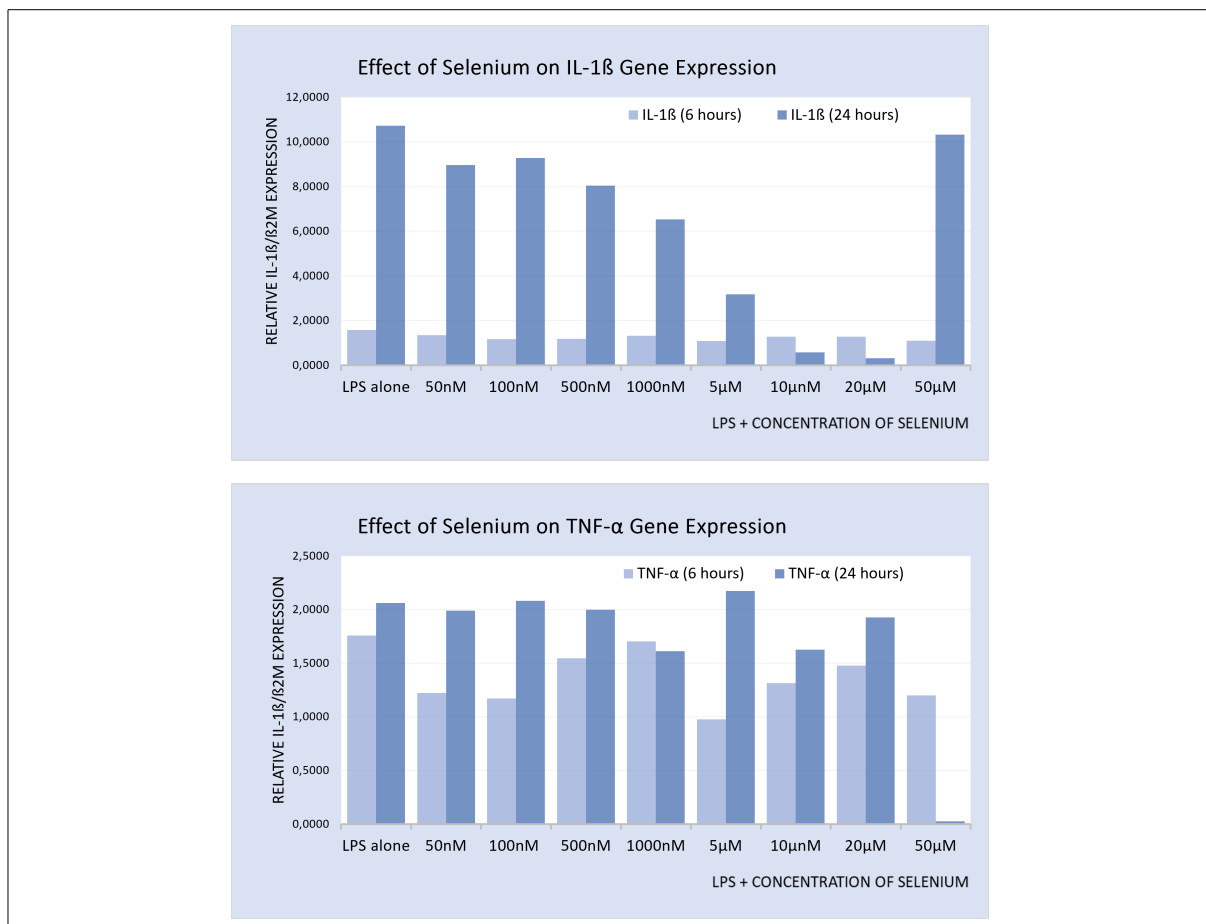


Figure 4.4. The impact of Selenium on the gene expression of IL-1 β (on top) and TNF- α (at the bottom) in THP-1 monocytic cell lines under LPS stimulation was examined at two distinct incubation periods, namely 6 and 24 hours.

4.3.B. Selenium Intervention on the Frequencies of Monocyte Subsets and Expression of Monocyte Migration Markers in CAD Mononuclear Cells

These findings correspond to parts of the third aim of the study. Here, PBMC of eight CAD patients were exposed to two different doses of selenium (100nM and 5 μ M), as stated in section 3.5.B. The aim was to assess the impact of selenium on the frequencies of monocyte subsets and the intensities of monocyte migration markers. Figure 4.5 represents the FACS data obtained from selenium treated and untreated monocytes for 24 hours. Although no significant differences were observed among various conditions in different monocyte sub-populations, a marked reduction was apparent when monocytes were treated with 5 μ M of selenium, particularly in the M2 and M3 monocytes.

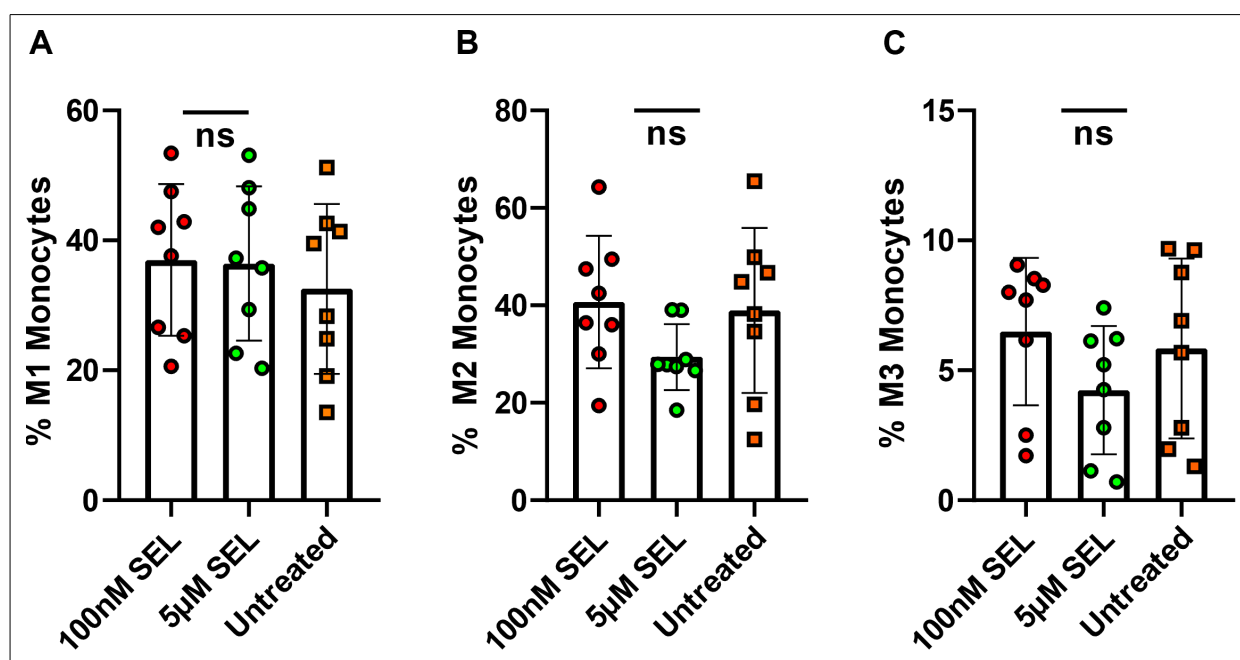


Figure 4.5. Comparison of the frequencies of blood monocyte subsets (A: M1, B: M2 and C: M3 monocytes) when mononuclear cells were treated with two doses of selenium (100 nM and 5 μ M). Here, untreated cells were used as control. Statistical analyses were performed by a one way-ANOVA non-parametric test. The coloured dot plots represent individual data values. The vertical lines in the scatter dot plot with bar represent the median with range.(ns: non-significant)

The subsequent figure, Figure 4.6, presents the expression pattern of migration markers (CX₃CR₁, CCR5, CCR2 and CCR1) on the monocyte subpopulations (M1, M2, M3). However, the results indicate that selenium had no discernible impact on the expression of these migration markers in this study.

4.3. THERAPEUTIC INTERVENTION WITH SELENIUM ON CAD MONONUCLEAR CELLS

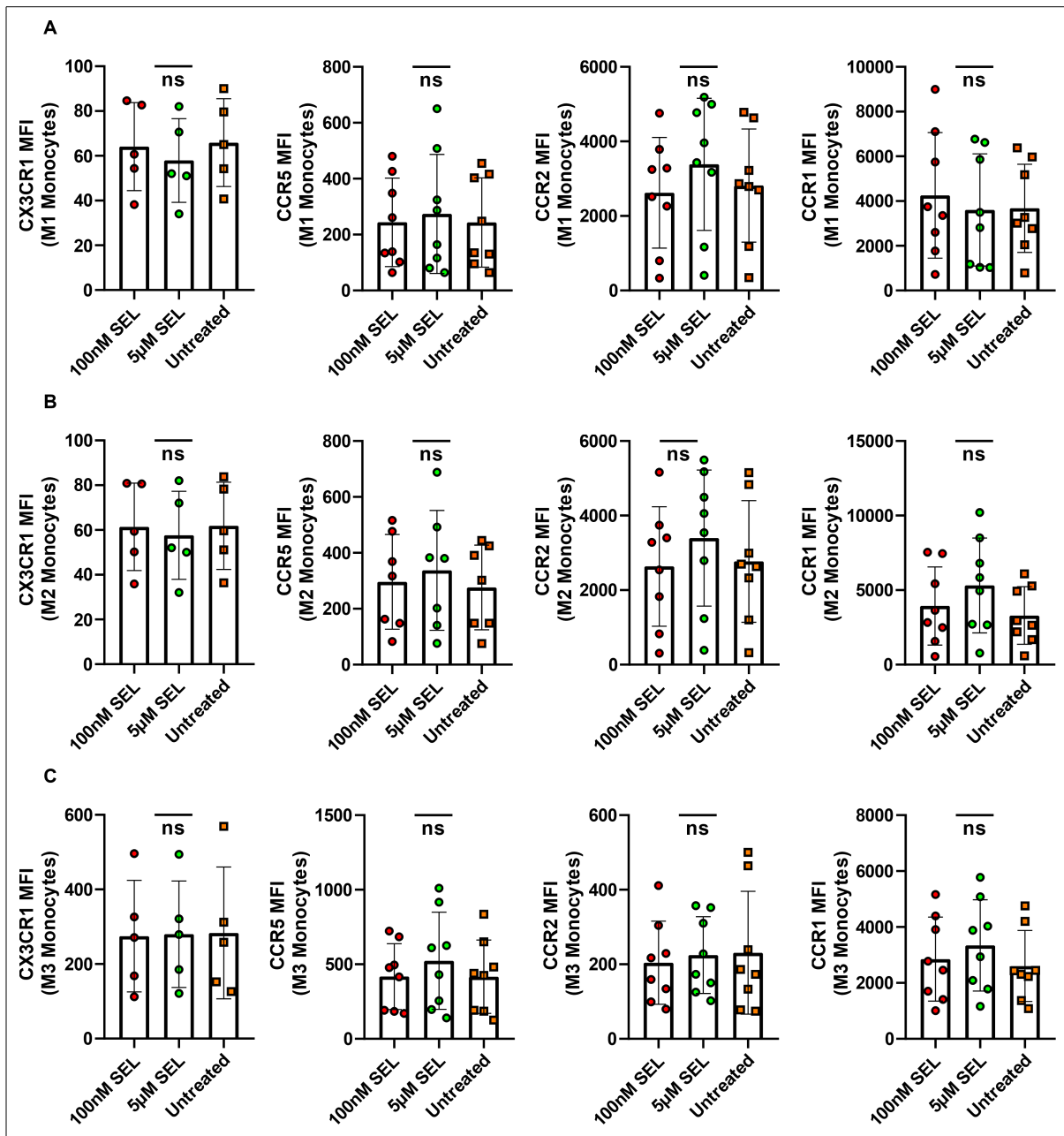


Figure 4.6. Comparison of median fluorescent intensities (MFI) of expressed monocyte migration markers (CX₃CR₁, CCR2, CCR5, and CCR1) in **A**: M1, **B**: M2 and **C**: M3 monocytes of CAD patients after 24h cell culture with selenium treatment (100 nM and 5 μ M selenium) and untreated. Statistical analyses were performed by a one way-ANOVA non-parametric test. The coloured dot plots represent individual data values. The vertical lines in the scatter dot plot with bar represents the median with range.(ns: non-significant)

4.3.C. Selenium Intervention on Phosphorylation Status of STAT3 Transcription Factor in CAD Mononuclear Cells

These findings correspond to parts of the third aim of the study. PBMC isolated from five CAD patients were seeded (3 million cells/well) and exposed to two different concentrations of selenium (100nM and 5 μ M selenium), as described in section 3.5.B. Subsequently, these cells were stimulated with recombinant IL-6 to determine role of selenium on STAT-3 phosphorylation. This study was conducted using WB technique, which has the following target proteins pSTAT-3 as well as STAT-3 and α -Tubulin was used as loading protein for normalization. Figure 4.7, shows the ratio of pSTAT-3 to STAT-3 (normalized to the loading protein) with four different culture conditions, including (i) IL-6 alone, (ii) selenium (100nM+IL-6), (iii) selenium (5 μ M+IL-6) and (iv) untreated control. Several observations can be assessed based on these results. Firstly, it is evident that under IL-6 stimulation, there is an elevated STAT-3 activity. Secondly, there is a baseline level of STAT-3 activity observed in the CAD samples even without any external stimulation. Finally, selenium demonstrates a clear tendency to reduce STAT-3 activity, particularly when exposed to 5 μ M of selenium dose, although this reduction did not reach the level of statistical significance.

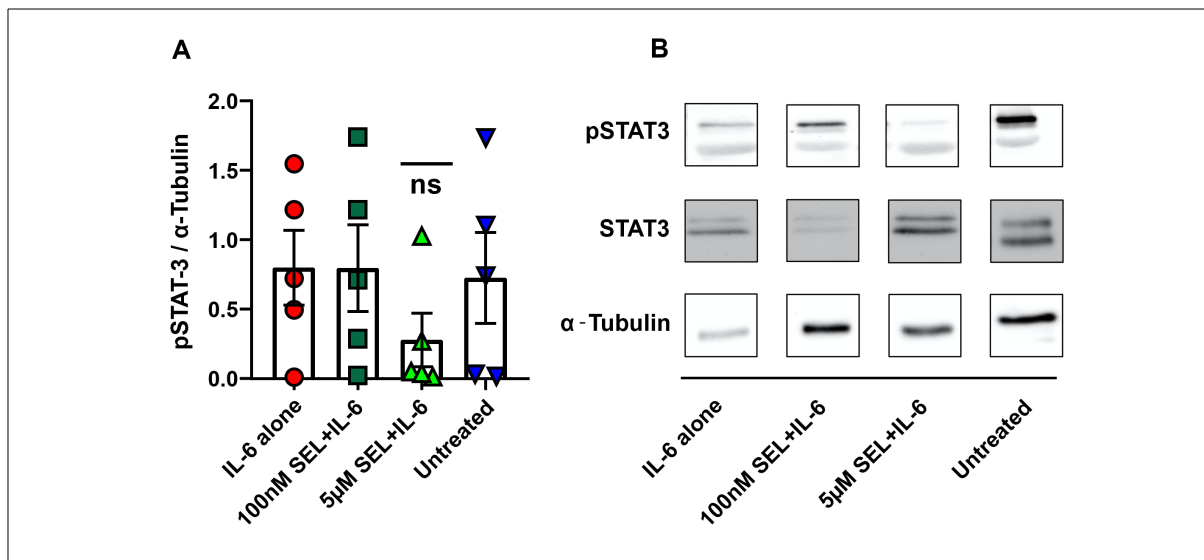


Figure 4.7. Effect of selenium on phosphorylation of the STAT-3 transcription factor in CAD mononuclear cells. **A:** PBMC from CAD patients were incubated with two different concentrations of selenium (100 nM and 5 μ M) for 24 h at 37 $^{\circ}$ C. These cells were subsequently treated with recombinant rIL-6 cytokine (100 ng/mL) for the last 30 min of incubation, and thereby compared with rIL-6 alone and untreated control. **B:** Representative bands of pSTAT-3, STAT-3, and α -Tubulin proteins in CAD mononuclear cells with corresponding treatment strategy. Statistical analyses were performed by a one way-ANOVA non-parametric test. The coloured dot plots represent individual data values. The vertical lines in the scatter dot plot with bar represents the median with range. (ns: non-significant)

4.3.D. Selenium Intervention on the Cell Supernatant Levels of Pro-inflammatory Cytokines from CAD Mononuclear Cells

These findings correspond to parts of the third aim of the study. PBMC isolated from six CAD patients were exposed to two different doses of selenium (100 nM and 5 μ M), as described in section 3.5.B. Upon 24 hours of cell culture, the therapeutic effect of selenium on the produced levels of pro-inflammatory cytokines (IL-6 and TNF- α) were determined. Figure 4.8 shows cell supernatant concentrations of IL-6 as well as TNF- α under different conditions, including selenium treated (100 nM and 5 μ M) and untreated controls. Strikingly, a significant reduction of IL-6 production was observed when these cells were treated with 5 μ M selenium compared to the IL-6 production of cells treated with 100 nM selenium. Interestingly, the IL-6 production of untreated cells compared to cells treated with 5 μ M selenium almost reached the level of significance with a p-value of 0.06. In parallel, the TNF- α concentrations were also markedly reduced with 5 μ M selenium treatment, though not reaching the level of statistical significance.

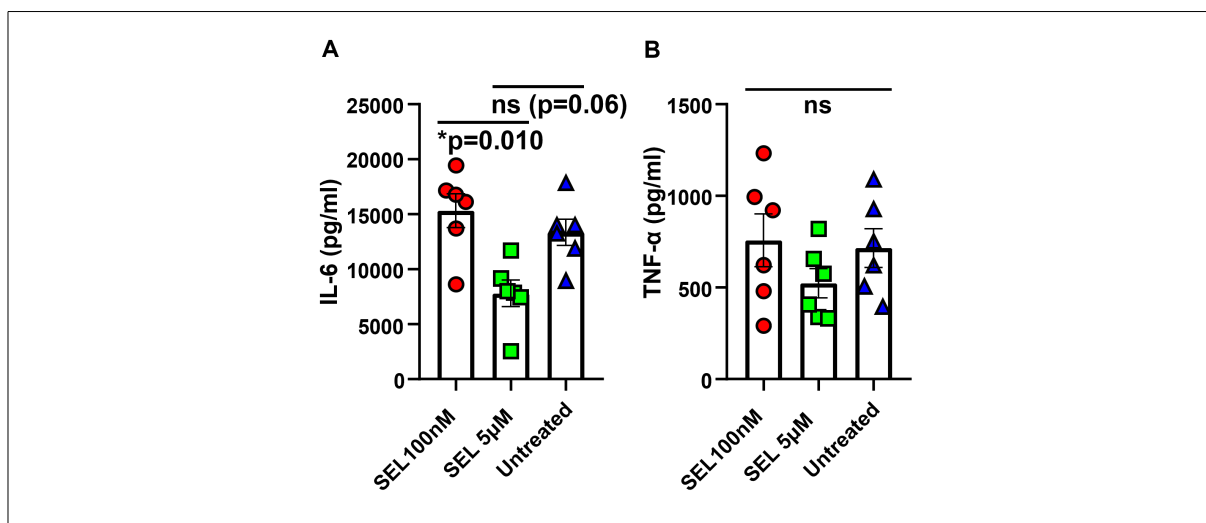


Figure 4.8. Effect of selenium on cell supernatant levels of IL-6 and TNF- α from CAD mononuclear cells. The cell supernatant levels of **A:** IL-6 and **B:** TNF- α cytokines from PBMC of CAD patients when incubated with two different concentrations of selenium, 100 nM and 5 μ M, for 24 hours at 37 °C. Statistical analyses were performed by a one way-ANOVA non-parametric test. The coloured dot plots represent individual data values. The vertical lines in the scatter dot plot with bar represents the median with range. (* $p \leq 0.05$; ** $p \leq 0.01$; ns: non-significant)

5. Discussion

5.1. Phenotyping of Monocyte Subsets and Migration Markers in CAD Patients and Normal Control

Since inflammatory atherosclerosis, underlying coronary artery disease (CAD), mainly consist of monocyte-driven macrophages in addition to the lipid deposition at subendothelial space, the frequencies of blood circulating monocytes, and the expression of migration markers were investigated in postoperative CAD patients and compared with normal controls. The illustration of the pathological mechanism underlying atherosclerosis can be found in Figure Figure 1.5. Detailed results are presented in Section section 4.1. In this study, CAD patients were examined to classify their circulating monocytes into three distinct subsets: **classical monocytes (M1)** identified as $CD14^{++} CD16^{-}$, **intermediate monocytes (M2)** marked as $CD14^{++} CD16^{+}$, and **non-classical monocytes (M3)** recognized as $CD14^{+} CD16^{++}$.

A noticeable increase in the frequencies of total monocytes in CAD patients could obviously relate to the process of monocyte-macrophage differentiation steps in atherosclerosis. This may further account for a direct relationship between the monocyte abundance and subsequent generation of plaque-associated macrophages, potentially leading to larger atherosclerotic lesions [84]. Therefore, an increase in circulating monocytes might lead to an increase in the number of macrophages in the atherosclerotic zone that needs further investigation. Nevertheless, such correlation may not always be direct or linear, as the immune response is a complex and dynamic process influenced by various factors.

In this study, a remarkable increase in M3 monocytes in the peripheral blood of CAD patients, together with the decrease in M1 monocytes, both reaching the level of significance, corroborates with the report [35], that M1 monocytes give rise to both M2 and M3 monocytes in the bloodstream during inflammatory conditions. The results align with prior research, [30], indicating that M3 monocytes exhibit inflammatory properties, given that elevated M3 monocytes levels consistently correlate with inflammatory conditions in humans, including diseases like CAD, atherosclerosis, rheumatoid arthritis, hemophagocytic syndrome, and Crohn's disease [30]. Interestingly, the report also notes a decrease in M1 monocytes counts especially in atherosclerosis, which mirrors the observations made in the present study. Moreover, the increased number of M3 monocytes, as observed,

5.1. PHENOTYPING OF MONOCYTE SUBSETS AND MIGRATION MARKERS IN CAD PATIENTS AND NORMAL CONTROL

aligns with another study [53] that found a significant rise in circulating $CX_3CR_1^+$ monocytes in individuals experiencing acute myocardial infarction (AMI). Here, there was a direct connection demonstrated between the elevated M3 monocytes and increased levels of acute phase proteins, a main factor in the contribution and progression of inflammation. Additionally, one could also argue that the reduced frequencies of M1 monocytes might be attributed to their rapid recruitment to atherosclerotic zone, as reported in previous studies [79]. All of this re-emphasizes the ongoing inflammation in CAD patients. However, potential drawbacks should be considered: In current research, a biphasic monocyte recruitment pattern has been described during the repair of cardiac tissues [85, 21, 86, 87]: There exists a pro-inflammatory and healing monocyte-macrophage-response after myocardial infarction [85], where the endothelium of infarcted areas of the heart alter their chemokine expression pattern over time, recruiting $Ly-6C^{high}$ monocytes through CCR2 initially, followed by $Ly-6C^{low}$ monocytes via CX_3CR_1 [87]. Here, during an acute inflammatory phase (phase I) the M1 are recruited to the site to remove dead cardiomyocytes by phagocytosis. Thereafter, the M3 monocytes promote resolution of inflammation and tissue repair (phase II). A report [86] has stated that the blood collected from mice around day 7 post-AMI showed an increased magnitude of non-classical monocytes. Certainly, the individuals enrolled in the study to finalize this doctoral dissertation had suffered NSTEMI, within a week prior to the collection of blood samples. The findings presented offer a suggestion that human monocyte behaviour, following myocardial infarction, may exhibit a comparable pattern to that observed in the mouse model, displaying a two-phase recruitment process. Here, one can argue that the elevated M3 monocytes count could also be beneficial, as it may promote resolution and tissue repair.

Strikingly, in the current study, M1 and M2 monocytes of CAD patients have shown a significant overexpression of CCR1. In fact, $CCR1^{high}$ monocytes were reported in several other progressive inflammatory diseases, such as knee osteoarthritis, multiple sclerosis, systemic sclerosis, interstitial lesions of glomerular diseases, and hypertension [79]. The significant elevation of CCR1 is accompanied by a marked decrease in CCR2 expression within M1 monocyte subsets, indicating an ongoing transition from monocytes to macrophages. According to Kaufmann [88], there is a time-dependent switch described as monocytes differentiate into plaque-associated macrophages. Monocytes lose their CCR2 marker as they differentiate into CCR1-positive macrophages. The alterations observed in the migration marker pattern of M1 and M2 monocytes may suggest an enhanced capability for their subsequent differentiation into macrophages associated with plaques. Intriguingly, it was demonstrated that the CCR1 receptor plays a pivotal role in orches-

5.1. PHENOTYPING OF MONOCYTE SUBSETS AND MIGRATION MARKERS IN CAD PATIENTS AND NORMAL CONTROL

trating the STAT-3 activity and consequently influencing the production of IL-6 cytokine in monocytic cells [89]. The capacity of CCR1 to manage IL-6/STAT-3 signalling pathways results in inflammation and the vulnerability of atherosclerotic plaques to rupture [89]. This correlation is in line with the demonstrated heightened STAT-3 activity together with elevated production of IL-6 (discussed in section 5.3). This alignment of results undoubtedly verifies the escalated inflammatory condition and the increased susceptibility to atherosclerotic plaque rupture among CAD patients.

Taken together, slight tendencies and significant differences were observed in the frequencies of total monocytes and monocyte subsets, as well as variations in the expression pattern of monocyte migration markers. These results are summarised in Figure 5.1 and collectively indicate an ongoing inflammatory status among CAD patients in the context of atherosclerosis.

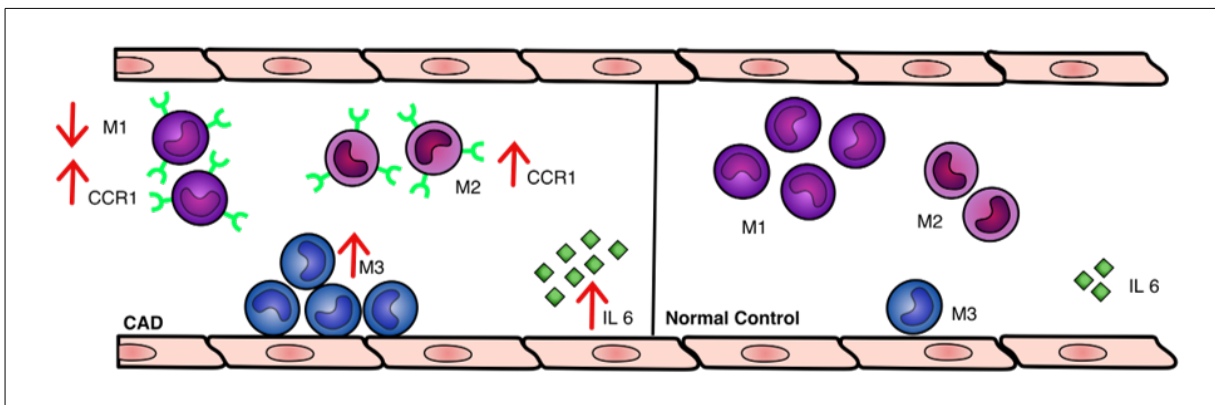


Figure 5.1. Inflammatory status of CAD patients compared to normal control

These results collectively indicate an inflammatory status among CAD patients in the context of atherosclerosis. The observed differences include a higher total count of monocytes in CAD patients (not shown); a shift in monocyte subsets with a decreased number of classical monocytes (M1) and increased number non-classical monocytes (M3); an indication of ongoing transformation of monocytes into macrophages with heightened CCR1 expression; and finally the strikingly elevated plasma level of IL-6.

5.2. Plasma Quantification of Pro-inflammatory Cytokines in CAD Patients and Normal Control

Next, inflammatory status in patients and normal controls were evaluated by determining the plasma concentrations of pro-inflammatory cytokines (IL-6 and TNF- α). The results are presented in section 4.2. A significant increase in plasma IL-6 levels in CAD compared to normal control was observed and this corresponds to the well-known role of IL-6 in ongoing pro-inflammatory status among CAD patients [90, 91]. The severity of CAD is correlated with progressively increased IL-6 levels [90]. In fact, IL-6 has been shown to possess a strong relationship in the development of future cardiac events and CAD mortality [92, 93]. Additionally, plasma IL-6 levels were reported to be independently associated with increased mortality in unstable CAD patients [94].

Surprisingly, plasma TNF- α levels were significantly lowered among CAD patients when compared with controls. Controversially, some studies have found that TNF- α level are higher in CAD patients compared to normal controls with increased risk for atherosclerosis [95, 96]. However, there were decreased frequencies of M1 monocytes among CAD patients (Figure 4.1) observed, which could correspond to the decreased levels of TNF- α production in these patients. Because, these M1 monocytes are the primary producers of TNF- α among monocyte subsets [28]. Another reason could be that the drug, statins, are commonly prescribed to CAD patients as a first-line treatment for secondary prophylaxis after a myocardial infarction. This statin could inhibit NF- κ B activity that is mainly responsible for the production of TNF- α cytokines [97].

In summary, the inflammatory status of CAD patients was confirmed with the strikingly elevated plasma level of IL-6, as pictured in Figure 5.1.

5.3. Therapeutic Intervention with Selenium

The current study has demonstrated a heightened inflammatory status among CAD patients when compared with normal control. One of the main aims of this study was to minimize the increased magnitude of inflammation in CAD patients by intervening with selenium.

Upon treatment with selenium, the frequencies of monocyte subsets and the expression pattern of monocyte migration markers on PBMCs were investigated. The results are demonstrated in section 4.3.B. Though no substantial changes were found in the expression pattern of monocyte migration markers, decreased tendencies for monocyte subsets (M2 and M3), when treated with 5 μ M of selenium, were found. Plausible reasoning for reduced tendencies in M2 and M3 monocytes could be that the STAT-3 activity is involved in monocyte differentiation. Loperna et al. [98] have investigated the effect of hypertension and subsequent endothelial stretch on monocyte differentiation, where they found that STAT-3 activation commences in monocytes to promote differentiation of M1 to M2 monocytes, and subsequently to M3 monocytes. Specifically, they found that endothelial cells undergoing hypertensive mechanical stretch induces an increase in STAT-3 within these monocyte populations. Moreover, it was recently shown, that in individuals with gain-of-function mutations in the STAT-3 gene, exhibit reduced M2 and M3, alongside an elevated percentage of M1 monocytes, which implies STAT3's involvement in shaping the shift from M1 to M3 monocytes [99]. This is consistent with findings in the current study, displayed in section 4.3.C, as selenium was noticed to inhibit STAT-3 activity, particularly intervening the phosphorylation status of STAT-3. Hence, one can speculate that a decreased STAT-3 activity may prevent the conversion of M1 to M2 and M3 subsets, under the influence of selenium. As discussed before (section 5.1), such interruption of monocyte differentiation could lead to reduced inflammation.

The impact of selenium intervention on the phosphorylation status of STAT-3 in CAD-mononuclear cells yields various conclusions, especially in the context of exposure to 5 μ M selenium. The results are illustrated in section 4.3.C. To begin, it is obvious that IL-6 stimulation amplifies the activity of STAT-3. Secondly, there is a baseline level of STAT-3 activity observed in the CAD samples even without any external stimulation. This correlation can be reasoned by the well-established understanding that CCR1, which is overexpressed in M1 and M2 monocytes, possesses the ability to trigger the IL-6/STAT-3 signalling pathways, resulting in inflammation [89]. Finally, it was demonstrated that sele-

nium reduces STAT-3 activity, especially when exposed to 5 μ M of selenium dose. STAT3 plays a crucial role in the regulation of monocyte-to-macrophage differentiation, and the suppression of STAT3 activity does not only reduces inflammation but also inhibits the differentiation of monocytes into macrophages [23]. Additionally, STAT3 signalling is a vital factor in determining the alternative M2 phenotype associated with anti-inflammatory properties and stability of the atherosclerotic plaque [23]. Prior studies have demonstrated that other STAT-3 inhibitors, such as ruxolitinib and metformin, have reduced inflammation, monocyte-to-macrophage differentiation, and atherogenesis [77, 76]. Therefore, the received results of reduced STAT-3 activity together with the striking result of reduced IL-6 levels (discussed below), may serve as compelling evidence that selenium also acts as a STAT-3 inhibitor. Thus, exploring the inhibition of JAK2/STAT-3 pathway and utilizing selenium as potential complementary therapeutic strategy warrants further investigation in the management of CAD.

Finally, the therapeutic effect of selenium could successfully circumvent the production of IL-6 and TNF- α by these CAD mononuclear cells, as shown in section 4.3.D, which might further aid in reducing the process of inflammation. This finding aligns with a previous report that showed a decrease in IL-6 levels when treated with selenium in the ApoE-/- mouse model of atherosclerosis [69]. In the context of atherosclerosis, it was shown that the increase in ICAM-1, VCAM-1, and E-selectin levels induced by TNF- α could be suppressed by selenium in a dose-dependent manner [100]. A recent study, [101], unveiled a correlation between elevated levels of IL-6 and the prevalence of vulnerable atherosclerotic plaque within patients, suggesting involvement of IL-6 in destabilization of atherosclerotic plaques. This underscores the pro-atherogenic properties of IL-6. Thus, selenium could potentially offer benefits to CAD patients by mitigating inflammation through the reduction of IL-6 production and TNF- α .

In conclusion, this study satisfactorily shows the therapeutic effects of selenium, which is pictured in Figure 5.2, in (i) diminishing the conversion of M1 into M2 and M3 monocytes subsets, (ii) markedly reducing the phosphorylation of STAT-3 activity and thereby (iii) decreasing the synthesis of IL-6 and TNF- α levels. All of these aspects are lowering inflammatory status in mononuclear cells obtained from CAD patients. Taken together, selenium could be regarded as a highly promising treatment strategy for CAD, and further investigations should be pursued to build upon these findings.

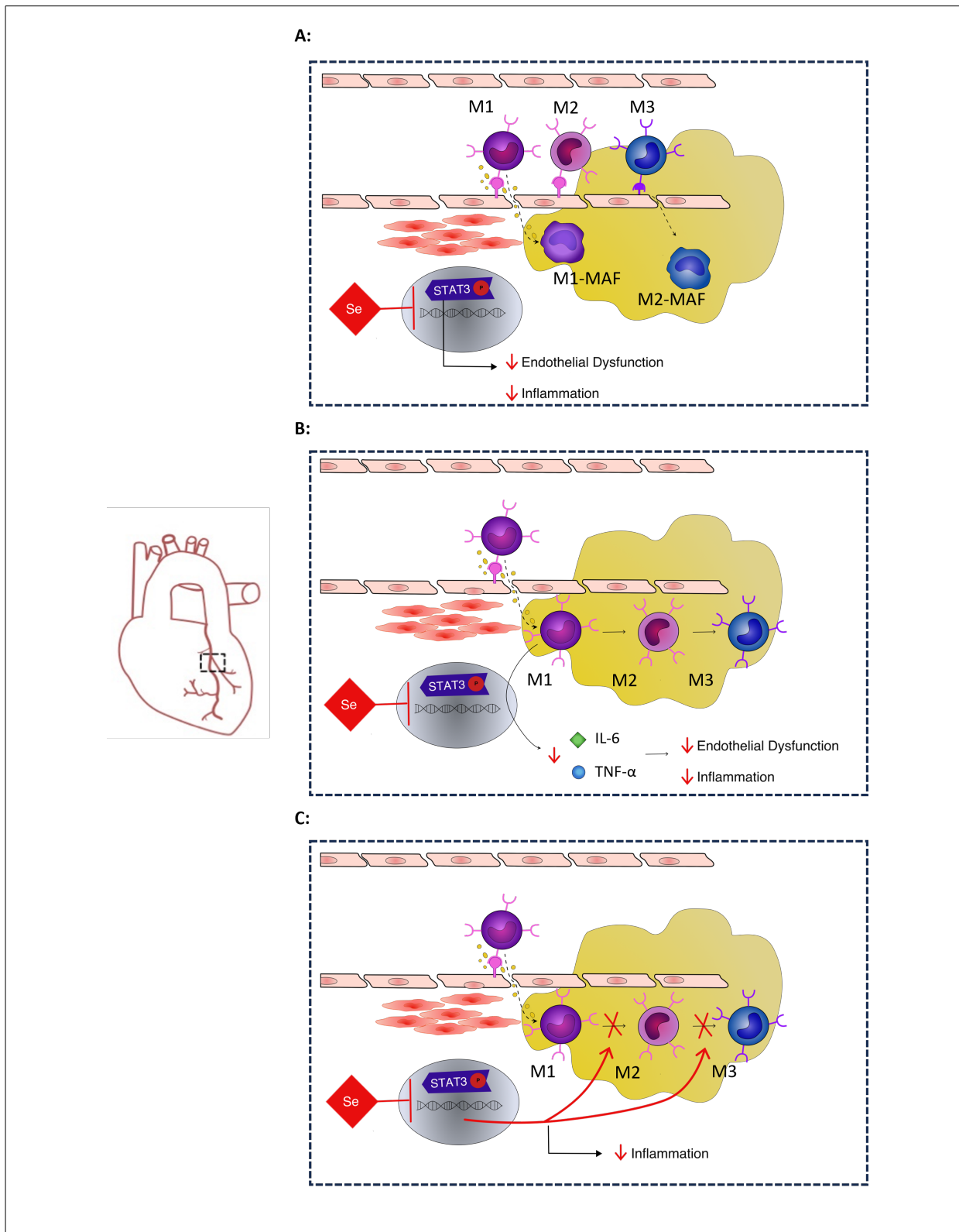


Figure 5.2. Anti-inflammatory therapeutic impact of selenium

In summary, this study effectively showcased the therapeutic impact of selenium. Selenium is mitigating STAT-3 activity (A) and thereby lowering IL-6 and TNF- α levels in mononuclear cells of CAD patients (B). This is mitigating both endothelial dysfunction and inflammation. Moreover, selenium is diminishing the conversion of monocytes into the intermediate (M2) and non-classical (M3) subsets (C).

5.4. Conclusion and Outlook

The received results can be concluded regarding the three main aims of the doctoral thesis (shown in Figure 1.6) as the following:

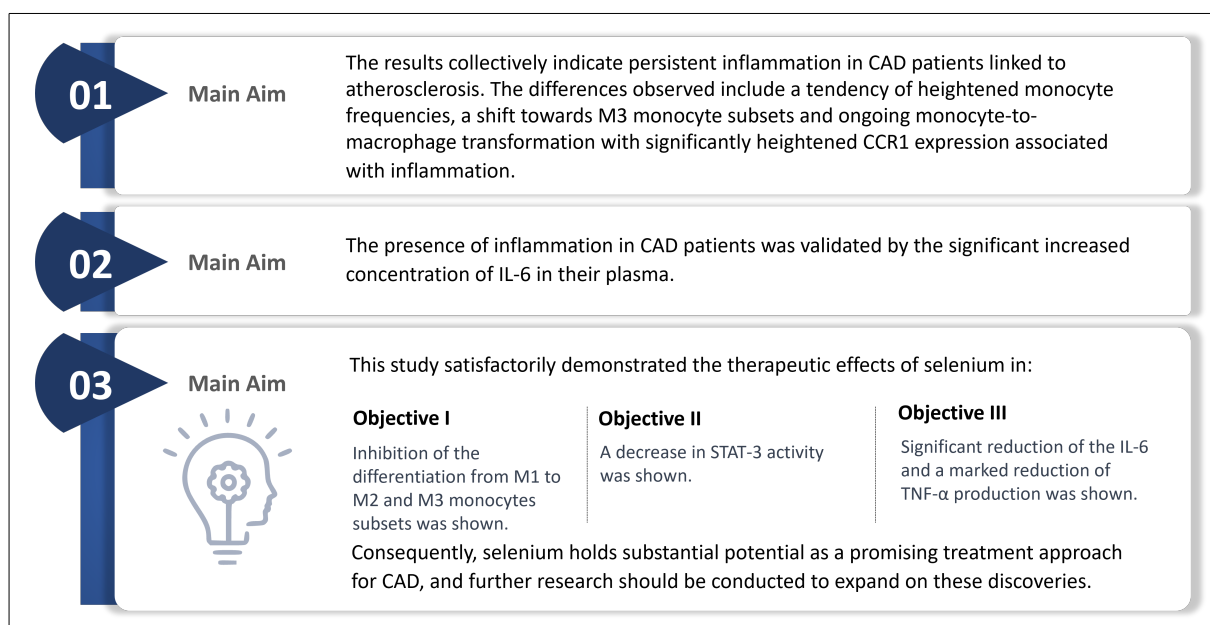


Figure 5.3. Conclusion of the main aims

The present doctoral thesis has provided valuable insights into the complex interplay between chronic inflammation, monocyte subtypes, and the role of selenium as a potential treatment strategy for patients with CAD. However, the obtained results also strike out a multitude of open questions and offer prospects for future research directions. The following are some potential areas for further investigation:

- **Clinical Studies on Selenium Supplementation:** The potential benefits of selenium supplementation highlighted in this work open the door to clinical studies. It would be of great interest to investigate the effects of targeted selenium treatment on the clinical outcomes of CAD patients. Such studies could shed light on the effectiveness, safety, and optimal dosage of selenium.
- **Mechanistic Investigations on Inflammation Regulation:** To gain a deeper understanding of the anti-inflammatory effects of selenium, further investigations could delve into the intricate molecular mechanisms underlying the interaction between selenium and key cellular signalling pathways, with a particular focus on the STAT-3 pathway, especially focusing on mechanistic investigations involving

STAT-3 in monocyte/macrophage differentiation. Here, a more specific elaboration on the potential effects of selenium on the differentiation of monocytes into macrophage subtypes could have a special focus. Moreover, investigation on therapeutic selenium to skew monocyte differentiation towards M2-like macrophages that contribute to tissue repair and resolution of inflammation, could be done.

- **Long-Term Effects on Prognosis:** As elevated IL-6 levels are associated with unfavourable prognosis in CAD patients, long-term studies could be conducted to examine the impact of selenium on IL-6 plasma levels and long-term prognosis and the progression of CAD. This could help assess the potential of selenium as a long-term treatment strategy.
- **Effects on Other CVD:** In addition to CAD, the effects of selenium on other CVD could be explored. This could allow for the expansion of treatment strategies to other disease entities.

Overall, the present work provides a promising starting point for further research in the field of inflammation modulation with selenium therapy in CAD. Continuing these research efforts could lead to innovative treatment approaches that could significantly enhance the management and prognosis of patients with CVD.

6. Summary

According to the estimates from the World Health Organization (WHO) cardiovascular diseases (CVDs) were ranked as the primary cause of death in 2020, globally. CAD is a chronic disease, where deposition of atherosclerotic plaques and subsequent blockage of the arteries cause ischaemia and necrosis. Though atherosclerosis arises due to multiple risk factors in the epicardial arteries of the CAD patients, chronic inflammations are the main driving force for the progression of atherosclerosis. In this process, circulating blood monocytes serve as one of the inflammatory cell subsets.

In this study, CAD patients were characterized for circulating monocytes subsets into three categories, **classical monocytes (M1)** (CD14⁺⁺ CD16⁻), **intermediate monocytes (M2)** (CD14⁺⁺ CD16⁺) and **non-classical monocytes (M3)** (CD14⁺ CD16⁺⁺), where classical monocytes were reduced (**p=0.0096) indicating the possibility of these inflammatory subsets to be migrated to the atherosclerotic plaques. This was evident with CCR1^{high} classical monocytes among CAD patients (*p=0.031), indicating their increased potential for the further differentiation into plaque-associated macrophages. In line with this, intermediate monocytes also exhibited elevated CCR1 expression among CAD patients (*p=0.035). At the same time, increased shift to non-classical monocytes among CAD patients (**p=0.0029) indicate existence of patrolling monocytes that are also known to aggravate inflammation. Furthermore, CAD patients also have higher levels of IL-6 cytokines (****p<0.0001), adding a layer of complexity that plays a crucial role in the development, progression, and complications of CAD. It has been shown that elevated IL-6 levels are predictive of CAD and associated with increased mortality among CAD patients.

To circumvent these inflammatory parameters, this study has effectively shown the inflammation mitigating effects of selenium. The reduced STAT-3 activity (ns) was demonstrated, as well as reduced levels of IL-6 (p=0.06) and TNF- α (ns) cytokines from CAD mononuclear cells. Further, the conversion of differentiation of monocytes into the intermediate (M2) and non-classical (M3) subsets was markedly diminished (ns). Hence, one can speculate that selenium treatment decreases the monocyte differentiation process, with reduced STAT-3 activity that further mitigates the production of IL-6 and TNF- α cytokines to reduce overall inflammation that has great impact at the atherosclerotic site where plaque-associated macrophages may be drastically reduced due to reduced monocyte differentiation at the periphery. These findings indicate that selenium could be a promising treatment strategy for CAD patients, especially in their post-operative phase.

Bibliography

- [1] European Society of Cardiology (ESC). *ESC Guidelines on Chronic Coronary Syndromes (Previously Titled Stable Coronary Artery Disease)*. Aug. 2019. URL: <https://www.escardio.org/Guidelines/Clinical-Practice-Guidelines/Chronic-Coronary-Syndromes> (visited on 09/12/2023).
- [2] L. Peng, X. Guo, Y. Gao, Q. Guo, J. Zhang, B. Fang, et al. “Impact of Right Coronary Dominance on Triple-Vessel Coronary Artery Disease: A Cross-Sectional Study”. In: *Medicine* 97.32 (Aug. 2018), e11685. DOI: 10.1097/MD.00000000000011685.
- [3] J. S. Lawton, J. E. Tamis-Holland, S. Bangalore, E. R. Bates, T. M. Beckie, J. M. Bischoff, et al. “2021 ACC/AHA/SCAI Guideline for Coronary Artery Revascularization: A Report of the American College of Cardiology/American Heart Association Joint Committee on Clinical Practice Guidelines”. In: *Circulation* 145.3 (Jan. 2022). DOI: 10.1161/CIR.0000000000001038.
- [4] F.-J. Neumann, R. A. Byrne, D. Sibbing, A. Kastrati, N. Frey, T. Doenst, et al. “Kommentar zu den Leitlinien (2018) der ESC und EACTS zur Myokardrevaskularisation”. In: *Der Kardiologe* 13.4 (Aug. 2019), pp. 181–192. DOI: 10.1007/s12181-019-0336-z.
- [5] J. J. Squiers, J. M. Schaffer, J. K. Banwait, W. H. Ryan, M. J. Mack, and J. M. DiMaio. “Long-Term Survival After On-Pump and Off-Pump Coronary Artery Bypass Grafting”. In: *The Annals of Thoracic Surgery* 113.6 (June 2022), pp. 1943–1952. DOI: 10.1016/j.athoracsur.2021.07.037.
- [6] M. S. Khan, M. Y.-u. Islam, M. U. Ahmed, F. I. Bawany, A. Khan, and M. H. Arshad. “On Pump Coronary Artery Bypass Graft Surgery Versus Off Pump Coronary Artery Bypass Graft Surgery: A Review”. In: *Global Journal of Health Science* 6.3 (Mar. 2014), p186. DOI: 10.5539/gjhs.v6n3p186.
- [7] S. Bundesamt. *Die 10 häufigsten Todesfälle durch Herz-Kreislauf-Erkrankungen*. Dec. 2022. URL: <https://www.destatis.de/DE/Themen/Gesellschaft-Umwelt/Gesundheit/Todesursachen/Tabellen/sterbefaelle-herz-kreislauf-erkrankungen-insgesamt.html> (visited on 09/12/2023).
- [8] W. H. Organization, ed. *Prevention of Cardiovascular Disease: Guidelines for Assessment and Management of Cardiovascular Risk*. Geneva: World Health Organization, 2007. ISBN: 978-92-4-154717-8.

-
- [9] WHO. *Fact Sheet CVDs*. 2020. URL: [https://www.who.int/news-room/fact-sheets/detail/cardiovascular-diseases-\(cvds\)](https://www.who.int/news-room/fact-sheets/detail/cardiovascular-diseases-(cvds)) (visited on 08/15/2023).
- [10] J. C. Brown, T. E. Gerhardt, and E. Kwon. “Risk Factors for Coronary Artery Disease”. In: *StatPearls*. Treasure Island (FL): StatPearls Publishing, 2023.
- [11] S. Bundesamt. *Destatis.De*. 2023. URL: https://www.destatis.de/DE/Themen/Gesellschaft-Umwelt/Gesundheit/Todesursachen/_inhalt.html (visited on 08/27/2023).
- [12] Deutsche Gesellschaft and für Thorax-, Herz- und Gefäßchirurgie [DGTHG]. *German Heart Surgery Report 2021: The Annual Updated Registry of the German Society for Thoracic and Cardiovascular Surgery*. 2022. URL: https://www.dgthg.de/sites/default/files/GermanHeartSurgeryReport2021_0.pdf (visited on 12/12/2022).
- [13] Aerzteblatt. *Fast 185.000 Herzoperationen in Deutschland pro Jahr*. Jan. 2018. URL: <https://www.aerzteblatt.de/nachrichten/87651/Fast-185-000-Herzoperationen-in-Deutschland-pro-Jahr> (visited on 07/30/2020).
- [14] R. Hajar. “Risk Factors for Coronary Artery Disease: Historical Perspectives”. In: *Heart Views* 18.3 (2017), p. 109. DOI: 10.4103/HEARTVIEWS.HEARTVIEWS_106_17.
- [15] DGK. *Prävention Herz-Kreislauf-Erkrankung (Pocket Guidelines)*. 2016. (Visited on 03/31/2020).
- [16] A. S. Simon and T. Vijayakumar. “Molecular Studies on Coronary Artery Disease—A Review”. In: *Indian Journal of Clinical Biochemistry* 28.3 (July 2013), pp. 215–226. DOI: 10.1007/s12291-013-0303-6.
- [17] R. Ross, Glomset, and Harker. *Response to Injury and Atherogenesis*. 1977.
- [18] S. Dihlmann, A. S. Peters, and M. Hakimi. “Entstehung der Arteriosklerose”. In: *Der Pathologe* 40.5 (Sept. 2019), pp. 559–572. DOI: 10.1007/s00292-019-00656-z.
- [19] R. J. Frink. “The Beginnings. A Multicentric Disease”. In: *Inflammatory Atherosclerosis: Characteristics of the Injurious Agent*. Heart Research Foundation, 2002.
- [20] B. Herrero-Fernandez, R. Gomez-Bris, B. Somovilla-Crespo, and J. M. Gonzalez-Granado. “Immunobiology of Atherosclerosis: A Complex Net of Interactions”. In: *International Journal of Molecular Sciences* 20.21 (Oct. 2019), p. 5293. DOI: 10.3390/ijms20215293.

-
- [21] A. Ghattas, H. R. Griffiths, A. Devitt, G. Y. Lip, and E. Shantsila. “Monocytes in Coronary Artery Disease and Atherosclerosis”. In: *Journal of the American College of Cardiology* 62.17 (Oct. 2013), pp. 1541–1551. DOI: 10.1016/j.jacc.2013.07.043.
- [22] H. Jiang, Y. Zhou, S. M. Nabavi, A. Sahebkar, P. J. Little, S. Xu, et al. “Mechanisms of Oxidized LDL-Mediated Endothelial Dysfunction and Its Consequences for the Development of Atherosclerosis”. In: *Frontiers in Cardiovascular Medicine* 9 (June 2022), p. 925923. DOI: 10.3389/fcvm.2022.925923.
- [23] Q. Chen, J. Lv, W. Yang, B. Xu, Z. Wang, Z. Yu, et al. “Targeted Inhibition of STAT3 as a Potential Treatment Strategy for Atherosclerosis”. In: *Theranostics* 9.22 (2019), pp. 6424–6442. DOI: 10.7150/thno.35528.
- [24] M.-Y. Wu, C.-J. Li, M.-F. Hou, and P.-Y. Chu. “New Insights into the Role of Inflammation in the Pathogenesis of Atherosclerosis”. In: *International Journal of Molecular Sciences* 18.10 (Sept. 2017), p. 2034. DOI: 10.3390/ijms18102034.
- [25] H. Shu, Y. Peng, W. Hang, J. Nie, N. Zhou, and D. W. Wang. “The Role of CD36 in Cardiovascular Disease”. In: *Cardiovascular Research* 118.1 (Jan. 2022), pp. 115–129. DOI: 10.1093/cvr/cvaa319.
- [26] M. MANUAL. *Atherosclerosis - Cardiovascular Disorders*. URL: <https://www.msmanuals.com/professional/cardiovascular-disorders/arteriosclerosis/atherosclerosis> (visited on 09/15/2023).
- [27] L. G. Spagnoli, E. Bonanno, G. Sangiorgi, and A. Mauriello. “Role of Inflammation in Atherosclerosis”. In: *Journal of Nuclear Medicine* 48.11 (Nov. 2007), pp. 1800–1815. DOI: 10.2967/jnumed.107.038661.
- [28] L. B. Boyette, C. Macedo, K. Hadi, B. D. Elinoff, J. T. Walters, B. Ramaswami, et al. “Phenotype, Function, and Differentiation Potential of Human Monocyte Subsets”. In: *PLOS ONE* 12.4 (Apr. 2017). Ed. by G. Zissel, e0176460. DOI: 10.1371/journal.pone.0176460.
- [29] S. Gómez-Olarte, N. I. Bolaños, M. Echeverry, A. N. Rodríguez, A. Cuéllar, C. J. Puerta, et al. “Intermediate Monocytes and Cytokine Production Associated With Severe Forms of Chagas Disease”. In: *Frontiers in Immunology* 10 (July 2019), p. 1671. DOI: 10.3389/fimmu.2019.01671.

-
- [30] J. Yang, L. Zhang, C. Yu, X.-F. Yang, and H. Wang. “Monocyte and Macrophage Differentiation: Circulation Inflammatory Monocyte as Biomarker for Inflammatory Diseases”. In: *Biomarker Research* 2.1 (2014), p. 1. DOI: 10.1186/2050-7771-2-1.
- [31] K. Murphy and C. Weaver. *Janeway Immunologie*. Berlin, Heidelberg: Springer Berlin Heidelberg, 2018. DOI: 10.1007/978-3-662-56004-4.
- [32] I. F. Charo and R. M. Ransohoff. “The Many Roles of Chemokines and Chemokine Receptors in Inflammation”. In: *New England Journal of Medicine* 354.6 (Feb. 2006), pp. 610–621. DOI: 10.1056/NEJMra052723.
- [33] H. Williams, C. Mack, R. Baraz, R. Marimuthu, S. Naralashetty, S. Li, et al. “Monocyte Differentiation and Heterogeneity: Inter-Subset and Interindividual Differences”. In: *International Journal of Molecular Sciences* 24.10 (May 2023), p. 8757. DOI: 10.3390/ijms24108757.
- [34] L. Ziegler-Heitbrock, P. Ancuta, S. Crowe, M. Dalod, V. Grau, D. N. Hart, et al. “Nomenclature of Monocytes and Dendritic Cells in Blood”. In: *Blood* 116.16 (Oct. 2010), e74–e80. DOI: 10.1182/blood-2010-02-258558.
- [35] C. N. França, M. C. Izar, M. N. Hortêncio, J. B. do Amaral, C. E. Ferreira, I. D. Tuleta, et al. “Monocyte Subtypes and the CCR2 Chemokine Receptor in Cardiovascular Disease”. In: *Clinical Science* 131.12 (June 2017), pp. 1215–1224. DOI: 10.1042/CS20170009.
- [36] R. Rua and D. B. McGavern. “Elucidation of Monocyte/Macrophage Dynamics and Function by Intravital Imaging”. In: *Journal of Leukocyte Biology* 98.3 (Sept. 2015), pp. 319–332. DOI: 10.1189/jlb.4RI0115-006RR.
- [37] K. L. Wong, J. J.-Y. Tai, W.-C. Wong, H. Han, X. Sem, W.-H. Yeap, et al. “Gene Expression Profiling Reveals the Defining Features of the Classical, Intermediate, and Nonclassical Human Monocyte Subsets”. In: *Blood* 118.5 (Aug. 2011), e16–e31. DOI: 10.1182/blood-2010-12-326355.
- [38] A. M. Zawada, K. S. Rogacev, B. Rotter, P. Winter, R.-R. Marell, D. Fliser, et al. “SuperSAGE Evidence for CD14⁺⁺CD16⁺ Monocytes as a Third Monocyte Subset”. In: *Blood* 118.12 (Sept. 2011), e50–e61. DOI: 10.1182/blood-2011-01-326827.

-
- [39] A. M. van der Laan, A. Hirsch, L. F. Robbers, R. Nijveldt, I. Lommerse, R. Delewi, et al. “A Proinflammatory Monocyte Response Is Associated with Myocardial Injury and Impaired Functional Outcome in Patients with ST-segment Elevation Myocardial Infarction”. In: *American Heart Journal* 163.1 (Jan. 2012), 57–65.e2. DOI: 10.1016/j.ahj.2011.09.002.
- [40] M. Kashiwagi, T. Imanishi, H. Tsujioka, H. Ikejima, A. Kuroi, Y. Ozaki, et al. “Association of Monocyte Subsets with Vulnerability Characteristics of Coronary Plaques as Assessed by 64-Slice Multidetector Computed Tomography in Patients with Stable Angina Pectoris”. In: *Atherosclerosis* 212.1 (Sept. 2010), pp. 171–176. DOI: 10.1016/j.atherosclerosis.2010.05.004.
- [41] K. S. Rogacev, C. Ulrich, L. Blomer, F. Hornof, K. Oster, M. Ziegelin, et al. “Monocyte Heterogeneity in Obesity and Subclinical Atherosclerosis”. In: *European Heart Journal* 31.3 (Feb. 2010), pp. 369–376. DOI: 10.1093/eurheartj/ehp308.
- [42] J. Cros, N. Cagnard, K. Woollard, N. Patey, S.-Y. Zhang, B. Senechal, et al. “Human CD14dim Monocytes Patrol and Sense Nucleic Acids and Viruses via TLR7 and TLR8 Receptors”. In: *Immunity* 33.3 (Sept. 2010), pp. 375–386. DOI: 10.1016/j.immuni.2010.08.012.
- [43] A. Mongirdienė and J. Liobikas. “Phenotypic and Functional Heterogeneity of Monocyte Subsets in Chronic Heart Failure Patients”. In: *Biology* 11.2 (Jan. 2022), p. 195. DOI: 10.3390/biology11020195.
- [44] G. Thomas, R. Tacke, C. C. Hedrick, and R. N. Hanna. “Nonclassical Patrolling Monocyte Function in the Vasculature”. In: *Arteriosclerosis, Thrombosis, and Vascular Biology* 35.6 (June 2015), pp. 1306–1316. DOI: 10.1161/ATVBAHA.114.304650.
- [45] A. Ciesielska, M. Matyjek, and K. Kwiatkowska. “TLR4 and CD14 Trafficking and Its Influence on LPS-induced pro-Inflammatory Signaling”. In: *Cellular and Molecular Life Sciences* 78.4 (Feb. 2021), pp. 1233–1261. DOI: 10.1007/s00018-020-03656-y.
- [46] N. C. Olson, I. Koh, A. P. Reiner, S. E. Judd, M. R. Irvin, G. Howard, et al. “Soluble CD14, Ischemic Stroke, and Coronary Heart Disease Risk in a Prospective Study: The REGARDS Cohort”. In: *Journal of the American Heart Association* 9.6 (Mar. 2020), e014241. DOI: 10.1161/JAHA.119.014241.

-
- [47] L. Rink, H. Haase, and A. Kruse. *Immunologie für Einsteiger*. 2., neu bearb. und aktualisierte Aufl. SpringerLink. Berlin [u.a.]: Springer Spektrum, 2015. ISBN: 978-3-662-44843-4.
- [48] C. Schütt and B. Bröker. *Grundwissen Immunologie*. 3. Aufl. Heidelberg: Spektrum Akademischer Verlag, 2011. ISBN: 978-3-8274-2646-8.
- [49] P. Marques, A. Collado, S. Martinez-Hervás, E. Domingo, E. Benito, L. Piqueras, et al. “Systemic Inflammation in Metabolic Syndrome: Increased Platelet and Leukocyte Activation, and Key Role of CX3CL1/CX3CR1 and CCL2/CCR2 Axes in Arterial Platelet-Proinflammatory Monocyte Adhesion”. In: *Journal of Clinical Medicine* 8.5 (May 2019), p. 708. DOI: 10.3390/jcm8050708.
- [50] S. Zhu, M. Liu, S. Bennett, Z. Wang, K. D. G. Pflieger, and J. Xu. “The Molecular Structure and Role of CCL2 (MCP-1) and C-C Chemokine Receptor CCR2 in Skeletal Biology and Diseases”. In: *Journal of Cellular Physiology* 236.10 (Oct. 2021), pp. 7211–7222. DOI: 10.1002/jcp.30375.
- [51] X. Deng, M. Xu, C. Yuan, L. Yin, X. Chen, X. Zhou, et al. “Transcriptional Regulation of Increased CCL2 Expression in Pulmonary Fibrosis Involves Nuclear Factor- κ B and Activator Protein-1”. In: *The International Journal of Biochemistry & Cell Biology* 45.7 (July 2013), pp. 1366–1376. DOI: 10.1016/j.biocel.2013.04.003.
- [52] J. K. Damás, A. Boullier, T. Wæhre, C. Smith, W. J. Sandberg, S. Green, et al. “Expression of Fractalkine (CX3CL1) and Its Receptor, CX3CR1, Is Elevated in Coronary Artery Disease and Is Reduced During Statin Therapy”. In: *Arteriosclerosis, Thrombosis, and Vascular Biology* 25.12 (Dec. 2005), pp. 2567–2572. DOI: 10.1161/01.ATV.0000190672.36490.7b.
- [53] X. Shao, B. Wu, P. Chen, F. Hua, L. Cheng, F. Li, et al. “Circulating CX3CR1+/-CD163+ M2 Monocytes Markedly Elevated and Correlated with Cardiac Markers in Patients with Acute Myocardial Infarction”. In: *Annals of Translational Medicine* 8.9 (May 2020), pp. 578–578. DOI: 10.21037/atm-20-383.
- [54] F. V. e. S. Castanheira, K. A. de Lima, G. C. M. Cebinelli, F. Sônego, A. Kanashiro, D.-F. Colon, et al. “CCR5-Positive Inflammatory Monocytes Are Crucial for Control of Sepsis:” in: *SHOCK* 52.5 (Nov. 2019), e100–e106. DOI: 10.1097/SHK.0000000001301.

- [55] V. Braunersreuther, A. Zerneck, C. Arnaud, E. A. Liehn, S. Steffens, E. Shagdarsuren, et al. “Ccr5 But Not Ccr1 Deficiency Reduces Development of Diet-Induced Atherosclerosis in Mice”. In: *Arteriosclerosis, Thrombosis, and Vascular Biology* 27.2 (Feb. 2007), pp. 373–379. DOI: 10.1161/01.ATV.0000253886.44609.ae.
- [56] W. A. Kuziel, T. C. Dawson, M. Quinones, E. Garavito, G. Chenuaux, S. S. Ahuja, et al. “CCR5 Deficiency Is Not Protective in the Early Stages of Atherogenesis in apoE Knockout Mice”. In: *Atherosclerosis* 167.1 (Mar. 2003), pp. 25–32. DOI: 10.1016/S0021-9150(02)00382-9.
- [57] C. Shi and E. G. Pamer. “Monocyte Recruitment during Infection and Inflammation”. In: *Nature Reviews Immunology* 11.11 (Nov. 2011), pp. 762–774. DOI: 10.1038/nri3070.
- [58] X. Zhao, M. Gu, X. Xu, X. Wen, G. Yang, L. Li, et al. “CCL3/CCR1 Mediates CD14+CD16- Circulating Monocyte Recruitment in Knee Osteoarthritis Progression”. In: *Osteoarthritis and Cartilage* 28.5 (May 2020), pp. 613–625. DOI: 10.1016/j.joca.2020.01.009.
- [59] M. Kieliszek. “Selenium—Fascinating Microelement, Properties and Sources in Food”. In: *Molecules* 24.7 (Apr. 2019), p. 1298. DOI: 10.3390/molecules24071298.
- [60] Deutsche Gesellschaft für Ernährung e. V. *Selenium Daily Intake*. 2015. URL: <http://www.dge.de/wissenschaft/referenzwerte/selen/> (visited on 12/16/2022).
- [61] L. Smith and U. Garg. “Disorders of Trace Metals”. In: *Biomarkers in Inborn Errors of Metabolism*. Elsevier, 2017, pp. 399–426. DOI: 10.1016/B978-0-12-802896-4.00015-8.
- [62] L. H. Duntas. “Selenium and Inflammation: Underlying Anti-inflammatory Mechanisms”. In: *Hormone and Metabolic Research* 41.06 (June 2009), pp. 443–447. DOI: 10.1055/s-0029-1220724.
- [63] J. K. MacFarquhar. “Acute Selenium Toxicity Associated With a Dietary Supplement”. In: *Archives of Internal Medicine* 170.3 (Feb. 2010), p. 256. DOI: 10.1001/archinternmed.2009.495.
- [64] M. de Lorgeril and P. Salen. “Selenium and Antioxidant Defenses as Major Mediators in the Development of Chronic Heart Failure”. In: *Heart Failure Reviews* 11.1 (Mar. 2006), pp. 13–17. DOI: 10.1007/s10741-006-9188-2.
- [65] H. Liu, H. Xu, and K. Huang. “Selenium in the Prevention of Atherosclerosis and Its Underlying Mechanisms”. In: *Metallomics* 9.1 (2017), pp. 21–37. DOI: 10.1039/C6MT00195E.

-
- [66] L. Cui, J. Zhang, J. Guo, M. Zhang, W. Li, J. Dong, et al. “Selenium Suppressed the LPS -induced Inflammation of Bovine Endometrial Epithelial Cells through NF- κ B and MAPK Pathways under High Cortisol Background”. In: *Journal of Cellular and Molecular Medicine* 27.10 (May 2023), pp. 1373–1383. DOI: 10.1111/jcmm.17738.
- [67] H. Häcker and M. Karin. “Regulation and Function of IKK and IKK-Related Kinases”. In: *Science’s STKE* 2006.357 (Oct. 2006). DOI: 10.1126/stke.3572006re13.
- [68] C. Stoppe, B. McDonald, S. Rex, W. Manzanares, R. Whitlock, S. Fremes, et al. “Sodium Selenite Administration in Cardiac Surgery (SUSTAIN CSX-trial): Study Design of an International Multicenter Randomized Double-Blinded Controlled Trial of High Dose Sodium-Selenite Administration in High-Risk Cardiac Surgical Patients”. In: *Trials* 15.1 (Dec. 2014), p. 339. DOI: 10.1186/1745-6215-15-339.
- [69] J. Xiao, N. Li, S. Xiao, Y. Wu, and H. Liu. “Comparison of Selenium Nanoparticles and Sodium Selenite on the Alleviation of Early Atherosclerosis by Inhibiting Endothelial Dysfunction and Inflammation in Apolipoprotein E-Deficient Mice”. In: *International Journal of Molecular Sciences* 22.21 (Oct. 2021), p. 11612. DOI: 10.3390/ijms222111612.
- [70] C. Zhang, Y. Deng, Y. Lei, J. Zhao, W. Wei, and Y. Li. “Effects of Selenium on Myocardial Apoptosis by Modifying the Activity of Mitochondrial STAT3 and Regulating Potassium Channel Expression”. In: *Experimental and Therapeutic Medicine* 14.3 (Sept. 2017), pp. 2201–2205. DOI: 10.3892/etm.2017.4716.
- [71] A. Mahmoodpoor, E. Faramarzi, A. Reyhanifard, A. Shamekh, S. Nikanfar, A. Azizi-Zeinalhajlou, et al. “The Effects of Selenium Supplementation on Inflammatory Markers in Critically Ill Patients”. In: *SN Applied Sciences* 4.12 (Dec. 2022), p. 326. DOI: 10.1007/s42452-022-05208-4.
- [72] M. W. A. Angstwurm, J. Schottdorf, J. Schopohl, and R. Gaertner. “Selenium Replacement in Patients with Severe Systemic Inflammatory Response Syndrome Improves Clinical Outcome:” in: *Critical Care Medicine* 27.9 (Sept. 1999), pp. 1807–1813. DOI: 10.1097/00003246-199909000-00017.
- [73] C. Stoppe, G. Schälte, R. Rossaint, M. Coburn, B. Graf, J. Spillner, et al. “The Intraoperative Decrease of Selenium Is Associated with the Postoperative Develop-

- ment of Multiorgan Dysfunction in Cardiac Surgical Patients*.” in: *Critical Care Medicine* 39.8 (Aug. 2011), pp. 1879–1885. DOI: 10.1097/CCM.0b013e3182190d48.
- [74] D. R. Hodge, E. M. Hurt, and W. L. Farrar. “The Role of IL-6 and STAT3 in Inflammation and Cancer”. In: *European Journal of Cancer* 41.16 (Nov. 2005), pp. 2502–2512. DOI: 10.1016/j.ejca.2005.08.016.
- [75] T. Alonzi, D. Maritano, B. Gorgoni, G. Rizzuto, C. Libert, and V. Poli. “Essential Role of STAT3 in the Control of the Acute-Phase Response as Revealed by Inducible Gene Activation in the Liver”. In: *Molecular and Cellular Biology* 21.5 (Mar. 2001), pp. 1621–1632. DOI: 10.1128/MCB.21.5.1621-1632.2001.
- [76] X. Yang, J. Jia, Z. Yu, Z. Duanmu, H. He, S. Chen, et al. “Inhibition of JAK2/STAT3/SOCS3 Signaling Attenuates Atherosclerosis in Rabbit”. In: *BMC Cardiovascular Disorders* 20.1 (Dec. 2020), p. 133. DOI: 10.1186/s12872-020-01391-7.
- [77] S. B. Vasamsetti, S. Karnewar, A. K. Kanugula, A. R. Thatipalli, J. M. Kumar, and S. Kotamraju. “Metformin Inhibits Monocyte-to-Macrophage Differentiation via AMPK-Mediated Inhibition of STAT3 Activation: Potential Role in Atherosclerosis”. In: *Diabetes* 64.6 (June 2015), pp. 2028–2041. DOI: 10.2337/db14-1225.
- [78] Z. Lin, N. Y. Chiang, N. Chai, D. Seshasayee, W. P. Lee, M. Balazs, et al. “In Vivo Antigen-Driven Plasmablast Enrichment in Combination with Antigen-Specific Cell Sorting to Facilitate the Isolation of Rare Monoclonal Antibodies from Human B Cells”. In: *Nature Protocols* 9.7 (July 2014), pp. 1563–1577. DOI: 10.1038/nprot.2014.104.
- [79] M. Wacker, A. Ball, H.-D. Beer, I. Schmitz, K. Borucki, F. Azizzadeh, et al. “Immunophenotyping of Monocyte Migration Markers and Therapeutic Effects of Selenium on IL-6 and IL-1 β Cytokine Axes of Blood Mononuclear Cells in Preoperative and Postoperative Coronary Artery Disease Patients”. In: *International Journal of Molecular Sciences* 24.8 (Apr. 2023), p. 7198. DOI: 10.3390/ijms24087198.
- [80] B. Rad. *Mini-PROTEAN Tetra_CellInstruction Manual*. May 2019. URL: <https://www.bio-rad.com/webroot/web/pdf/lsr/literature/10007296D.pdf> (visited on 03/18/2020).
- [81] Wikipedia. *Western Blot Wiki*. Mar. 2020. URL: https://en.wikipedia.org/wiki/Western_blot (visited on 03/18/2020).
- [82] Wikipedia. *SDS Page Wiki*. Feb. 2020. URL: <https://de.wikipedia.org/wiki/SDS-PAGE#Probenvorbereitung> (visited on 03/19/2020).

-
- [83] T. Scientific. *SuperSignal West Femto Maximum Sensitivity Substrate*. Mar. 2020. URL: https://www.thermofisher.com/document-connect/document-connect.html?url=https%3A%2F%2Fassets.thermofisher.com%2FFTFS-Assets%2FSLG%2Fmanuals%2FMAN0011345_SupSig_West_Femto_MaxSensi_Subs_UG.pdf (visited on 03/23/2020).
- [84] S. E. Engelen, A. J. B. Robinson, Y.-X. Zurke, and C. Monaco. “Therapeutic Strategies Targeting Inflammation and Immunity in Atherosclerosis: How to Proceed?” In: *Nature Reviews Cardiology* 19.8 (Aug. 2022), pp. 522–542. DOI: 10.1038/s41569-021-00668-4.
- [85] M. Wardak. “⁶⁸Ga-labeled Exendin-4 to Image Cardiac Repair after Myocardial Infarction: From Lizard Venom to Laboratory and Beyond”. In: *Journal of Nuclear Cardiology* 27.6 (Dec. 2020), pp. 2398–2401. DOI: 10.1007/s12350-019-01641-y.
- [86] C. Peet, A. Ivetic, D. I. Bromage, and A. M. Shah. “Cardiac Monocytes and Macrophages after Myocardial Infarction”. In: *Cardiovascular Research* 116.6 (May 2020), pp. 1101–1112. DOI: 10.1093/cvr/cvz336.
- [87] M. Nahrendorf, F. K. Swirski, E. Aikawa, L. Stangenberg, T. Wurdinger, J.-L. Figueiredo, et al. “The Healing Myocardium Sequentially Mobilizes Two Monocyte Subsets with Divergent and Complementary Functions”. In: *The Journal of Experimental Medicine* 204.12 (Nov. 2007), pp. 3037–3047. DOI: 10.1084/jem.20070885.
- [88] A. Kaufmann, R. Salentin, D. Gemsa, and H. Sprenger. “Increase of CCR1 and CCR5 Expression and Enhanced Functional Response to MIP-1 α during Differentiation of Human Monocytes to Macrophages”. In: (2000), p. 5.
- [89] M. M. K. Lee, R. K. S. Chui, I. Y. S. Tam, A. H. Y. Lau, and Y. H. Wong. “CCR1-Mediated STAT3 Tyrosine Phosphorylation and CXCL8 Expression in THP-1 Macrophage-like Cells Involve Pertussis Toxin-Insensitive G α 14/16 Signaling and IL-6 Release”. In: *The Journal of Immunology* 189.11 (Dec. 2012), pp. 5266–5276. DOI: 10.4049/jimmunol.1103359.
- [90] M. V. Wainstein, M. Mossmann, G. N. Araujo, S. C. Gonçalves, G. L. Gravina, M. Sangalli, et al. “Elevated Serum Interleukin-6 Is Predictive of Coronary Artery Disease in Intermediate Risk Overweight Patients Referred for Coronary Angiography”. In: *Diabetology & Metabolic Syndrome* 9.1 (Dec. 2017), p. 67. DOI: 10.1186/s13098-017-0266-5.

-
- [91] H. Susilo, M. Thaha, B. S. Pikir, M. Y. Alsagaff, S. D. Suryantoro, C. D. K. Wungu, et al. “The Role of Plasma Interleukin-6 Levels on Atherosclerotic Cardiovascular Disease and Cardiovascular Mortality Risk Scores in Javanese Patients with Chronic Kidney Disease”. In: *Journal of Personalized Medicine* 12.7 (July 2022), p. 1122. DOI: 10.3390/jpm12071122.
- [92] Y. Feng, D. Ye, Z. Wang, H. Pan, X. Lu, M. Wang, et al. “The Role of Interleukin-6 Family Members in Cardiovascular Diseases”. In: *Frontiers in Cardiovascular Medicine* 9 (Mar. 2022), p. 818890. DOI: 10.3389/fcvm.2022.818890.
- [93] G. M. Gager, B. Biesinger, F. Hofer, M.-P. Winter, C. Hengstenberg, B. Jilma, et al. “Interleukin-6 Level Is a Powerful Predictor of Long-Term Cardiovascular Mortality in Patients with Acute Coronary Syndrome”. In: *Vascular Pharmacology* 135 (Dec. 2020), p. 106806. DOI: 10.1016/j.vph.2020.106806.
- [94] E. Lindmark, E. Diderholm, L. Wallentin, and A. Siegbahn. “Relationship Between Interleukin 6 and Mortality in Patients With Unstable Coronary Artery Disease: Effects of an Early Invasive or Noninvasive Strategy”. In: *JAMA* 286.17 (Nov. 2001), p. 2107. DOI: 10.1001/jama.286.17.2107.
- [95] S. Yuan, P. Carter, M. Bruzelius, M. Vithayathil, S. Kar, A. M. Mason, et al. “Effects of Tumour Necrosis Factor on Cardiovascular Disease and Cancer: A Two-Sample Mendelian Randomization Study”. In: *eBioMedicine* 59 (Sept. 2020), p. 102956. DOI: 10.1016/j.ebiom.2020.102956.
- [96] P. M. Ridker, N. Rifai, M. Pfeffer, F. Sacks, S. Lepage, and E. Braunwald. “Elevation of Tumor Necrosis Factor- α and Increased Risk of Recurrent Coronary Events After Myocardial Infarction”. In: *Circulation* 101.18 (May 2000), pp. 2149–2153. DOI: 10.1161/01.CIR.101.18.2149.
- [97] A. Hilgendorff, H. Muth, B. Parviz, A. Staubitz, W. Haberbosch, H. Tillmanns, et al. “Statins Differ in Their Ability to Block NF- κ B Activation in Human Blood Monocytes”. In: *Int. Journal of Clinical Pharmacology and Therapeutics* 41.09 (Sept. 2003), pp. 397–401. DOI: 10.5414/CP41397.
- [98] R. Loperena, J. P. Van Beusecum, H. A. Itani, N. Engel, F. Laroumanie, L. Xiao, et al. “Hypertension and Increased Endothelial Mechanical Stretch Promote Monocyte Differentiation and Activation: Roles of STAT3, Interleukin 6 and Hydrogen Peroxide”. In: *Cardiovascular Research* 114.11 (Sept. 2018), pp. 1547–1563. DOI: 10.1093/cvr/cvy112.

- [99] D. Korenfeld, K. Roussak, S. Dinkel, T. P. Vogel, H. Pollack, J. Levy, et al. “STAT3 Gain-of-Function Mutations Underlie Deficiency in Human Nonclassical CD16+ Monocytes and CD141+ Dendritic Cells”. In: *The Journal of Immunology* 207.10 (Nov. 2021), pp. 2423–2432. DOI: 10.4049/jimmunol.2000841.
- [100] S. A. Dabravolski, V. N. Sukhorukov, A. A. Melnichenko, V. A. Khotina, and A. N. Orekhov. “The Role of Selenium in Atherosclerosis Development, Progression, Prevention and Treatment”. In: *Biomedicines* 11.7 (July 2023), p. 2010. DOI: 10.3390/biomedicines11072010.
- [101] M. Basiak, M. Kosowski, M. Hachula, and B. Okopien. “Plasma Concentrations of Cytokines in Patients with Combined Hyperlipidemia and Atherosclerotic Plaque before Treatment Initiation—A Pilot Study”. In: *Medicina* 58.5 (Apr. 2022), p. 624. DOI: 10.3390/medicina58050624.

Acknowledgment

With great joy and gratitude, I look back on the successful completion of my doctoral thesis, which I accomplished from February 2019 to September 2023 at the Clinic for Cardiothoracic Surgery of the Faculty of Medicine at Otto-von-Guericke University, Magdeburg. The choice of the topic for my doctoral thesis was driven by a personal motivation. On one hand, I have always been interested in experimental research, and on the other, the field of cardiology and cardiothoracic surgery has always fascinated me. My professional background in emergency services as a paramedic further solidified my connection to the medical condition of heart attack. Next to its high frequency of occurrence, it is one of the most impressive emergencies regarding both clinical presentations and treatment options, as well as treatment strategies. It was my desire to contribute on a scientific level to provide innovative approaches and new treatment options for patients with CAD.

In this regard, I would like to express my sincere appreciation. First and foremost, my deep thanks go to Dr. Priya Veluswamy, who guided me through the topic and assisted me in writing this dissertation with her expertise and leadership. Likewise, I hold profound appreciation for Prof. Dr. med. Wippermann who not only entrusted me with the topic of this doctoral thesis but also offered valuable insights. I want to express a special thanks to the entire team at the Cardiothoracic Surgery Research division. The support of Dr. Priya Veluswamy, Dr. med. Max Wacker and Mrs. Elena Densk, along with the cooperative atmosphere in the laboratory, provided me with the opportunity to conduct experiments under optimal conditions. The generous provision of space and materials, as well as expert guidance, significantly contributed to the positive outcomes of my work. It was a great pleasure to benefit from the team's expertise and dedication. In our regular team meetings, Mrs. Prof. Dr. rer. biol hum. Walles and Mr. Prof. Dr. Walles also contributed valuable thoughts and ideas that enhanced the quality of the work.

At the same time, I would not want to omit mentioning my family in this acknowledgment. I extend my heartfelt thanks to my parents, Elke Hänicke-Hurlin and Udo Hänicke, for accompanying and encouraging me on my journey, including pursuing my medical studies. To my husband, Alexander Ball, my sincere gratitude for his unwavering support throughout the entire research process.

My doctoral thesis journey was influenced by several individuals who supported, advised, and encouraged me. The experiences and insights I gained will stay with me.

With profound gratitude, Anna Ball

Ehrenerkärung

Ich erkläre, dass ich die der Medizinische Fakultät der Otto-von-Guericke-Universität Magdeburg zur Promotion eingereichte Dissertation mit dem Titel:

**Blood Monocyte Phenotypes and Effect of Selenium on Mononuclear Cells
in Coronary Artery Disease: A Special Focus on Monocyte Migration
Markers and STAT-3/IL-6 Axis**

an der Universitätsklinik für Herz- und Thoraxchirurgie

mit Unterstützung durch

**Prof. Dr. med. Jens Wippermann, Dr. Priya Veluswamy,
Dr. med. Max Wacker**

ohne sonstige Hilfe durchgeführt und bei der Abfassung der Dissertation keine anderen als die dort aufgeführten Hilfsmittel benutzt habe.

Bei der Abfassung der Dissertation sind Rechte Dritter nicht verletzt worden.

Ich habe diese Dissertation bisher an keiner in- oder ausländischen Hochschule zur Promotion eingereicht. Ich übertrage der Medizinischen Fakultät das Recht, weitere Kopien meiner Dissertation herzustellen und zu vertreiben.

Potsdam, August 26, 2024

Anna Ball

Curriculum Vitae

The Curriculum Vitae has been excluded from this version due to data protection considerations.